THE UNIVERSITY OF CALGARY

THE DYNAMIC SIMULATION OF A THREE PHASE SEPARATOR

by

Marc M. Dionne

A THESIS

SUBMITTED TO THE FACULTY OF GRADUATE STUDIES

IN PARTIAL FULFILLMENT OF THE REQUIREMENTS FOR THE

DEGREE OF MASTER OF SCIENCE IN CHEMICAL ENGINEERING

DEPARTMENT OF CHEMICAL AND PETROLEUM ENGINEERING

CALGARY, ALBERTA

November, 1998

ABSTRACT

A nonequilibrium rate based model for the dynamic simulation of a horizontal three phase separator was developed. The rate based model included the calculation of mass and heat transfer rates which were accomplished through the use of a mass and heat transfer correlation. Several simulation runs were performed in order to test the model. Additional tests were performed to verify the effect of various chemical mixtures upon the separator design, the effect of feed disturbances and the effect of weir width. The simulations included various separator operation scenarios such as dry startup, feed disturbance and shutdown.

The results obtained showed that the model was successful in describing the three phase separator. The separator behaved as expected to the applied disturbances.

ACKNOWLEDGMENTS

Many individuals have contributed to the work presented in this thesis. The author would like to thank the following people:

Dr. W. Y. Svrcek, his supervisor, for guidance and direction.

Dr. Marco Satyro for his wealth of information and his words of encouragement.

Kent Berkley, for his expertise in computer programming and his knowledge of the HYCON package.

The Hyprotech staff, for answering numerous questions.

Hyprotech Ltd., for allowing the author to use a copy of HYCON.

Deb, his wife, for her words of encouragement and patience.

TABLE OF CONTENTS

LIST OF TABLES

LIST OF FIGURES

NOMENCLATURE

a	interficial area (m^2/m^3)
c	concentration ($kmol/m^3$)
C	number of component (Degree of freedom analysis)
D	diffusivity coefficient (cm^2/s)
E	energy holdup (kJ)
e	energy transfer rate (kJ/s)
F	feed flowrate (kmol/s)
Fa	F-factor
G	Gibbs free energy
H	enthalpy (kJ)
h	liquid height above weir edge (m) or heat transfer coefficient (kJ/m^2 s)
HV	vapour holdup (kmol)
HL	liquid holdup (kmol)
K	equilibrium ratio (y/x)
K	overall mass transfer coefficient (kmol/s)
ka	mass transfer coefficient interfacial area product (kmol/s)
L	liquid flowrate (kmol/s) or weir width (m)
L1	light liquid flowrate (kmol/s)
L2	heavy liquid flowrate (kmol/s)
M	mass condensed or vapourized (kmol)
M	molecular weight (kg/kmol)
m	slope of equilibrium curve
N	mass transfer flowrate (kmol/s) or number of moles (kmol)
N_D	degrees of freedom
N_V	number of variables
N_E	number of equations
P	pressure (kPa)
Q	energy into separator/stage (kJ/s)
R	universal gas constant (K Pa m^3 / K kmol)
t	time step or time (s or min)
T	temperature (K)
V	vapour phase or vapour flowrate (kmol/s) or system volume (m^3)

Vc	critical volume (cm^3/mol)
x	liquid composition in mole fraction
y	vapour composition in mole fraction
z	feed composition or compressibility factor

superscript/subscript

‘	liquid1 fraction
“	liquid2 fraction
*	equilibrium value
cond	mass condensed
ex	excess Gibbs free energy
flash	mass vapourized
i	individual component index or interface composition
j	component index or stage index
L	liquid
L’	light liquid
L”	heavy liquid
o	at infinite dilution
U	holdup
V-L’ or V-'	vapour to light liquid transfer
L’-L” or '-"	light liquid to heavy liquid transfer
L'-V or '-V	light liquid to vapour transfer
L"-L' or "-'	heavy liquid to light liquid transfer
t	total
v	vapour fraction or vapour
out	exiting streams
in	feed streams
L_1	light liquid
L_2	heavy liquid

Symbols

α	NRTL non randomness parameter
τ	NRTL interaction parameter
ρ	density (g/cm^3 or kg/m^3)
σ	surface tension ($dyne/cm^2$)
Δ	difference
μ	viscosity (cp)
γ	NRTL activity coefficient

Chapter 1- Introduction

Simulation and simulators of chemical processes and unit operations are an integral part of today's process engineers' repertoire. There has been a continuing effort starting in the 1950's to develop and validate mathematical models of all the unit operations that are in refineries, oil and gas facilities and chemical plants. The models of the 1950's focused on the steady state behaviour with simplistic or non-existent thermodynamic models. However, some of the early models were dynamic models and their solutions were obtained using hybrid or analog computers.

In the 1960's, further development of the mathematical models allowed the simulation emphasis to change from individual unit operation simulations to complete process simulations (Lacey and Svrcek, 1990). As plant problems to be simulated increased in complexity, like safety related problems, an increased urge to consider dynamic simulations arose. Near the late 1960's, engineering companies produced sequential modular simulators, where the individual modules used detailed models and rigorous thermodynamics to simulate operations of compressors and distillation columns (Lacey and Svrcek, 1990).

The 1970's were greeted with enhancements in process engineering software from engineering and software companies. There were advancements made in the thermodynamic packages with improvements in unit operations, convergence techniques, technical manuals and software support (Lacey and Svrcek, 1990). These improved thermodynamic packages produced more efficient and accurate simulations. The computer hardware also improved over the decades with enhancements in computer speed and storage capability.

The 1980's marked the decade of microcomputers and personal computers (Lacey and Svrcek, 1990). Along with the hardware improvement, industry focused on operating

systems and the refinement of the interaction between the user and the software. Interfacing marked the next step in the development of steady state simulators which allowed simulation results to be graphically displayed during the simulations. Some examples of these simulators are HYSIM and HYSYS, which are simulation software developed at Hyprotech Ltd.

In the 1990's, the mathematical models were further developed in order to dynamically simulate entire plants. These models consisted of the equilibrium model and the nonequilibrium or rate based models. An example of this software is RATEFRAC developed at Aspen Tech Ltd.

The emphasis was changed from the equilibrium model to the nonequilibrium model in an attempt to model transient mass and energy fluxes. The increase in the complexity of the nonequilibrium model by estimating the mass and energy transfer coefficients does not guarantee an increase in the model's accuracy.

Virtually all simulators use an equilibrium based model which many types of equipment to be simulated accurately such as separators, distillation towers and liquid-liquid extractors. But as the engineers' responsibility required them to simulate more equipment, the associated complexity of the equipment increased; therefore, the simulator's mathematical model had to increase in complexity. It was noticed that the equilibrium model was no longer adequate and as a result, engineers turned to the nonequilibrium model which involves mass transfer as part of the mathematical model.

An extensive literature search was performed and revealed that very little work has been done on the dynamic simulation of three phase separators. Due to the lack of literature on the subject of separator simulation, the focus turned to the simulation of distillation towers since the equilibrium tray and the separator models are very similar.

Chapter 2- Literature Survey

2.1 Introduction

The interest and need for dynamic simulators (Marquardt, 1991) has been known for decades. Throughout the years, simulators have been written to simulate single phase systems, two phase systems, and finally three or multiple phase systems. These simulators can be used for evaluating the safety in the operation of certain processes, for the design of process units, and in the evaluation and design of process control schemes.

As a result of these needs and applications, there was a growing number of separation processes which were routinely simulated, such as drum separators, liquid-liquid extractors, absorbers, strippers, and distillation columns. The latter separation process will be the unit operation of interest for this literature review.

This literature survey will focus on the state of the art for steady-state and dynamic simulations of three phase distillation towers. This work will summarize the models used, the accompanying necessary assumptions, and finally the solution methods employed to solve the system of equations. The first section of this chapter will present the various models employed in process simulators and is divided into steady state and dynamic modeling.

2.2 Mathematical Models

For steady-state simulations, the equilibrium stage model had been used for over 50 years and has provided satisfactory results for such equipment as flash tanks and distillation columns. The first dynamic simulators (for example a flash tank) incorporated an equilibrium stage model. Then, eventually the nonequilibrium model was developed because the model creators wanted to more realistically represent physical processes.

They wanted to consider the incomplete approach to thermodynamic equilibrium by the model itself as opposed to introducing an arbitrary efficiency as some have done with the equilibrium stage model.

There are other models (Taylor and Lucia, 1995) that are being used in dynamic simulations such as the compartmental model (Benallon et al., 1986), the collocation model (Carta et al., 1995) and the bubble residence contact time model (Morris, 1980).

2.2.1 Equilibrium Model

The equilibrium stage model had been used by engineers for over 50 years (Taylor and Lucia, 1995). It had been the base model adapted to simulate various separation processes. Figure 2.1 illustrates an equilibrium stage. The equations used to describe the basic equilibrium stage model are the material balances, equilibrium relations, the composition summation equations, and the enthalpy equations (MESH equations). The major assumption made for the equilibrium stage model was that the vapour and liquid phases exiting a stage were in thermodynamic, mechanical, and thermal equilibrium. Some have added an efficiency factor in order to take into account the incomplete approach to thermodynamic equilibrium. Many other authors (Luyben, 1973) have added to or modified this model in an attempt to more accurately model mass and energy transfer in a contact stage.

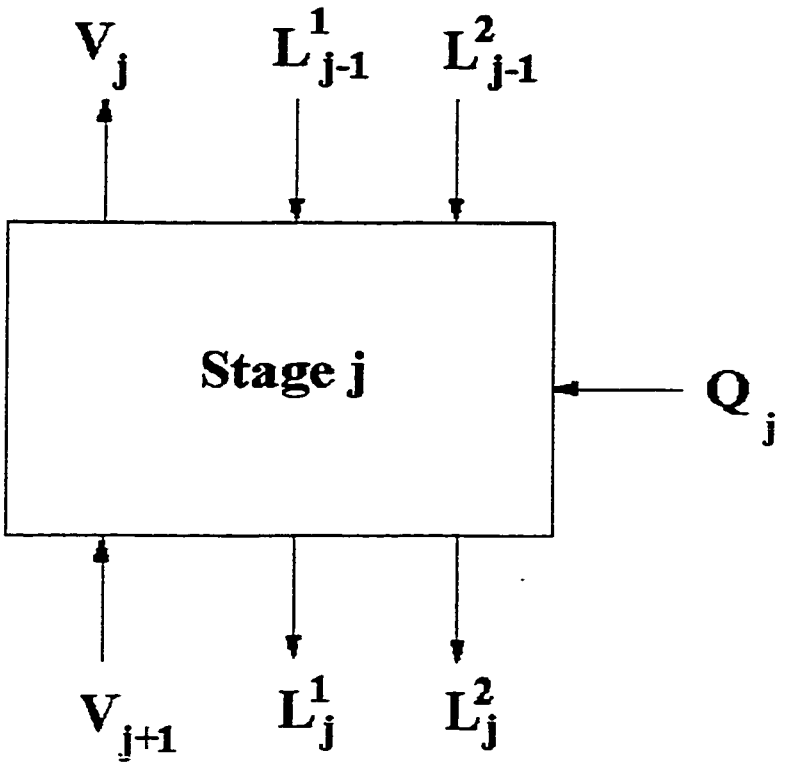

Figure 2.1 Diagram of an equilibrium stage

Sayama et al. (Sayama et al., 1990) only added a stoichiometric equation to the basic model for their steady-state simulator. Their assumptions included ideal dispersion of the liquid phase and the thermodynamic equilibrium in all stages.

Landwehr et al. (Landwehr et al., 1992) used the basic model with the addition of equilibrium relations, the Murphree tray efficiency, stoichiometric equation, and the definition of the second liquid phase. Their equations were based on the assumptions that there was liquid vapor equilibrium at the liquid surface, the liquid phases were ideally mixed, there was liquid-liquid equilibrium, and the Murphree tray efficiency model was valid. They applied their simulator on several steady state examples of three phase distillation operations from the literature. One example verified was a high pressure distillation column separating a four component mixture. The results could be successfully

simulated if the model parameters for the NRTL (Non-Random Two-Liquid) or UNIQUAC (Universal Quasi-Chemical) models were available.

Salazar-Sotelo (Salazar-Sotelo, 1992) took the MESH equations and removed the summation and enthalpy equations and replaced them with the equilibrium equations. The equations were based upon the assumption that all exiting streams from a stage were at thermodynamic equilibrium. He used a two step solution method, the first step solved the liquid-liquid equations stage by stage, while the second step involved the application of the Naphtali and Sandholm technique to solve the remaining equations. Salazar-Sotelo simulated an eleven stage atmospheric column to separate propanol and butanol from water. The simulation converged after five iterations. The simulations were sensitive to the accuracy of the initial guesses for the liquid-liquid equilibrium distribution coefficients.

Cairns and Furzer (Cairns and Furzer, 1990) had used the basic model with the following assumptions: negligible vapour holdup, no sidestreams removed, and the passing streams were equal (composition-wise). Cairns and Furzer performed twenty nine total reflux runs in the various distillation regions of the compositional diagram. All the experimental runs tended towards a common heterogeneous azeotrope overhead. They found that the bottoms approached different compositions along various paths. These paths depended upon the overall feed mixture. They found that a seven ideal stage column would best represent the experimental data for the runs. They claimed that the simulations gave adequate results and that there were some problems with internal behaviour such as frothing and dry stages.

Pucci et al. (Pucci et al., 1986) also utilized the basic MESH equations but made these assumptions: the reboiler operates with a homogeneous mixture, either the bottom flowrate or reboiler duty was given, and the reflux or distillate flowrate could be given. They applied their simulator to the separation of fermentation products. They claim that their proposed computation procedure was reliable and efficient. They also noted that

their procedure was flexible for the simulation of any kind of distillation column with two or three co-existing phases.

The results obtained by Block and Hegner (Block and Hegner, 1976) have been used as a benchmark for many other results obtained from various authors. Their model equations consisted of the component material balance, the enthalpy balance, stoichiometric equation, and the phase equilibrium equation. These equations were based upon the assumptions such as phase equilibrium at each stage, and values were given to the gas phase enthalpy, liquid phase enthalpy, the vapor-liquid equilibrium ratio and the liquid-liquid equilibrium ratio. Their example was the distillation of a propanol-butanol-water mixture.

Kingsley and Lucia (Kingsley and Lucia, 1988) had as well included the MESH equations into their model, but had broken down the mass balance into two separate equations, one for the individual component balance and the second for the overall component balance. They had also added the equilibrium equations and the Murphree tray efficiency into the model to aid in increasing the accuracy of the simulation. When performing the pressure-vapor fraction (PV) flash to determine the heterogeneous behaviour, temperature was a variable but they exclude the energy balances from the set of equations.

Wasylkiewicz (Wasylkiewicz, 1992) proposed a simulation of a three phase distillation tower, using a stage by stage calculation method. His model consisted of the MESH equations including the Vapor-Liquid and Liquid-Liquid equilibrium equations. The data required to complete the set of equations were the saturation pressures, activity coefficient relationships, as well as the vapor and liquid enthalpies. Wasylkiewicz also noted that if the pressure, feed composition and the feed enthalpy were supplied, then only one piece of information was required to solve the equilibrium distillation stage, namely the temperature or heat input. Wasylkiewicz compared his results to those generated by

Block and Hegner, and concluded that they were in agreement. Wasylkiewicz claimed that his simulation technique was robust and could solve systems with initial approximations that were far from the final solution.

Baden and Michelsen (Baden and Michelsen, 1987) also used the equilibrium model, but dealt only with the energy and mass balances as well as the equilibrium relations. They did not note any assumption made to simplify the model and calculation method. Their solution method was declared robust and easy to implement.

Heh et al. (Heh et al., 1987) had adapted the standard equilibrium model for their simulator. They removed the summation equations and replaced them with the equilibrium equations. The assumptions necessary for their model were: the stage flash was isobaric and isothermal, the vapour phase was ideal, and the enthalpy of mixing was zero. They simulated a twelve stage column separating a propanol-butanol-water mixture. Their converged solution was identical to results obtained from other simulations with slightly different columns. They claim that their new method was less computationally efficient but could predict correct phase regions. They had also indicated that the application of the global Newton method produced a solution algorithm that was more efficient and robust than their previous algorithm.

Ross and Seider (Ross and Seider, 1980) employed the standard MESH model for the basis of their simulator. They did add equilibrium equations as well as a pseudo equilibrium factor which was comparable to a normalized K factor (Ross and Seider, 1980). The only assumption that they mention was that the column model assumed constant molal overflow.

Kruse et al. (Kruse et al., 1995) added the Murphree stage efficiency, and the equilibrium relations to the model in order to increase the accuracy of their dynamic simulator. They made the following assumptions: constant pressure profile throughout the entire column, ideally mixed liquid phase, negligible vapour holdup (to simplify the

model), and high contact times. They had observed that both the steady state and dynamic simulation results were not in agreement with the calculated and experimental concentration profiles. Only with the peripheral systems (condenser and reboiler) did the results agree between the calculated and experimental profiles.

Eckert and Kubícek (Eckert and Kubícek, 1994) added component hold-ups, internal energy hold-ups, volume balances, pressure drop equations and the Francis weir formula to their dynamic simulator. The Francis weir formula allowed them to predict the exiting liquid molar flowrates.

Wong et al. (Wong et al., 1991) added the Francis weir formula and the equilibrium relations. In order to simplify their dynamic simulation, they made several assumptions such as: liquid-vapour phases were in equilibrium, liquid-liquid phases were also in equilibrium, the tray efficiency was neglected, one term of the Francis weir formula did not depend upon the liquid density, the partial derivatives were negligibly small, the liquid in the reboiler was at its bubble point, and for the condenser-decanter the temperature was constant, volume hold-up was constant, the two liquid phases were in equilibrium, and the two liquid phases were perfectly split (so that the flowrates and hold-ups were equal to the equilibrium phase fraction).

Kinoshita et al. (Kinoshita et al., 1986) removed the heat balances from their model and added the vapour hold-ups and equilibrium relationships. The assumptions required to complete this model were: volatility was constant, the molar holdups of both the liquid and vapor were considered constant, hydraulic effects were negligible, there was perfect mixing between the liquid and vapor phase and within each individual phase, and pressure was independent of time.

Iribarren and Chiotti (Iribarren and Chiotti, 1991) used the standard equilibrium model but through algebraic manipulations of the model equation, they produced an equation capable of predicting the startup time of a distillation column operating at total

reflux. Their assumptions were the following: binary system with constant relative volatilities, instantaneous equilibrium of vapor composition, negligible molar holdups on each stage, constant molar liquid holdups, liquid and vapor flowrate were identical, liquid phase was still uniform throughout the entire column after hydraulic steady state was achieved.

2.2.2 Nonequilibrium Model

The equilibrium stage model was a conceptually simple model (Taylor and Lucia, 1995). It had been used to design and simulate actual distillation columns . But the stages of a real column are not equilibrium stages. As a result, efficiency factors had been implemented in order to take into account the incomplete approach to thermodynamic equilibrium. When the efficiencies were used, it was usually either the Murphree tray efficiencies or the overall efficiencies. The nonequilibrium stage model used the equilibrium stage model plus other equations to estimate or predict the mass and energy transfer fluxes. The equations used to describe the nonequilibrium stage model were the mass balances, energy balances, the equilibrium relations, and the mass and energy transfer equations. There were separate balance equations written for each individual phase. There were no efficiencies required for this model, due to the mass and energy transfer equations. The rates of energy and mass that were transferred across the phase interfaces depended upon the degree from which the phases were not in equilibrium (Taylor and Lucia, 1995). The rates were determined by the use of multicomponent mass transfer models.

Overjero et al. (Overjero et al., 1994) designed a non-equilibrium model composed of conservation equations, heat and mass rate equations and interface equations. The conservation and interface equations were the component material balances, ratio of side

stream to interstage flowrate, energy balances, and balances around the interface. The only assumption that the authors mentioned was that the interface was a singular surface without resistance; therefore, equilibrium was attained. The results obtained from their experiments had a 6% average deviation from compared results. They claim that they adequately estimated the molar fluxes in every stage of the column and that the overall results were in agreement with the measured results. They estimated the mass transfer rates using three different methods resulting from equations that were based upon the film model steady state one-dimensional diffusion (Overjero et al, 1994). The three different solution methods were the method based upon the use of effective mass transfer coefficients, the implicit interactive method and the explicit interactive method.

Kooijman and Taylor (Kooijman and Taylor, 1995) had taken the basic non-equilibrium model and enhanced it. The model equations they used were the vapor and liquid holdup, the component molar balance, the molar holdup summation, the holdup energy balances, the energy holdup summation, interface energy transfer equations, the interface composition summation, equilibrium relations, mass transfer ratios, and the pressure calculations. Kooijman and Taylor indicate that the non-equilibrium model included the tray sizing parameters and the mass transfer models, where both of these factors would influence the column dynamics. The authors did list their assumptions as follows: the trays operated at different flow regimes (froth, emulsion, bubbling liquid and foam), the holdups were required (there are different types of holdups), the froth would contain more holdup if the tray had multiple phases, the trays were in mechanical equilibrium, the thermodynamic equilibrium was assumed only at the interface between the vapor and liquid, the condenser and reboiler operated at equilibrium, the mass transfer occurred only between the liquid and vapor on the tray and it was dictated by resistance to transport in each phase. Finally there was constant molar vapor holdup above the froth. The results obtained showed differences between the equilibrium and nonequilibrium

models used. The difference in results obtained from the equilibrium and nonequilibrium methods had been attributed to the fact that the nonequilibrium stage model used both heat and mass transfer limitations that the equilibrium stage model ignored.

Rovaglio and Doherty (Rovaglio and Doherty, 1990) claimed to have developed a new dynamic model for heterogeneous azeotropic distillation capable of automatically detecting and noting the multiple liquid phase on each tray. Their model equations were the material and energy balances, the fluid dynamics relationships, the vapor-liquid equilibrium equation, and the definition of a total energy stage. The model also included the following assumptions: the condenser-decanter was a liquid-liquid equilibrium stage, the condenser-decanter was a subcooled total condenser, the decanter temperature was the same as the condenser temperature, the condenser-decanter operated at atmospheric pressure, the capacitance terms due to downcomer were neglected, the vapor holdup over the plate was neglected, the liquid and vapor phases were well mixed and the liquid and vapor streams leaving each tray were in phase equilibrium. The authors indicated that most of their results showed that the simulations were stable and responded well to disturbances. Some oscillating behaviour was observed in the lower stages while trying to reach steady state.

2.2.3 Other Nonequilibrium Models

As the need for accurate and efficient dynamic simulators developed, there was need to develop different models that did not require a large number of assumptions and that would simulate complex systems. Some of the more interesting models were the collocation model, the compartmental model and the residence time model.

2.2.3.1 Collocation Model

The collocation model (Carta et al. 1995) was a reduced-order model that interpolated values for state variables at well defined mesh points, that can be regarded as fictitious stages. The problem with this model was that during a column transient state, the state variable could take on values that had no physical meaning, hence these values were useless to the column performance interpretation. This modeling approach has had little acceptance Carta et al., (1995) and Stewart et al., (1985).

2.2.3.2 Compartmental Model

The compartmental model was a low order modeling technique that took a stage column as a compartmental system where a known number of stages was selected and lumped together to form an equivalent single stage. This technique leads to a lower order model without the need of linearization.

The compartmental analysis involved breaking a distillation column into several sections or compartments, where each section was made up of several stages. The material balance involved in the set of equations incorporated the compartmental sections. The major assumption in this model was that the dynamic behaviour of a compartment can be represented by a single stage with equal holdup to that of the total compartment holdup and the composition of the compartment sensitive stage (Benallon et al., 1986). With this assumption, the model could represent the dynamic behaviour of the compartmental stage by one differential equation derived from the dynamic material balance. Therefore, the compartmental model is composed of a set of single dynamic material balance equations from each section. The material balance equations were based upon absorption factors and as a result, the tray tower was treated as a packed column. A second assumption

made was that the column operated with equimolar overflow and piecewise linear equilibrium.

The full compartment model used the stripping factor for both the rectification and stripping section of the column. In this model, no energy balances were performed or required. The final assumption needed was to assign the condenser and reboiler, as the first and last compartment, as the sensitive stages. Benallon et al. (Benallon et al., 1986) noted that a minimum of two compartments were required to achieve an approximate dynamic model that would match the desired bottoms and distillate compositions. Benallon et al. claimed that their compartmental model showed an adequately close representation of dynamics and initial and final steady state. They mentioned that the system response to changes in feed composition gave good representation of the dynamics and arrive at a proper steady state.

2.2.3.3 Residence Time Contact Model

Morris (Morris, 1980) developed a non-equilibrium model where the mass transfer was modeled by bubbles flowing through a stratified mass of liquid. This semi empirical approach resulted in a residence time model. There were no other authors that had published papers on distillation tower simulators using a similar model.

2.3 Solution Methods

There have been many proposed methods to solve the set of non-linear model equations. These methods can be categorized as follows: 1) simultaneous-correction methods (ex: Newton-Raphson), 2) stage-to-stage methods, 3) equation tearing methods

(ex: tridiagonal matrix method) (Sayama et al. 1990), 4) continuation methods, and 5) collocation methods. The solution methods explanations would also include examples of systems that the authors had solved and compared.

2.3.1 The Simultaneous-correction Methods

The most common example of the class of simultaneous-correction methods was Newton's method. This method was the most widely used method for solving the set of equations that were required to model separation processes. It was also used in equilibrium and non-equilibrium models as well as in steady state and dynamic simulators. Various authors (Landwehr et al., 1992) had mentioned the use of separate techniques to linearize the set of non-linear equations prior to the application of Newton's method.

Kruse et al. (Kruse et al., 1995) had developed a solution method using the Newton-Raphson algorithm to solve for steady-state conditions. These conditions were required as the initial starting point for the dynamic simulation. During each time step of the dynamic simulation, the algorithm used a modified Euler method to transform the differential equations into a new variable vector. These new equations were then treated as above and solved for steady-state. Kruse et al. had used long chain hydrocarbons (C_{10}+) and fatty alcohols (C_{12} +) distillation as a test of their model.

Eckert et al. (Eckert et al., 1995) solved their set of differential and algebraic equations in two steps. The differential equations were solved by a simple Euler integration method and the algebraic equations were solved using an adaptive iteration algorithm based on Newton's method. Eckert and his colleagues had tested two separate systems , the n-butanol-water- n-propanol system and the nitromethane dodecane ethylene glycol system.

Landwehr et al. (Landwehr et al., 1992) used the global Newton-Raphson method to solve the model equations. The Jacobian matrix had a tridiagonal structure, but as side-streams were added and multiple coupled columns were added, the diagonal structure widens. The systems presented in their paper were the butanol-water-butyl acetate and the 2 column plant required for the acetonitrile-acrylonitrile-water system.

Salazar-Sotelo (Salazar-Sotelo, 1992) described a two step solution procedure to solve the set of equations. The first step involved solving the stage to stage liquid-liquid equations. The second step consisted of solving the remainder of the equations by the Naphtali-Sandholm method, which was based upon the Newton method and was applied to the entire block of equations. The only system that was used as a simulation example in his paper was the propanol-butanol-water system.

Cairns and Furzer (Cairns and Furzer, 1990) had employed the Newton-Raphson method to solve for the change in variable values. The Jacobian had been formed by applying the Naphtali-Sandholm technique to the set of equations. In the event that the Newton-Raphson method produced negative mol fractions, these values were reset to a very small positive number such as 10^{-8}. Cairns and Furzer had found that if some of the equations were simplified, then the block equations could be solved by back-substitution using Gaussian elimination. The systems used as examples in their paper were the methanol-acetone-chloroform system and the ethanol-water-2,2,4-Trimethylpentane.

Block and Hegner (Block and Hegner, 1976) had proposed the use of the Newton-Raphson method to solve the set of equations. Their procedure used the liquid compositions as the independent variables . In the procedure, the component mass balance equations were linearized with respect to the liquid compositions. This method was regarded as a bubble point procedure with a block tridiagonal structure instead of the tridiagonal structure. There were three separate process examples illustrated in this paper. The first example was a stripping column with a top separator having a system consisting

of butyl acetate, butyl alcohol and water. The second example was an industrial distillation column used to separate low boiling compounds from a partly miscible mixture. The feed to this column was composed of propanol, butanol and water. The last example was a distillation column with a sidestream phase remover. The component system used in this example was the same as the one in the second example.

Kingsley and Lucia (Kingsley and Lucia, 1988) had modified the Ferraris and Morbidelli method (Ferraris and Morbidelli, 1981). The Ferraris-Morbidelli method used a combination of three different methods, the boiling point type method, the global Newton-Raphson method and the multiflash method. This solution method switched from one method to another in order to optimize the computational time. The only drawback to Kingsley and Lucia's method was that it sometimes required a careful initialization of subproblems. The system tested and used as an example was the ethanol-benzene-water system.

Landwehr et al. (Landwehr et al., 1992) added a step prior to solving the equations by Newton's method. The differential equations were first modified with an implicit Euler method. This technique transformed the differential equations into algebraic equations that could be added to the set of equations that were solved by Newton-Raphson's method. However, when solving for the steady-state, the equations were solved using a modified Gauss algorithm for the mostly tridiagonal matrix, that included additional rows and columns for additional variable vectors. The examples used in this paper were the twelve stage propanol-butanol-water column (to compare results with those of Block and Hegner) and the seven stage butyl acetate-butanol-water column.

Baden and Michelson (Baden and Michelson, 1988) concluded that the Newton-Raphson method was the most effective method for solving non-linear systems of equations used to describe columns with non-ideal stages. This Newton-Raphson method was first applied to the solution of distillation columns by Naphtali and Sandholm. The set

of equations were setup in a block tridiagonal matrix composed of three different blocks that were either full or sparse matrices. The authors also used a block-diagonal Thomas algorithm to modify the set of equations in order to solve them by elimination. There were numerous examples presented in this paper, including a deethanizer, a debutanizer, extractive distillation columns, a conventional benzene-ethanol-water azeotropic distillation column, and a methanol hydrogen sulfide distillation column.

Heh et al. (Heh et al., 1987) developed a unique solution algorithm which combined the steepest descent method with the global Newton's method that is able to predict three phase patterns, to be computationally efficient and rapidly convergent. This solution procedure was used to solve the material balance, energy balance and the enthalpy balance equations. Heh and his colleagues used the n-propanol, n-butanol, water system and the acrylonitrile, acetonitrile, water systems as examples to demonstrate their new solution technique.

2.3.2 The Stage-to-stage Method

The stage-to-stage method solved the system either from the reboiler to the condenser or from the condenser to the reboiler. Many of the proposed algorithms performed the necessary flash calculations stage to stage, back and forth until convergence was reached. Other algorithms only solve the system unidirectionally, either from top to bottom or vice versa.

Liu et al. (Liu et al., 1993) carried out a three phase isenthalpic flash for each stage from the condenser to the reboiler. The algorithm required that values for the reflux ratio, distillate or bottoms flowrate, the feed conditions, and the number of theoretical stages be specified. Prior to the stage-to-stage flash calculations, initial estimates were required for the vapour and liquid flowrates, the vapour and overall liquid compositions, and the

temperature of all stages. These were determined by initially solving the steady state balance equations. Convergence was achieved once the various criteria were met. The system that was used in their work was the benzene-ethanol-water system.

Sayama et al. (Sayama et al., 1990) also proposed an algorithm that solved the problem stage-by-stage. Within their algorithm, a Gauss-Newton method was employed to solve for a vector representing the change in mol fraction. Sayama and his colleagues had tested ten different systems, where each system was composed of either three components or four components. These were the following components used: acetone, acetonitrile, water, furfural, methanol, ethanol, methyl acetate, ethyl acetate, butyl acetate, chloroform, propanol and butanol.

2.3.3 The Equation Tearing Method

The equation tearing method was a solution procedure that included the sum-rates and the bubble point methods (Taylor and Lucia, 1995). These methods make use of two loops, where the outer loop solved a part of the system of equations, and the inner loop solved the remaining set of equations. For example, the sum-rates method simultaneously solved the phase equilibrium equations and the mass balance for the flowrates and set the column pressure profile and the column temperature profile all in the inner loop. The outer loop was used to solve the energy equations in order to adjust the temperature profile (Taylor and Lucia, 1995).

Grottoli et al. (Grottoli et al., 1991) presented a tearing method to solve the block of equations for their actual stage column simulator. Their outer loop solved the balance equations, mass efficiency, equilibrium equations, stoichiometric equations, enthalpy balance equations, and the thermal efficiencies. The inner loop was used to solve the

mass transfer efficiencies and the thermal efficiencies by the Newton-Raphson method. Grottoli had used a benzene and hydrocarbon oil system for their simulations.

2.3.4 The Continuation Method

The homotopy or continuation method had been investigated as a separate way to solve difficult distillation simulation problems. Taylor and Lucia (Taylor and Lucia, 1995) claim that the homotopy method would succeed when the Newton method failed. The method consisted of transforming an easily solved problem through "parameterization" into a problem that would be solved. The first step would be to start with a problem that was dimensionally similar to the original problem that could be easily solved or already had a known solution. This meant that the new problem would be transformed by the "parameterization" of the original solution, and that the parameter's value would change from an initial value to a final value. This in turn generated a path by transforming the solution roots of the new problem to the solution roots of the original problem.

Vickery and Taylor (Vickery and Taylor, 1986) had indicated that the Newton homotopy was very easy to implement in their original code but was not the most reliable method to use. Vickery and Taylor developed a thermodynamic homotopy method that was superior to the Newton homotopy because their method removed the thermodynamics non-linearities of the original system. The authors do mention that the Newton homotopy should be used first and if it fails then one should switch to their thermodynamic homotopy. The systems that they tested were the methanol-acetone-water-ethanol, ethanol- t-butanol-water, water-acetone-furfural, methanol-ethanol-water, and methanol-acetone-chloroform mixtures.

2.3.5 The Collocation Method

There has been a very limited amount of work done with the collocation method. The few individuals (Carta et al. (1995) and Stewart et al. (1985)) that utilized this method have done so to solve the equilibrium stage problem, both in steady-state and dynamic simulations. They had noted that this particular method was useful for problems involving sets of partial differential equations (Taylor and Lucia, 1995). The systems tested by Carta et al. (Carta et al., 1995) and Stewart et al. (Stewart et al. 1985) were the methane-ethane-propane-butane-pentane-hexane mixture, and the methanol-ethanol-water mixture.

2.3.6 The Numerical Integration and Differentiation Methods

There were several other techniques that had been proposed as solution techniques to solve the set of equations for the distillation process. These methods included numerical integration and differentiation.

Wong et al. (Wong et al., 1991) used a semi-implicit Runge-Kutta technique to integrate their system. As long as assumptions, dealing mainly with the Francis weir formula, were met the procedure was applicable. The only system presented in their paper was the ethanol-benzene-water system, which was thoroughly tested.

Benallon et al. (Benallon et al., 1986) solved their compartmental model by finite difference. They had noted that their results were in agreement with the compartmental based techniques. The initial and final steady states were identical in both the compartmental and collocation methods.

Summary

An extensive literature search was performed in order to find what work has been done on the subject of the dynamic simulation of three phase separators. A result of this search revealed that little work has been done on the subject of the dynamic simulation of three phase separators. The search was then changed to the subject of the simulation of distillation towers. This subject has been extensively explored.

Many models were developed in order to describe various distillation towers. The equilibrium model was the first model to be developed. This model consisted of mass and energy balances, summation equations and equilibrium relations. The major assumption of this model was that the exiting streams were in equilibrium with each other. Many have then introduced an efficiency factor to the model in order to compensate for the incomplete approach to thermodynamic equilibrium. In an attempt to avoid arbitrary efficiency factors, engineers decided to try to predict mass and energy transfer. As a result the nonequilibrium model was developed. This model is simply the equilibrium model with the addition of mass and energy transfer calculations. Other models developed were the collocation model, the compartmental model and the residence time contact model.

The literature search also revealed the various solution methods used to solve the model equations. There were six main solution methods described. The different solution methods were the simultaneous-correction method, the stage-to-stage method, the equation tearing method, the collocation method, the continuation method, and the numerical integration and differentiation method.

Chapter 3- Available Model

As with all chemical engineering simulators, a mathematical model describing the unit operation to be simulated must first be developed. A literature survey was accomplished in order to investigate the work done on the subject of dynamic simulation of separation equipment. Little work has been performed in the field of three phase separators, therefore, the literature survey focused upon distillation towers. The literature survey allowed the author to choose an appropriate mathematical model that can be easily adapted for the purpose of this work. This chapter will present the chosen model.

3.1 The Separator Model

The result of the literature survey indicated that the Lao and Taylor (Lao and Taylor, 1994) model was the most suitable model for this thesis. However, it must be appropriately modified in order to correctly model the three phase separator. This chapter will discuss the modification of the Lao and Taylor model and its use in developing a dynamic model for a three phase separator.

3.2 Lao and Taylor Model

The purpose of this model was to simulate a non-equilibrium three phase distillation column stage, and combine the stage model to simulate trayed distillation column dynamic behaviour. Figure 3.1 displays an ideal vapour-liquid-liquid distillation tray that is the basis of Taylor's model. The interfaces account for mass transfer and heat transfer between the phases.

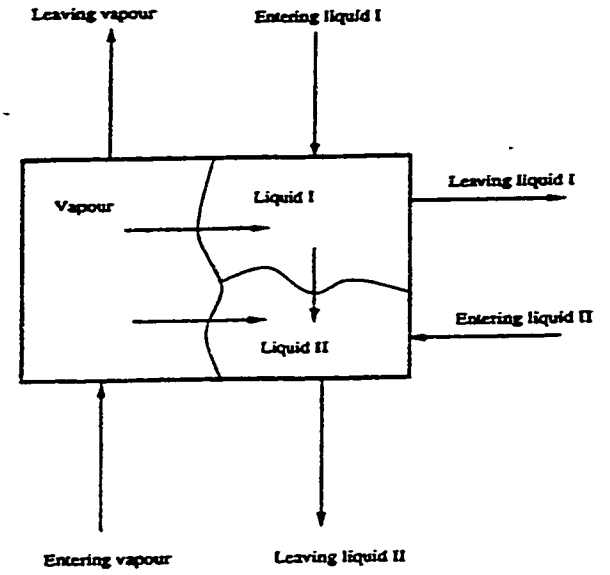

Figure 3.1 Schematic diagram of a nonequilibrium stage for three phase distillation. (Lao and Taylor, 1994, p. 2640)

3.2.1 Model Equations

The model equations used are the material (individual and overall) and energy balances, mass and energy transfer rate equations, and the equilibrium relations. For the material balances, the equations account for transfer from one phase to all the others plus material balances for the phase interfaces. The energy balance equations account for each phase. Any energy changes associated with mass transfer between the stages, and for any energy transfer across the phase boundaries are included in these equations. The mass and energy transfer rates (the fluxes) depend upon how far the phases are from equilibrium (driving force). The rate equations are a function of concentration and temperature differences. Lao and Taylor use both the convective and diffusive contributions to the mass transfer rate equations. The equations are solved using the solutions of the generalized Maxwell-Stefan equations. (Lao and Taylor, 1994) The driving force of the mass transfer rate is the difference in composition between the bulk value and the interface

value. The other equations that are necessary in this model are the interface model equations. These equations are simply the difference between the composition of one phase and the equilibrium ratio and phase composition product of the other phase, for example:

$$K_{ij}x_{ij} - y_{ij} = 0 \qquad (3.1)$$

The major assumption made in the Taylor stage model is that the interface offers no resistance to mass transfer. It is the interface compositions that are in equilibrium, not the bulk compositions.

The remaining equations that are necessary to complete this model are the summation equations that force the composition summation to reach a value of 1.0 for each of the phases present in the stage.

3.2.2 Vapour and Liquid Flow Models

Lao and Taylor (Lao and Taylor, 1994) have developed several vapour and liquid flow models to more accurately simulate the hydrodynamics of a distillation stage. They have proposed four different models: the homogeneous liquid model, the segregated liquid model, the stratified liquid model and finally the dispersed liquid model. Figures 3.2 to 3.4 displays the latter three flow models.

The homogeneous liquid model assumes that both liquid phases behave as a single phase. In this way a two phase theoretical stage model can be adapted to a three phase model as long as it uses the combined phase flow rates and average physical properties (Lao and Taylor, 1994). This model is too simplistic for a three phase system but it is a starting point from which the model could be expanded and improved.

The segregated liquid model (Figure 3.2) assumes that the vapour rises through the liquids in plug flow, as though the liquid phases are separated horizontally (in parallel) , not being in contact with each other. This model also assumes that each liquid phase is well mixed. This segregation of the liquid phases would mean that there is no mass transfer between the two liquids. This model is not valid because it is very unlikely that the phases would ever reach equilibrium. The variables x and y represent the bulk phase compositions. The subscripts i and j indicate the component index and the stage numbering, respectively.

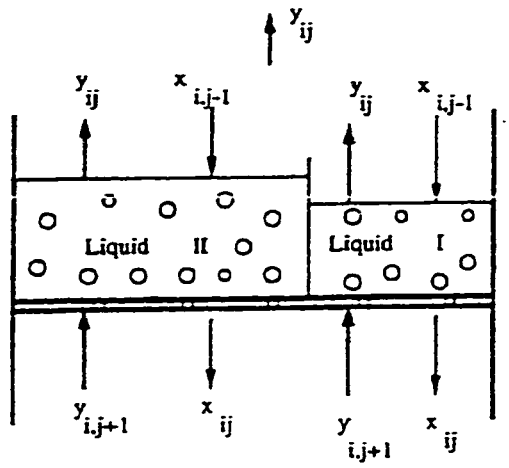

Figure 3.2 Schematic diagram of the segregated liquid model.

(Lao and Taylor, 1994, p. 2643)

The stratified liquid model is more appropriate for Lao and Taylor's model (Lao and Taylor, 1994) than the previous two models. In Lao and Taylor's model, it is assumed that the vapour rises through each of the liquid phases, one by one (Figure 3.3). However, this model would not allow significant mass transfer to occur between the two liquid phases because of their limited contact area.

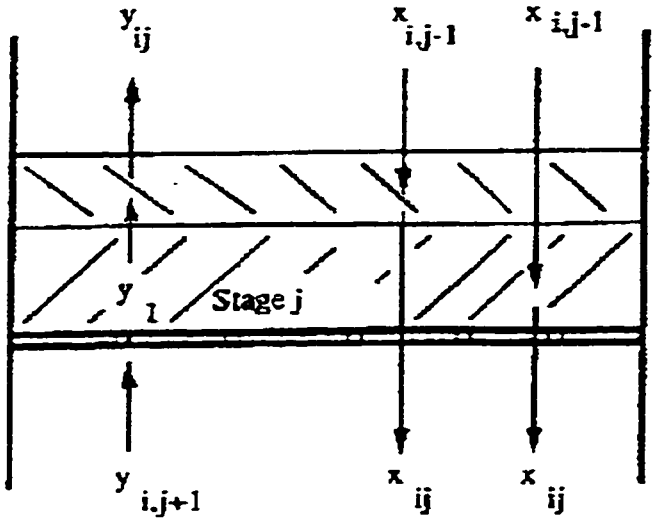

Figure 3.3 Schematic diagram of the stratified liquid model.

(Lao and Taylor, 1994, p. 2644)

The dispersed liquid model is considered the most realistic of the four models (Figure 3.4). The drawback to this liquid flow model is that the liquid-liquid mass transfer coefficients must be determined. It is assumed that one liquid phase is fully dispersed throughout the other; it is only the continuous phase that actually comes into contact with the vapour phase.

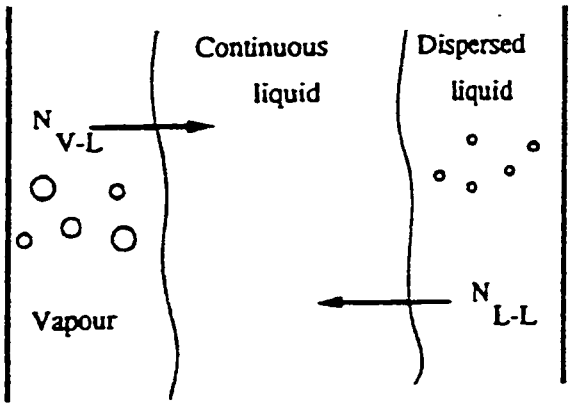

Figure 3.4 Schematic diagram of the dispersed liquid model.

(Lao and Taylor, 1994, p. 2644)

3.3 Solution Procedure

The dispersed liquid stage model has been developed for a single stage of a distillation tower. The advantage of this model is that there is no need for prior knowledge of the number of phases present on the tray of interest. The use of a thermodynamic model that performs a liquid phase stability test is used to determine the number of phases present. As a result, this solution procedure can be applied to a multi-stage tower when the algorithm solves the system stage by stage. Figure 3.5 outlines this solution procedure (Lao and Taylor, 1994). Model I represents the homogenous liquid model. Models II, III, and IV represents the segregated, stratified and dispersed liquid flow model, respectively.

Summary

The Lao and Taylor model offers the most adaptable model for a 3 phase separator. The equations consist of mass and energy balances, mass and energy transfer rate equations, and the equilibrium relations. The stratified liquid flow model combined with modified versions of the above equations would be best suited for this work.

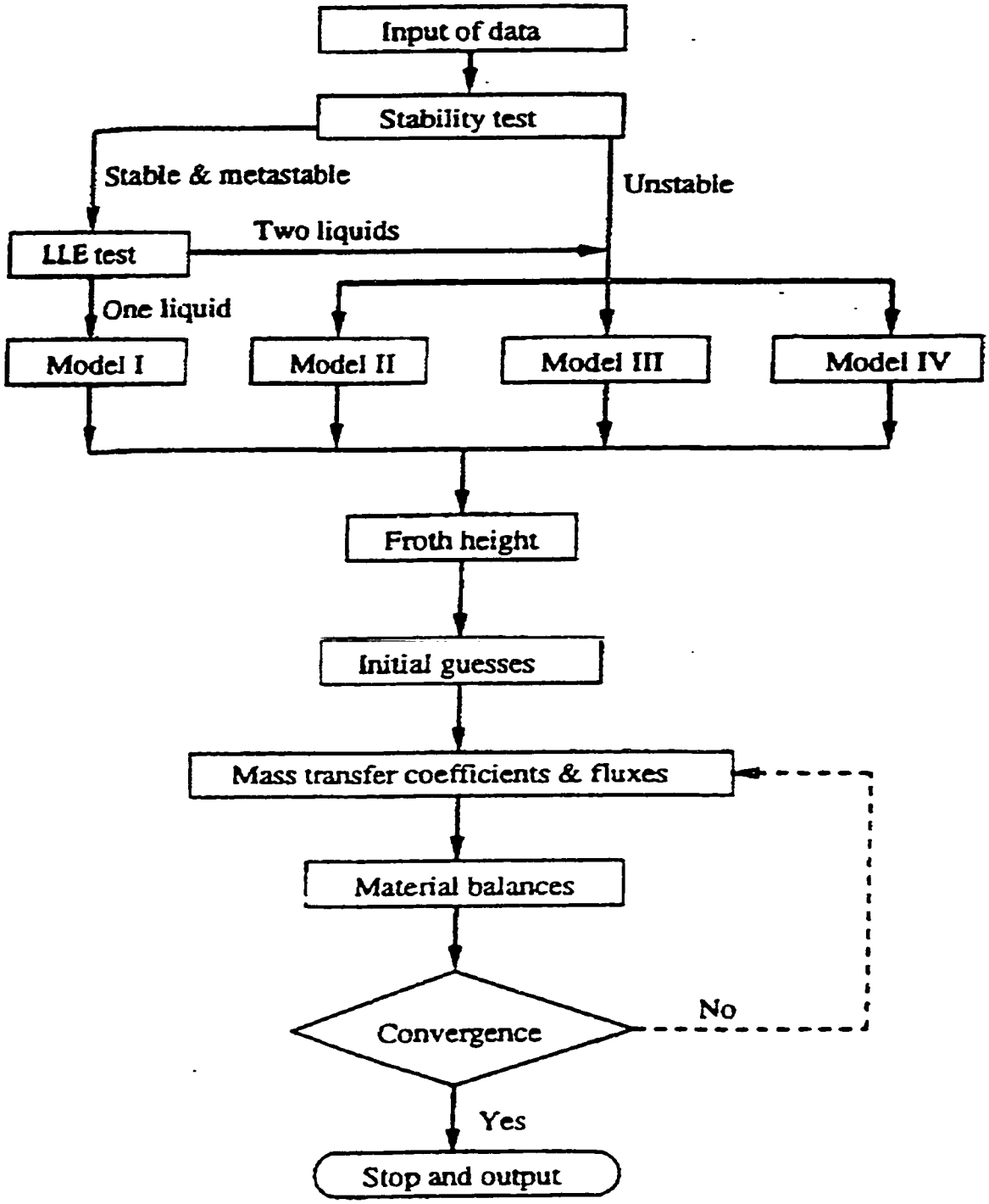

Figure 3.5 Outline of computational procedure.

(Lao and Taylor, 1994, p. 2645)

Chapter 4- Model Development

A mathematical model has been chosen for the purpose of simulating a three phase separator. The chosen model was originally used for simulating a tray of a distillation column by Lao and Taylor (Lao and Taylor, 1994). The Lao and Taylor model was chosen because Taylor and his colleagues are the leaders in the field of the three phase nonequilibrium distillation stage model. This chosen model must be modified in order to adapt it for the purpose of the three phase separator. This chapter is devoted to the development of the three phase separator model.

4.1 Three Phase Separator Model

The model equations have been taken from Taylor's model (Lao and Taylor, 1994). The equations required to describe the system include individual mass balances, total material and energy balances, summation equations (as a check), change of composition equations, and mass transfer equations. The model has been modified to include capability for multiple phases, multiple components, an energy stream into and/or out of the separator. Lao and Taylor's dispersed liquid model (Figure 3.4) will be used for this work. The model requires the liquid-liquid mass transfer coefficients be determined and this will be performed through the use of mass transfer correlations (refer to section 4.2.5) by Xu and Shen (Xu and Shen, 1992). The only modification made to the liquid flow model was that there was a very minimal contact between the vapour and the heavy liquid phase, thus, no mass transfer would occur between these two phases. As a result, necessary changes would be made to the associated model equations to adapt it to the

separator model. The modifications included removing any mass transfer between the vapour phase and the heavy liquid phase with the exception of any condensation or vapourization that might occur.

4.2 Model and Equations

An example of a three phase separator can be found in Figure 4.1. This form of the three phase separator is designated a "bucket and weir" separator. The weirs are designed to control the liquid flowrate and the buckets are used for appropriate holdup and surge times.

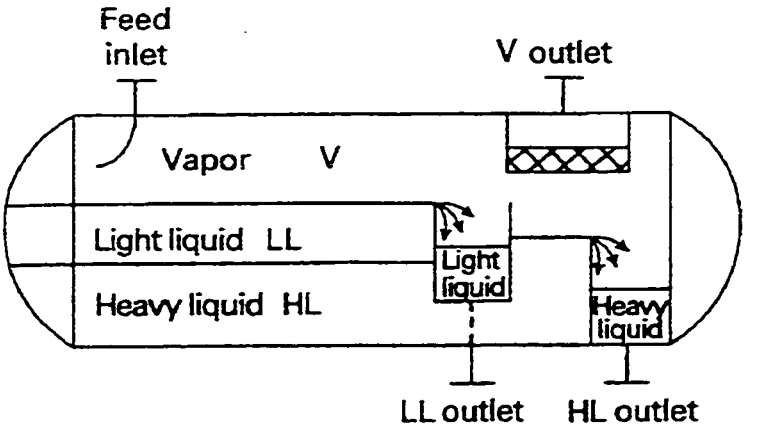

Figure 4.1 Diagram of a horizontal weir and bucket three phase separator.

(Monnery and Svrcek, 1994, p. 31)

By referring to Figure 4.2 a representation of a 3 phase non-equilibrium stage, the mass and energy balances for non-steady state are:

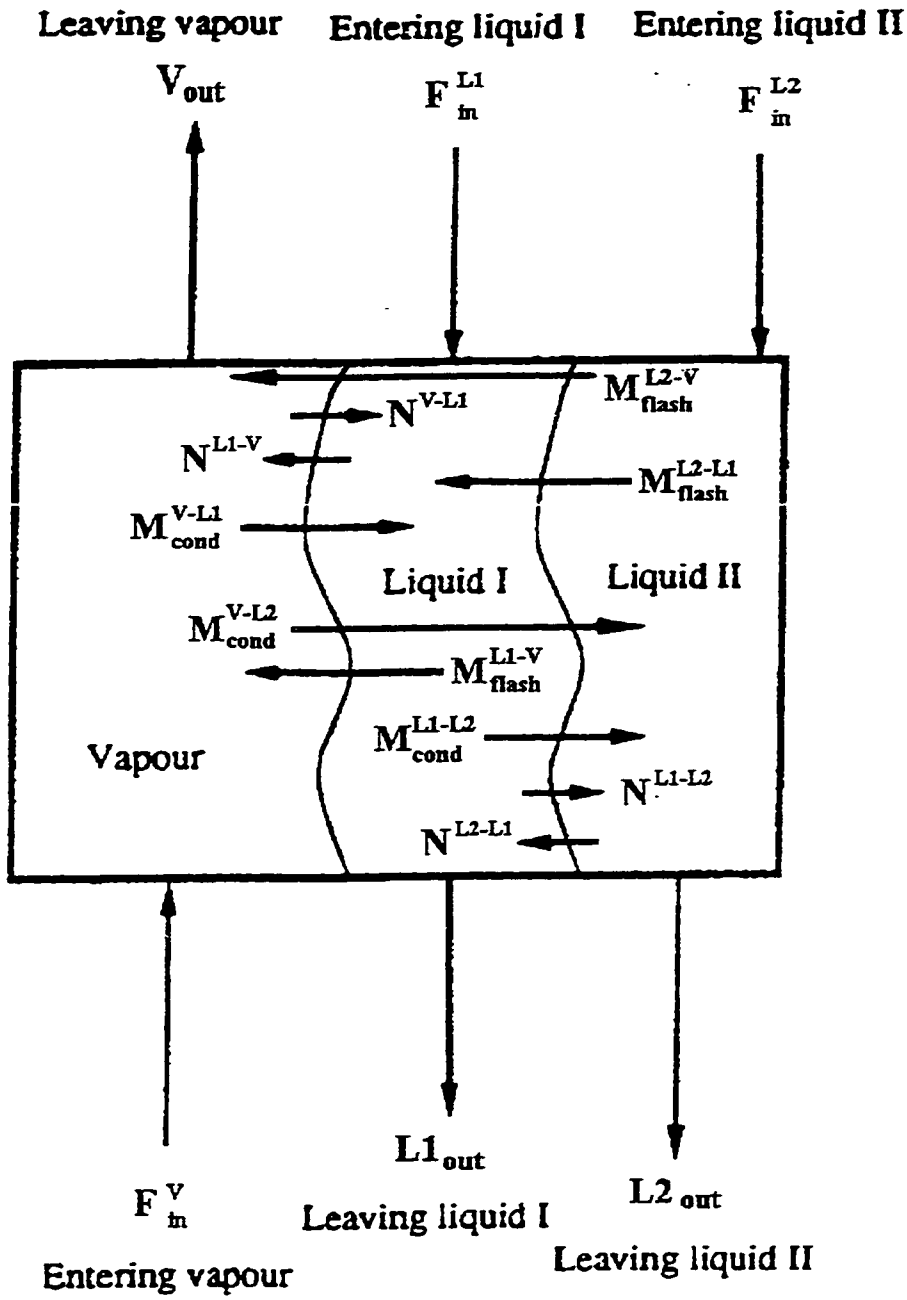

Figure 4.2 Diagram of the modified nonequilibrium stage for the three phase separator.

The model equations are listed as the following:

4.2.1 Overall Mass Balances

$$\frac{d(HV)}{dt} = F^{v} - V - N_t^{V-L'} + N_t^{L'-V} + M_{tflash}^{'-V} + M_{tflash}^{''-V} - M_{tcond}^{V-'} - M_{tcond}^{V-''} \quad (4.1)$$

$$\frac{d(HL')}{dt} = F' - L' + N_t^{V-L'} - N_t^{L'-L''} + N_t^{L''-L'} - N_t^{L'-V} + M_{tcond}^{V-'} - M_{tcond}^{'-''} + M_{tflash}^{''-'} - M_{tflash}^{'-V} \quad (4.2)$$

$$\frac{d(HL'')}{dt} = F'' - L'' + N_t^{L'-L''} - N_t^{L''-L'} + M_{tcond}^{V-''} + M_{tcond}^{'-''} - M_{tflash}^{''-'} - M_{tflash}^{''-V} \quad (4.3)$$

4.2.2 Individual Mass Balances

$$\frac{d(HVi)}{dt} = z_i^{V} F^{V} - y_i V - N_i^{V-L'} + N_i^{L'-V} + M_{iflash}^{'-V} + M_{iflash}^{''-V} - M_{icond}^{V-'} - M_{icond}^{V-''} \quad (4.4)$$

$$\frac{d(HL_i')}{dt} = z_i' F' - x_i' L' + N_i^{V-L'} - N_i^{L'-L''} + N_i^{L''-L'} - N_i^{L'-V} + M_{icond}^{V-'} - M_{icond}^{'-''} + M_{iflash}^{''-'} - M_{iflash}^{'-V} \quad (4.5)$$

$$\frac{d(HL_i'')}{dt} = z_i'' F'' - x_i'' L'' + N_i^{L'-L''} - N_i^{L''-L'} + M_{icond}^{V-''} + M_{icond}^{'-''} - M_{iflash}^{''-'} - M_{iflash}^{''-V} \quad (4.6)$$

4.2.3 Enthalpy/Energy balances

$$\frac{d(E^{HV})}{dt} = H^{F^V} F^V - H^{U^V} V - H^{U^V} N_t^{V-L'} + H^{U^{L'}} N_t^{L'-V} + H^{U^{L'}} M_{tflash}^{'-V} + H^{U^{L^*}} M_{tflash}^{*-V}$$
$$- H^{U^V} M_{tcond}^{V-'} - H^{U^V} M_{tcond}^{V-*} - ha_V (T_1 - T_2) \qquad (4.7)$$

where $E^{HV} = H^{HV} HV$

$$\frac{d(E^{HL'})}{dt} = H^{F'} F' - H^{L'} L' + H^{U^V} N_t^{V-L'} - H^{U^{L'}} N_t^{L'-L^*} + H^{U^{L^*}} N_t^{L^*-L'} - H^{U^{L'}} N_t^{L'-V}$$
$$+ H^{U^V} M_{tcond}^{V-'} - H^{U^{L'}} M_{tcond}^{'-*} + H^{U^{L'}} M_{tflash}^{'-'} - H^{U^{L'}} M_{tflash}^{'-V} + ha_V (T_1 - T_2) \qquad (4.8)$$
$$- ha_{L'} (T_2 - T_3)$$

$$\frac{d(E^{HL^*})}{dt} = H^{F^*} F'' - H^{L^*} L'' + H^{U^{L'}} N_t^{L'-L^*} - H^{U^{L^*}} N_t^{L^*-L'} + H^{U^V} M_{tcond}^{V-*}$$
$$+ H^{U^{L'}} M_{tcond}^{'-*} - H^{U^{L^*}} M_{tflash}^{*-'} - H^{U^{L^*}} M_{tflash}^{*-V} + ha_{L'} (T_2 - T_3) \qquad (4.9)$$

Depending upon the quantity of material that is transferred across the various interfaces, the energy associated with it could be negligible; thus, reducing the number of terms in equations 4.7 to 4.9.

The variable N is the interphase mass transfer rate. The superscript signifies the direction in which the transfer occurs. For example, V-L1 signifies the mass transfer that occurs from the vapour phase to the light liquid phase. The subscript L2-L1 represents the mass transfer from the heavy liquid phase to the light liquid phase.

The variable M represents any mass transfer that occurs due to either evaporation or condensation. The associated superscript was the same as those for the mass transfer variable N. The subscript *t* signifies the total overall transfer of all the components. The

subscript *cond* signifies any mass that condensed from the vapour phase to either liquid phases or from the light liquid phase to the heavy liquid phase. The subscript *flash* represent any mass that evaporate from either liquid phase to the vapour phase or the heavy liquid phase that changes density and transfers to the light liquid phase.

4.2.4 Change of Composition

The composition can be thought of as a fraction of a holdup, thus, a part of the total holdup or change in holdup divided by the total holdup, as seen below. The variables HV, HL' and HL" are the molar holdups of the vapour phase, light liquid and heavy liquid phase, respectively.

$$\frac{dy_i}{dt} = \frac{d(HV_i)}{dt} * \frac{1}{HV_t} \quad \text{or} \quad y_i = \frac{HV_i}{HV_t} \tag{4.10}$$

$$\frac{dx_i'}{dt} = \frac{d(HL_i')}{dt} * \frac{1}{HL_t'} \quad \text{or} \quad x_i' = \frac{HL'_i}{HL'_t} \tag{4.11}$$

$$\frac{dx_i''}{dt} = \frac{d(HL_i'')}{dt} * \frac{1}{HL_t''} \quad \text{or} \quad x_i'' = \frac{HL''_i}{HL''_t} \tag{4.12}$$

4.2.5 Mass transfer coefficients

A mass transfer coefficient correlation (Xu and Shen, 1992) found in the literature will be used. This correlation calculates the coefficient-interfacial area product and is suited for a fractionating column but can be applied to the separator. The equations used are the following:

$$k^L a = D_L^{0.5}\rho_L[(0.32 - 1.34E - 3(\frac{\Delta\sigma}{\Delta x})) + 50L] * 10^{-3} \text{ mol/s} \quad (4.13)$$

where $\frac{\Delta\sigma}{\Delta x}$ = average surface tension gradient

$$k^V a = D_V^{0.5}[0.7 + 71.42 + f(\frac{\Delta\sigma}{\Delta x}))Fa] * 10^{-3} \text{ mol/s} \quad (4.14)$$

where $f(\frac{\Delta\sigma}{\Delta x})$ depends upon the type of surface tensions whether negative or positive systems. The variable *ka* is the individual mass transfer coefficient interfacial area product. D is the diffusivity coefficient. The variable ρ is the bulk phase density. The variable E is the energy balance function or the differential term of the change in energy holdup of a phase. The term $\frac{\Delta\sigma}{\Delta x}$ is the average surface tension gradient. L is the total liquid flowrate. The superscripts L and V are the liquid phase and vapour phase designation. Fa is the F-factor which is determined by the product of gas flowrate through a unit separator cross section and the square root of the gas density.

In Xu and Shen's work, the $k^L a$ and $k^V a$ variables are the binary mass transfer coefficients-interfacial area products. This work uses multicomponent mixtures, therefore, the multicomponent mass transfer coefficients-interfacial area products are required.

The first step in calculating the multicomponent gas phase products $k^V a$ is to determine the gas binary pair diffusivity coefficients using the Chapman-Enskog prediction. Then the binary coefficients are converted to the effective multicomponent diffusivity coefficients by using the Wilke effective diffusivity equation (equation 4.15). These effective multicomponent diffusivity coefficients are fed to equation 4.14 in order to obtain the multicomponent gas phase products.

$$D_{AM} = \frac{1 - y_A}{\sum_{\substack{i=1 \\ i \neq A}}^{n+1} \left(\frac{y_i}{D_{Ai}} \right)} \tag{4.15}$$

The primary step in obtaining the multicomponent liquid phase products k^La is to estimate the liquid binary pair diffusivity coefficients at infinite dilution. This was performed by using a correlation (equation 4.16) developed by Wong and Hayduk (Wong and Hayduk, 1990). Using equation 4.17 the liquid binary pair diffusivity coefficients were determined. By applying equation 4.15 to the binary pair diffusivity coefficients, the liquid effective diffusivity coefficients are calculated. Finally the effective diffusivity coefficients are used in equation 4.13 to get the multicomponent liquid phase products k^La.

$$D_{AB}^{o} = 2.77(10^{-3}) \mu_B^{-0.559} \left(\frac{\bar{V}_{CB}}{V_{CA}^{1.59}} \right) \left(M_A M_B^{1.31} \right)^{-0.166} e^{\left(\frac{-685.5}{T} \right)} \tag{4.16}$$

D_{AB}°=diffusivity at infinite dilution in cm^2/s

μ=viscosity in cp

V_c=critical volume in cm^3/mole

M=molecular weight in kg/kgmol

T=temperature in K

$$D_{AB} = \left(D_{AB}^{o} \right)^{x1} \left(D_{BA}^{o} \right)^{x2} \tag{4.17}$$

$x1 = x_B / (x_A + x_B)$

$x2 = 1.0 - x1$

With these individual coefficient -interfacial area products, one can determine the overall mass transfer - interfacial area product by using the following equations :

$$\frac{1}{K_L} = \frac{1}{m'' k_V} + \frac{1}{k_L} \tag{4.18}$$

$$\frac{1}{K_V} = \frac{1}{k_V} + \frac{m'}{k_L} \tag{4.19}$$

where,

$$m' = \frac{y_{ai} - y_a^*}{x_{ai} - x_{aL}} \tag{4.20}$$

$$m'' = \frac{y_{aG} - y_{ai}}{x_a^* - x_{ai}} \tag{4.21}$$

If equimolar counter diffusion is assumed then this value can be substituted into equations 4.22 and 4.23

$$N_V = K_V a(y^* - y_B) \tag{4.22}$$

$$N_L = K_L a(x_B - x^*) \tag{4.23}$$

to find the molar flowrates.

4.2.6 Weir equation

In order to determine the exiting liquid molar flowrates, the weir formula used in the separator model was,

$$F = 3.33 * L * h^{3/2} \tag{4.24}$$

where F=volumetric flowrate ft^3/s

L=weir width ft

h=liquid level over weir height ft.

This equation was changed to,

$$F = \frac{3.33 * L * h^{3/2}}{v} * C \tag{4.25}$$

where C=conversion factor to convert from ft^3/s to m^3/s

v=molar volume $m^3/kmol$

in order to convert F to a molar flowrate in kmol/s.

4.2.7 Thermodynamic Model

The most common thermodynamic models used are the activity coefficient based models such as the UNIQUAC, UNIFAC, and NRTL (Walas, 1985). Lao and Taylor (Lao and Taylor, 1994) used the UNIQUAC model to calculate the activity coefficients in each liquid phase. They also used the UNIFAC model for obtaining missing pairs of UNIQUAC parameters. Krishnamurthy and Taylor (Krishnamurthy and Taylor, 1985) used the UNIQUAC model to determine equilibrium K values and excess enthalpies.

Due to certain factors, the NRTL model was chosen to represent the two mixtures used in the simulations. Walas (Walas, 1985) stated that the NRTL model represented liquid-liquid equilibria and vapour-liquid equilibria of multicomponent mixtures adequately and was often superior to other models for aqueous mixtures. On September, 1997

technical staff at Hyprotech Ltd. suggested to the author to use the NRTL model with the HYCON package (Hyprotech Ltd.) for thermodynamic calculations of the two chosen aqueous mixtures. HYCON's envelope utility produced three phase regions that were easier to find when using the NRTL model.

HYCON (HYSYS-Conceptual Design Application) is a software package, designed by Hyprotech Ltd., that offers state of the art methods of distillation, many electronic databases for thermodynamic equilibrium and thermophysical models, interactive parameter estimation and visualization techniques. The software package is a thermodynamic extension of HYSYS' steady state and dynamic simulators. "It provides an environment for exploration of alternative designs for distillation systems, thermodynamic model behaviour and proper determination and tuning of interaction parameters and physical properties" (HYSYS-Conceptual Design Application reference manual, p.1).

The NRTL or Non-Random-Two-Liquid equation was developed by Renon and Prausnitz (Smith and van Ness, 1985). The associated excess Gibbs free energy equation of multicomponent mixtures and the equation of activity coefficients of multicomponent mixtures will be presented to the reader to clarify the NRTL model. The excess Gibbs free energy equation of binary mixtures is the following:

$$\frac{G^{ex}}{RT} = \sum_i x_i [\sum_j \tau_{ji} G_{ji} x_j / \sum_k G_{ki} x_k]. \qquad (4.26)$$

The NRTL activity coefficient equation of multicomponent mixtures is,

$$\ln(\gamma_i) = \frac{\sum_{j=1}^{m} \tau_{ji} G_{ji} x_j}{\sum_{l=1}^{m} G_{li} x_l} + \sum_{j=1}^{m} \frac{x_j G_{ij}}{\sum_{l=1}^{m} G_{lj} x_l} \left(\tau_{ij} - \frac{\sum_{n=1}^{m} x_n \tau_{nj} G_{nj}}{\sum_{l=1}^{m} G_{lj} x_l} \right) \qquad (4.27)$$

where $_{ji} = \frac{(g_{ji} - g_{ii})}{RT}$ (4.28)

$$G_{ji} = \exp(-\alpha_{ji} \tau_{ji}) \qquad (4.29)$$

$$_{ii} = \tau_{jj} = 0 \quad \text{and} \quad G_{ii} = G_{jj} = 1.$$

The NRTL binary parameters used with the above equations are listed in Tables 4.1-4.4.

τ_{ij}	water	n-propanol	n-butanol
water	0.0000	444.3338	570.1362
n-propanol	1997.5500	0.0000	45.8986
n-butanol	2794.6660	-46.9043	0.0000

Table 4.1 The τ_{ij} binary parameters for water-propanol-butanol

α_{ij}	water	n-propanol	n-butanol
water	0.0000	0.4850	0.4700
n-propanol	0.4850	0.0000	0.3046
n-butanol	0.4700	0.3046	0.0000

Table 4.2 The α_{ij} binary parameters for water-propanol-butanol

τ_{ij}	water	ethanol	benzene
water	0.0000	-109.6339	4843.3760
ethanol	1332.3120	0.0000	991.5067
benzene	3719.3950	334.1524	0.0000

Table 4.3 The τ_{ij} binary parameters for water-ethanol-benzene

α_{ij}	water	ethanol	benzene
water	0.0000	0.3031	0.2000
ethanol	0.3031	0.0000	0.2911
benzene	0.2000	0.2911	0.0000

Table 4.4 The α_{ij} binary parameters for water-ethanol-benzene

4.2.8 Model Assumptions

In order for these equations to be applicable to the separator model, the following assumptions must be made:

1) The separator is always at mechanical equilibrium.

2) All phases are in contact with the exception of the vapour and heavy liquid. This assumption is associated with Lao and Taylor's stratified liquid flow model.

3) Each individual phase is always well mixed, there are no concentration or composition differences along the separator.

4) The mass transfer occurs in equimolar counter diffusion.

5) For mass transfer calculations, the phase with the largest resistance will be the rate determining phase and if the resistance is large enough then the resistance contribution from the other phase can be neglected.

6) The separator will behave like a stage of a distillation tower.

7) No heat loss to the environment (adiabatic system).

8) No entrainment.

4.3 Degrees of Freedom Analysis

In order to determine which variables should be specified before attempting to solve the system, a degrees of freedom analysis is performed on the separator. This particular problem will deal with 3 individual holdups or as many holdups as there are phases present when the feed is flashed. Each holdup within the separator will be considered individually. Figure 4.3 shows the basis for the degree of freedom analysis of the three phase separator.

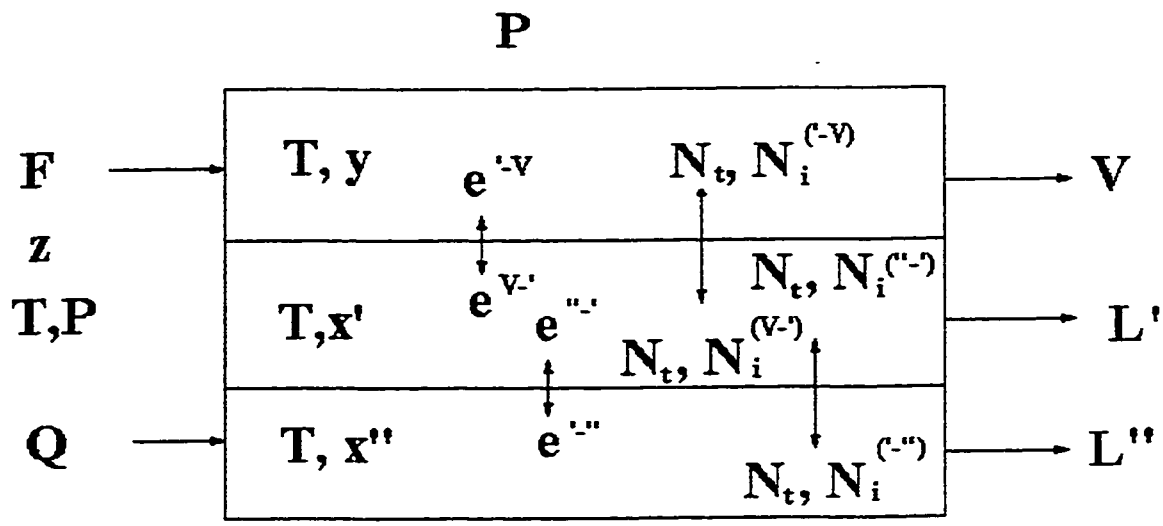

Figure 4.3 Degrees of freedom analysis diagram for the three phase separator

4.3.1 Variables

With the individual holdups taken into account, then the analysis is:

Temperatures	4
Pressures	2
flows	4
Heat input (Q)	1
compositions	4C

molar rates (mass transfer)	4C+4	
energy rates	2	
Number of variables	$N_v = 8C+17$	(4.30)

There are four temperatures available to the model. These include the single temperature of the incoming feed, then three temperatures of the individual phases within the separator. The pressures available are the vessel pressure and the pressure of the feed. There are four flows in the model which includes the feed stream and the three exiting streams. There is only one heat input into the system and that is specified at the head end of the separator. There are four distinct sections of the separator where the compositions can be determined, the feed stream and the three individual separator phases. As there can be C components the total number of variables for the compositions is 4C. The exiting stream compositions will be identical to those found within the separator, and thus are not included in the analysis. As the model has been developed to have only two phase contacts (vapour-liquid1 and liquid1-liquid2), there are two molar rates across each interface; therefore, there are four rates per component and a total of 4C rates for the entire system. There are four more mass transfer rate summation equations that define the total rate across each phase interface. There are two energy rates, one from the vapour to the light liquid and the other from the light liquid to the heavy liquid (these can also signify the reverse).

4.3.2 Equations

Total mass balances	3
component mass balances for each phase	3(C-1)
mass transfer rate equations	4C+6
energy balances	3

energy transfer rate equations	2
Number of equations	$N_E = 7C + 11$

The degrees of freedom would become,

$$N_D = 8C+17-(7C+11)=C+6 \qquad (4.31)$$

The mass transfer rate equations include the summation of the individual component rates ($N_t=\Sigma$ Ni) across the interface. The total mass transfer rates crossing the interface in counter direction must be equal due to the assumption of equimolar counter (ie: $N_t^{v-l}=N_t^{l-v}$). Thus, only one of the total transfer rate is calculated using the correlations and the other transfer rate is set equal to the first.

One would specify the following:

Feed flowrate	1
Feed temperature	1
Feed pressure	1
inlet heat (Q)	1
feed compositions	C
mass transfer rates	2

These specifications would render the system specified. $N_s = C+6$

Therefore, by specifying the feed temperature, pressure, flowrate and compositions and the heat inlet and the mass transfer rates and pressure setpoint, the separator model system is specified and can be solved.

4.4 Energy Input into the Separator

When energy (Q) is added to the separator, this quantity can be lumped with the energy or enthalpy of the feed into the system. In this way, the pressure enthalpy (PH) flash can be used to determine the energy input.

4.5 Solution Method

The dry startup is achieved by first using the PH flash to flash the feed. Next solve the set of equations (equations 4.1 to 4.9) for the change in holdups. Then solve the differentials (equations 4.10 to 4.12) for composition changes and the exiting streams V, L', L". The explicit Euler Integration method is used to solve the set of ordinary differential equations. Using this approach resulted in not requiring initial guesses for most or all of the variables.

The explicit Euler Integration method is described by equations 4.32 to 4.34.

$$\frac{dy_i}{dt} = f(x_{i-1}) \tag{4.32}$$

$$\frac{y_i - y_{i-1}}{\Delta t} = f(x_{i-1}) \tag{4.33}$$

$$y_i = y_{i-1} + \Delta t * f(x_{i-1}) = y_{i-1} + \Delta t * \frac{dy_i}{dt} \tag{4.34}$$

The only data required to solve the next time step variables were the values of the previous step. In this way, there was need for only one set of initial values or initial guesses for all variables at the beginning of the simulation. This solution technique is the most elementary method available and is simple to use (Franks, 1972).

The solution steps taken will be slightly different for the dynamic and shutdown mode. The shutdown mode is the same as the dry startup mode except the feed flowrate will be set to zero.

4.5.1 Solution Steps for the Dry Startup

1) Flash feed to get phase fractions and thermodynamic properties, required for separator design

2) Design separator.

3) Begin the time step.

4) Perform a PH flash on the feed which would give F^{V}, $F^{L'}$, $F^{L''}$ ..... and their compositions and enthalpies. The flash would be performed with the addition of Q (energy into the separator, if applicable).

5) Combine the individual feed streams (F^{V}, $F^{L'}$, $F^{L''}$ .....) and their corresponding energy streams with the appropriate holdups then perform the PH flash in order to get the equilibrium compositions x^{*}.

6) Determine overall mass transfer coefficients

7) Calculate the mass transfer rates.

8) Solve the mass balance equations to get the differentials (change in holdups). Integrate the differentials.

9) With the holdup differentials, calculate the new compositions.

10) Calculate the new liquid heights based on the new volumes.

11) Move to the next time step.

12) Continue steps 1-11 until all differential reach a set point (i.e. 10^{-7}) signifying that steady-state has been reached.

The dynamic scenario will be solved using the above mentioned steps but with minor modifications that account for the disturbance being simulated.

The shutdown will follow the steps outlined above and will be simpler to solve. All equations (algebraic and ODE) that have any variables associated with the feed will be simplified because those variables will no longer be required. As the feed will be set to 0, any other feed information will be neglected such as the feed temperature, pressure, compositions and molar enthalpy. As a result, the differential algebraic equations (DAE) (4.1 to 4.12) will not have as many terms.

4.6 Special Disturbance Consideration

In the event that the disturbance is a change in feed conditions such as superheated or subcooled feed stream, extra terms are required for certain equations. The variables are included in both the mass and energy. This will account for any vapourization or condensation that might occur. In the event of the introduction of a superheated or subcooled feed, the separator will be thermodynamically unstable. As a result, interphase heat flow will direct energy to the appropriate phases. This in turn will tend to equilibrate the phase temperatures. Depending on the feed condition, this change in phase temperature will force either a fraction of the liquid phases to vapourize or a fraction of the vapour phase to condense. This situation will require either heat transfer coefficients or individually setting the values of these interphase heat transfer rates.

In the case of a superheated feed stream, the temperature of the vapour and both of the liquid phases are smaller than that of the feed. This difference in temperature is the driving force for heat transfer from vapour to the light liquid and from the light liquid to the heavy liquid. The extra steps required to solve this problem include calculating the heat transfer rates by either employing heat transfer coefficients or setting these values

manually. This energy transfer is accumulated in changes in the overall energy holdups. Then a stability test and flash will be performed on all of the phases to determine if the vapour phase will partially condense or either of the liquid phases will partially vapourize.

These steps will be repeated for the case of a subcooled feed but obviously the heat transfer will be in the opposite directions than the above case.

An important variable in these simulations is the vessel pressure. This parameter is affected by many other operating parameters and will affect many other variables. Equation 4.35 shows what variables can affect the pressure. This equation is a derivative of the ideal gas law.

$$P = \frac{znRT}{V} \tag{4.35}$$

where z= compressibility factor

n= number of moles in system

R= universal gas constant

T= temperature of system

V= volume occupied by system

There are four variables that can affect the vessel pressure. The first variable is *z*, the compressibility factor. This factor can be determined by the thermodynamic property package used in these simulations. This value did not change significantly during the course of each run.

The second variable *n*, the number of moles in the system, can greatly affect the system pressure. A sudden increase in the number of moles of gas could cause an increase in pressure if the other variables stay reasonably constant. In these simulations, the increase in *n* could be caused by a step increase in vapour feed flowrate or a decrease in the exiting vapour molar flowrate. If the vapour feed increases while the vapour

temperature and volume remain constant, then the separator pressure would increase. As a result, a linear change in n would cause a proportional linear change in pressure.

The vapour temperature would have the same effect upon the pressure as the number of moles of vapour. A rise in vapour phase temperature would cause a rise in vessel pressure.

The pressure is also related to the vapour phase volume. As seen by equation 4.35, a change in the volume would cause a reciprocal effect upon the pressure.

Summary

The model presented by Lao and Taylor (Lao and Taylor, 1994) and Kooijman and Taylor (Kooijman and Taylor, 1995) was chosen and modified to appropriately describe a dynamic three phase separator. The equations involved are the overall and individual mass balances, the energy balances, the composition change equations and the composition summation equations (which are used only as a check). A mass transfer coefficient correlation was used (Xu and Shen, 1992) and modified for the separator model. A few assumptions were made so that Lao and Taylor's model could be applied to the separator model:

- All phases are in contact with the exception of the vapour and heavy liquid. This assumption is associated with Lao and Taylor's stratified liquid flow model.
- The separator will behave like a stage of a distillation tower.

Chapter 5- Results and Discussion

The Lao and Taylor (Lao and Taylor, 1994) mathematical model of a three phase distillation column tray had been modified and adapted to model a three phase separator. The separator was designed by following the steps presented in Monnery and Svrcek's paper (Monnery and Svrcek, 1995). The separator design was based upon the mixtures fed to the unit. The mixtures used in the separator were the water-propanol-butanol mixture and the water-ethanol-benzene mixture.

This chapter will present the experimental results obtained over the course of this work. Section 5.2 covers the effect of various chemical mixtures upon separator design. The results of the effect of a feed flowrate increase and decrease are described in Section 5.3. Finally, the experimental results of the effect of weir width are discussed in Section 5.4.

5.1 Results

The purpose of this work was to see if the data produced by the simulator indicated satisfactory separator behaviour in steady state and during transient periods. Another goal of this work was to see if the separator, once a disturbance was applied, would adequately reach steady state in a realistic manner. The data would show how the separator operating variables behaved during both the steady state and dynamic periods. The variables of most interest are the liquid levels, vessel pressure, and the exiting molar flowrate.

The only disturbances applied to the separator were a feed flowrate increase and a feed flowrate decrease. The magnitude of the disturbance had to be large enough to produce noticeable dynamic behaviour. The feed step increase was chosen at about 52%, and the feed step decrease was chosen at about 48%.

In order to simulate the most important operating scenarios, the following tests were performed:

1) dry startup

2) feed step changes (increase/decrease)

3) shutdown.

The run numbers and associated system running conditions are summarized in Table 5.1. The mixture used for Run # 1 was the water-ethanol-benzene mixture, and the remaining 4 Runs used the water-propanol-butanol chemical systems. These two different chemical systems were chosen because their associated three phase regions were easy to find.

Vessel parameters							
Run #	case	Feed flowrate	Temperature	Pressure	Weir width		System *
		(kmol/hr)	(K)	(kPa)	LL (cm)	HL (cm)	
1	S1	2300.0	346.50	140.0	202.83	223.98	WEB
2	S2	2300.0	378.90	176.0	206.15	229.76	WPB
3	w1.0	2300.0	378.90	176.0	206.15	229.76	WPB
4	w0.5	2300.0	378.90	176.0	103.08	114.88	WPB
5	w0.2	2300.0	378.90	176.0	41.23	45.95	WPB
* WEB water-ethanol-benzene Run 2 (case S2) is identical to Run 3 (w1.0) WPB water-propanol-butanol							

Table 5.1 Various runs performed

This chapter will demonstrate the following results:

1) Effects of various chemical systems on separator design

2) Effect of feed flowrate change upon vessel pressure,
temperature,
liquid heights,
exiting molar flowrate

3) Effect of weir width upon vessel pressure
temperature
liquid heights
exiting molar flowrate

The step disturbances in feed flowrate consisted of an increase to 152% of the original feed and secondly a decrease to 52% of the original feed flowrate of 2300 kmol/hr. The next set of disturbances involved changing the weir length from its original length to 0.5 of the original length then further reducing it to 0.2 of the original length. The property package chosen for the 2 mixtures was the NRTL-ideal, because the NRTL (activity coefficient) thermodynamic package predicts aqueous solutions with greater accuracy than certain other packages such as the equation of state Peng-Robinson.

For reference purposes, Appendix B contains two graphs demonstrating the residue curve maps of both chemical mixtures. The maps for the water-propanol-butanol mixture was determined at 176 °C and the water-ethanol-benzene mixture at 140 °C. By choosing the feed composition that pinpoints the feed mixture within the two liquid

mixture was determined at 176 °C and the water-ethanol-benzene mixture at 140 °C. By choosing the feed composition that pinpoints the feed mixture within the two liquid region, a three phase region could then be determined by varying the temperature of the mixture.

Table A.1 (Appendix A) is a tabular example of the results obtained from Run 3 (case w1.0) performed by the simulator in order to cover all of the operation scenarios.

5.2 Effects of Various Chemical Mixtures on Separator Design

There were two mixtures chosen for the simulations. The varying thermodynamic properties associated with these mixtures produced changes in the overall physical dimensions of the separator. The variables which have the greatest effect upon separator design (physical dimensions) are the phase fraction and total feed flowrate. Table 5.2 presents the physical dimensions of the two separators required for the water-ethanol-benzene mixture and the water-propanol-butanol mixture. Figure 4.1 shows a two dimensional representation of the horizontal separator being simulated.

	System*	
Parameter	WEB	WPB
Diameter (cm)	229.68	235.25
Total length (cm)	926.99	974.84
LL weir height (cm)	168.72	174.29
HL weir height (cm)	89.42	92.37
LL weir width (cm)	202.83	206.15
HL weir width (cm)	223.98	229.76
Surface Area (m^2)	83.46	89.43

* WEB = water-ethanol-benzene
WPB = water-propanol-butanol

Table 5.2 Separator dimensions

Table 5.2 shows that the designed separators are similar due to the fact that the two chosen aqueous mixtures are very similar.

5.3 Effect of a Feed Flowrate Increase and Decrease

Runs number one and two were performed to compare results obtained from the two different mixtures. As noted previously, the simulations were broken down into three groups: the dry startup, the feed increase or decrease and the shutdown.

Figure 5.1 shows the pressure and liquid heights time response of the dry start-up of the water-ethanol-benzene mixture. As the separator was being filled, the liquid levels were increasing, causing the available vapour volume (or molar holdup) to decrease, thus, forcing the pressure to increase. At time $t \approx 2$ min, the pressure peaked at 141.56 kPa due to the pressure control of the vapour outlet. This valve insured that the pressure does not spike possibly causing vessel damage. At approximately 11 minutes the heavy liquid level reached the height of the weir and this liquid height leveled off to the liquid height of 91.5 cm. At about this time the rate of increase of the light liquid decreased to almost a linear rate and the pressure decreased to a value of about 140.3 kPa. At about 54 minutes, the light liquid height reached the weir height and began to overflow, leveling off at 170.0 cm. The pressure's response to the leveling of the light liquid height was to finally decrease to the pressure setpoint of 140 kPa. Note that this small pressure variation would not be measurable by typical process instrumentation.

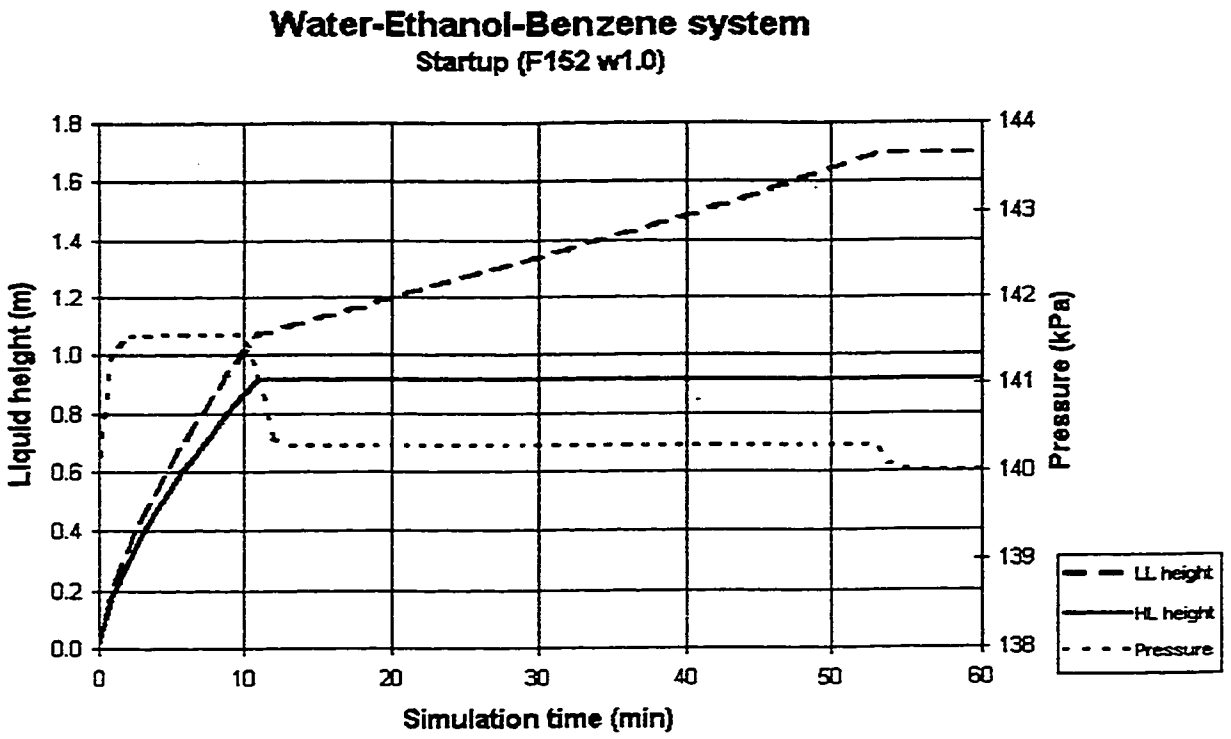

Figure 5.1 Pressure and Liquid Height-Time profile for Run#1 Dry Startup

Figure 5.2 shows the change in temperature during the startup. The changes in the vapour and light liquid phase properties can be attributed to minor changes in thermodynamic property calculations. These changes in temperature were very minimal and thus can be neglected.

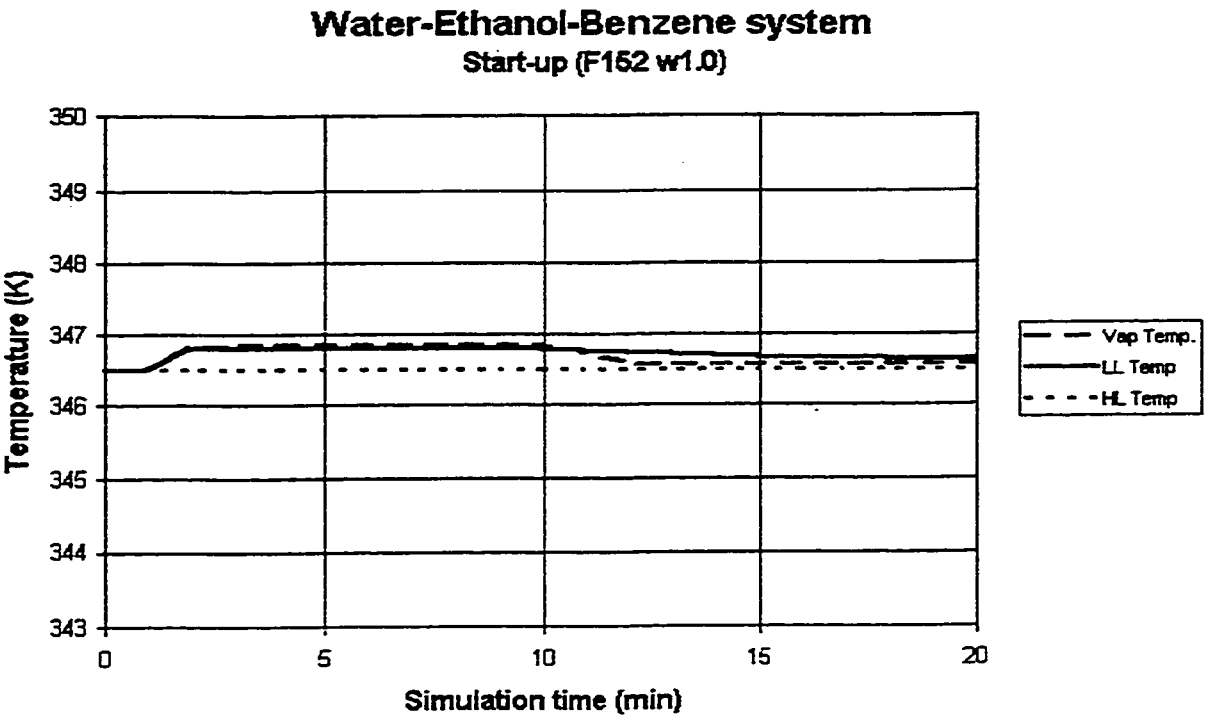

Figure 5.2 Temperature-Time profile for Run#1 Dry Startup

Figure 5.3 shows the changes in the exiting phase flowrates with time. From time 0 to about 14 minutes, there was a noticeable increase in the vapour outlet flow in response to the increase in pressure. The flowrate leveled off to 0.063 kmol/s. At t=15 min, the flowrate slowly decreased to 0.062 kmol/s (associated pressure of 140.3 kPa).

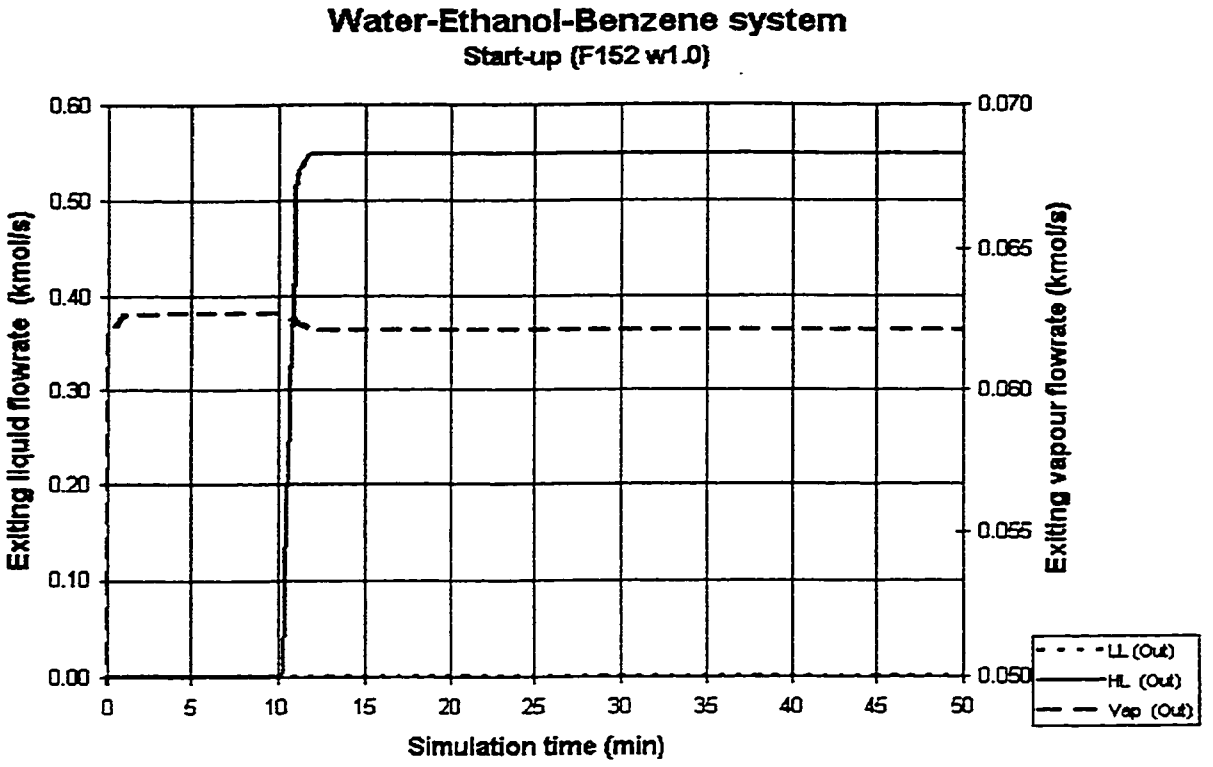

Figure 5.3 Exiting Molar Flowrate-Time profile for Run#1 Dry Startup

5.3.2 Run # 1 Feed Flowrate Increase

A step disturbance of 152% of the original feed flowrate was introduced to the separator. The pressure and liquid head response to the step change in feed flowrate can be seen in Figure 5.4. The liquid head that is shown in the following graphs signifies the liquid level that is above its corresponding weir height. With an increase in feed flowrate, one would expect an increase in vessel pressure until the separator adapts to the new flowrate by increasing all of the exiting flowrates. In this run the pressure was constant.

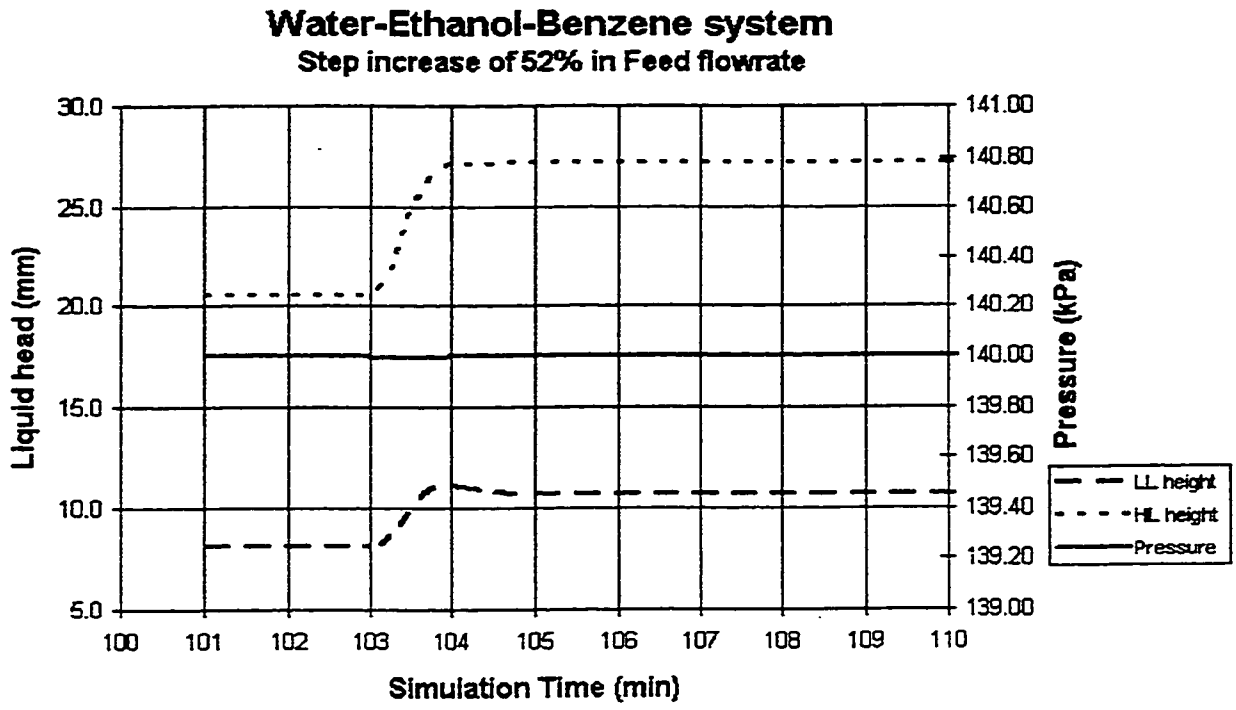

Figure 5.4 Pressure and Liquid Head-Time profile for Run#1 Feed increase

When observing the liquid heights or the liquid heads, there were appropriate responses to the feed increase. The heavy liquid head increased to compensate for the increase in the heavy liquid fraction of the feed. When observing the light liquid head, there was first an increase in height, from about 8 mm to 11.2 mm, then a small decrease to 10.7 mm. This overshoot in the light liquid head at about 104 minutes was due to the combined effects of the increasing volume of both the heavy liquid phase and the light liquid phase. From 104 minutes to 105 minutes, the light liquid head decreased then stabilized because at time 104 minutes, the heavy liquid head had stabilized (to 27 mm),

thus the light liquid dynamics depended solely upon the changes experienced by the light liquid phase. The light liquid weir assured that the exiting light liquid flowrate stabilized to match the incoming flowrate.

Figure 5.5 shows that the phase temperatures were constant and thus, indicated a stable system.

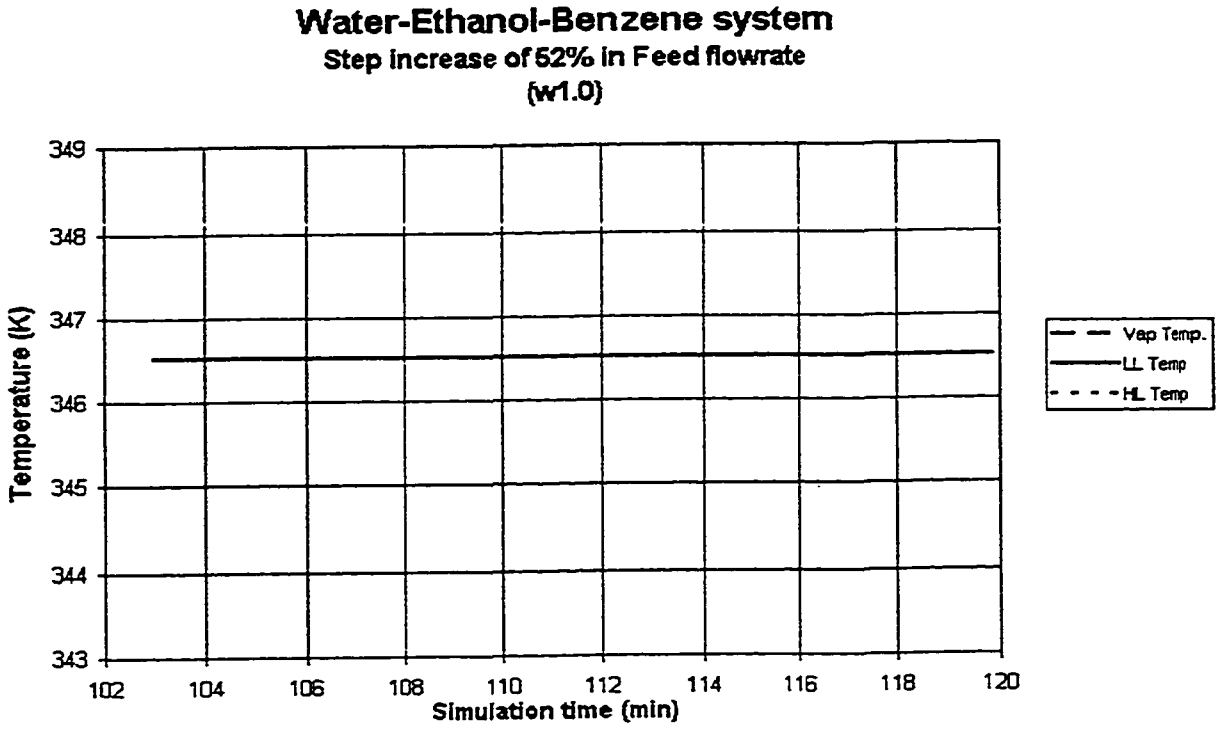

Figure 5.5 Temperature-Time profile for Run#1 Feed increase

Figure 5.6 shows the exiting flowrate responses to the feed increase. As mentioned above, due to the change in thermodynamic properties of certain phases, the

pressure decreased. The controller closes the vapour outlet valve in order to regulate the exiting vapour flowrate so that the pressure reached the setpoint of 140 kPa.

Both the light and heavy liquid exiting flowrate increased with the change in feed flowrate. The heavy liquid showed the greatest increase in the exiting flowrate because it must match the feed flowrate which is composed mainly of the heavy liquid (85.8%).

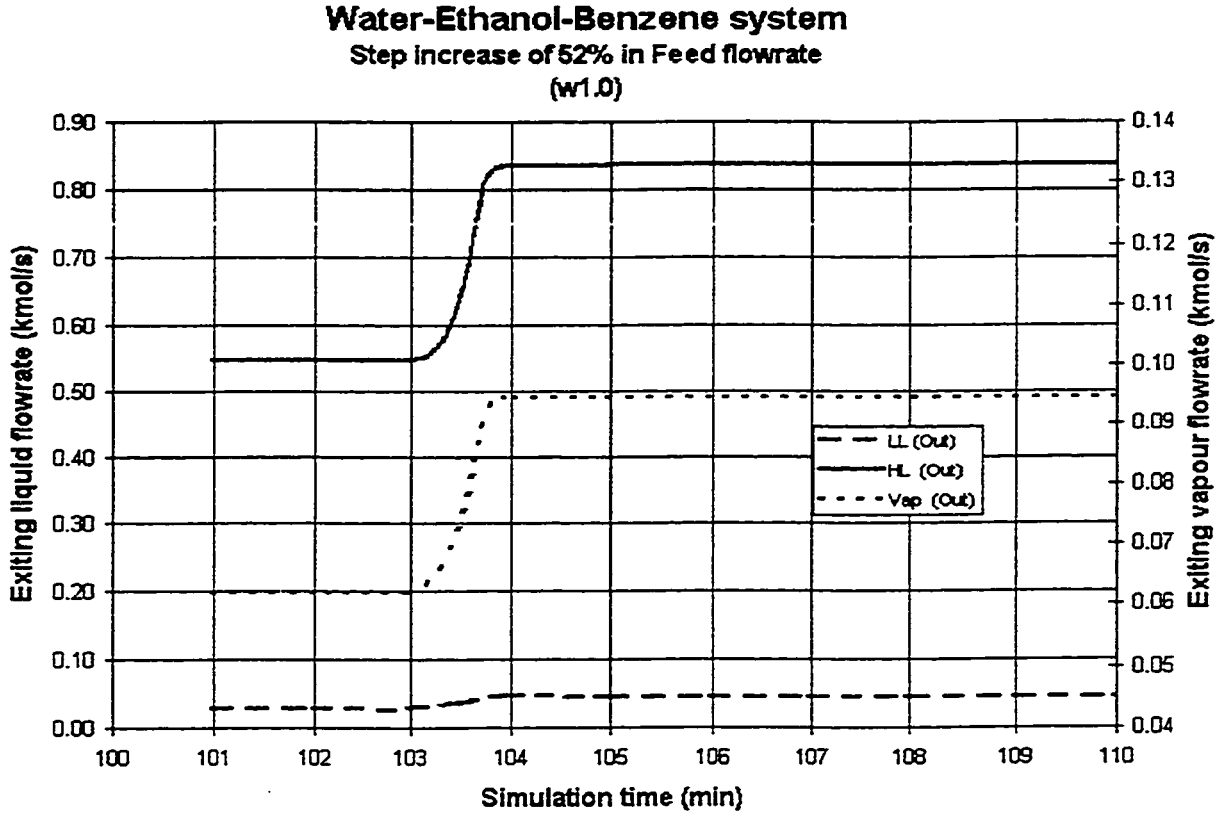

Figure 5.6 Exiting Molar Flowrate-Time profile for Run#1 Feed increase

5.3.3 Run # 1 Feed Flowrate Decrease

The feed flowrate was decreased next to 52% of the original value. In Figure 5.7, one can see that the pressure increased instead of decreasing. Again, this was due to minute changes in density and molar due to the property flash calculations.

The liquid heads responded as would be expected, decreasing appropriately to compensate for the step decrease in the feed flowrate. The temperature, again, stayed constant during this disturbance as seen in Figure 5.8, indicating thermal stability.

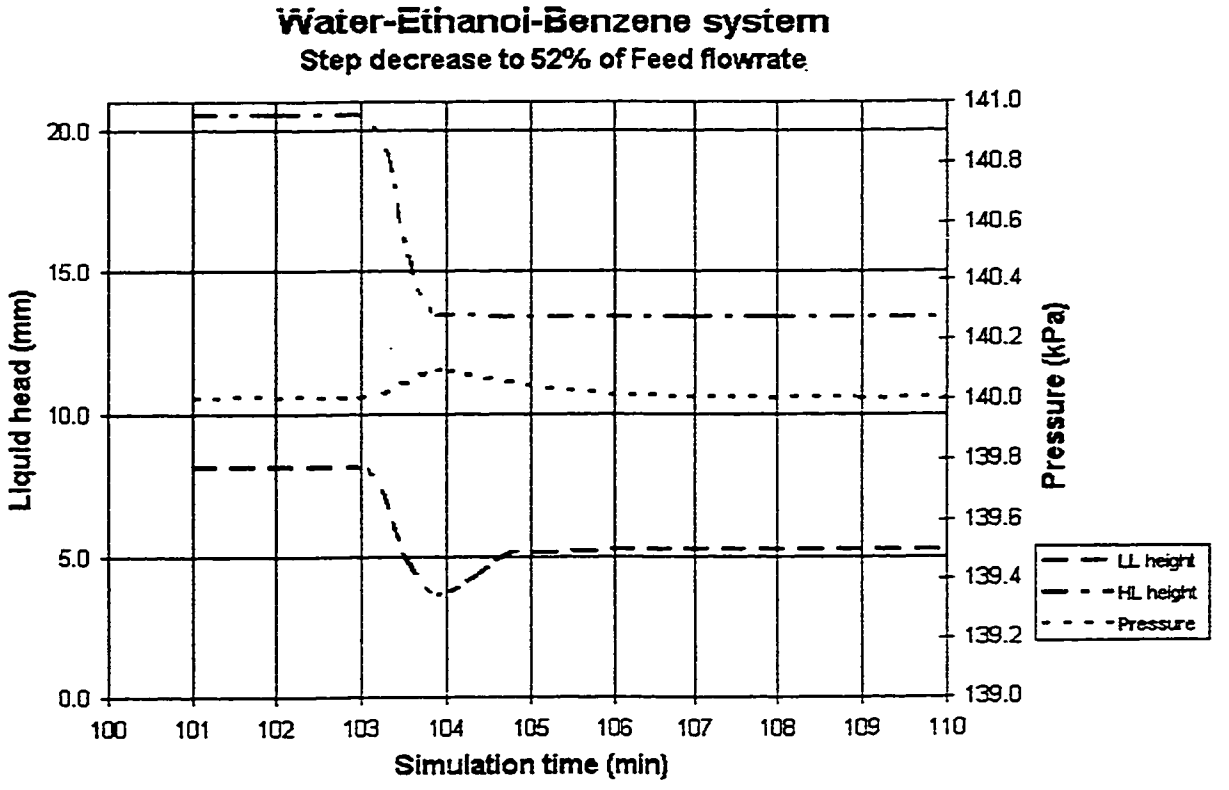

Figure 5.7 Pressure and Liquid Height-Time profile for Run#1 Feed decrease

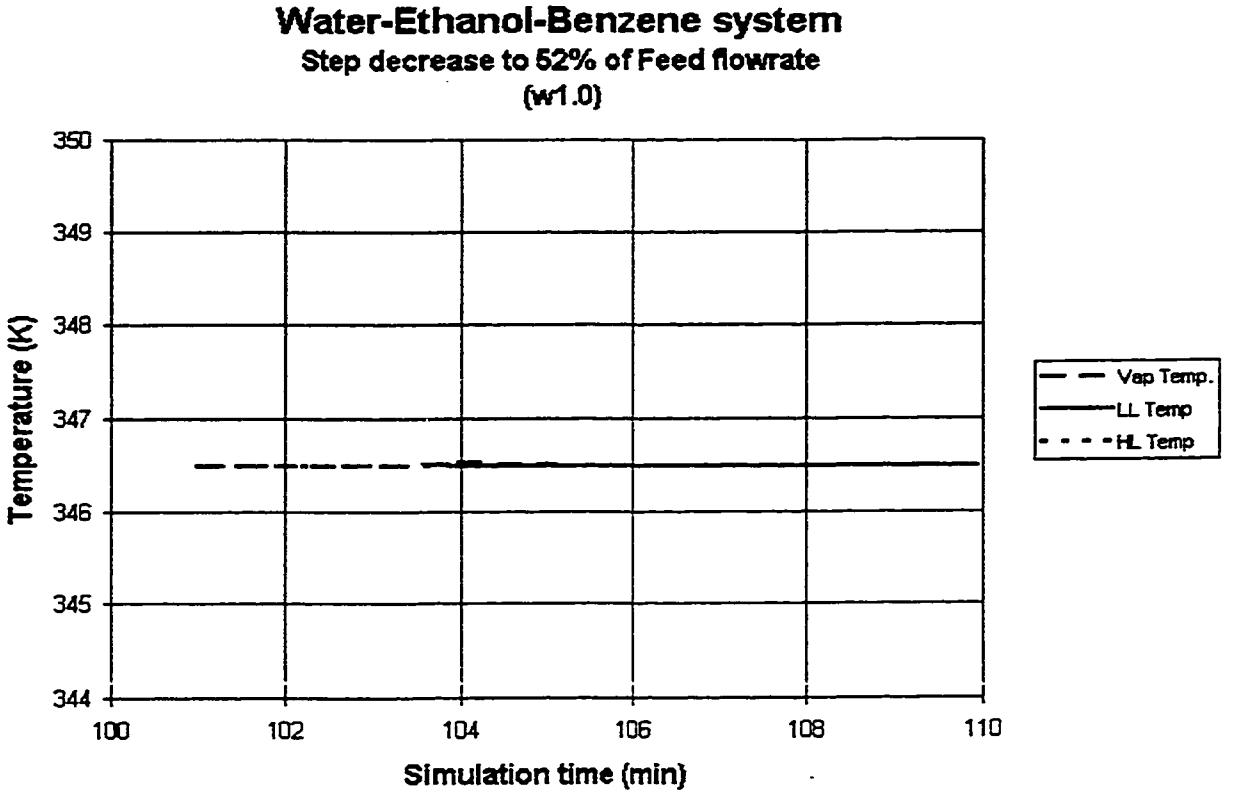

Figure 5.8 Temperature-Time profile for Run#1 Feed decrease

The exiting molar flowrates also responded appropriately to the step change. In Figure 5.9 the vapour flowrate decreased from 0.062 kmol/s to 0.033 kmol/s. The heavy liquid flowrate decreased from 0.548 kmol/s to 0.288 kmol/s. The light liquid response showed an interesting behaviour. Initially the light liquid flowrate is at 0.029 kmol/s, then it decreases to 0.008 kmol/s (which is more than a 52.45% decrease) and finally it increases to 0.015 kmol/s. The reason that the flowrate decreased to 0.008 kmol/s then increased to 0.015 kmol/s is that when the heavy liquid height was reduced to its stable

height, it lowered the light liquid level past its stable level. The light liquid volume had to increase so that the height could be brought back to the steady-state value.

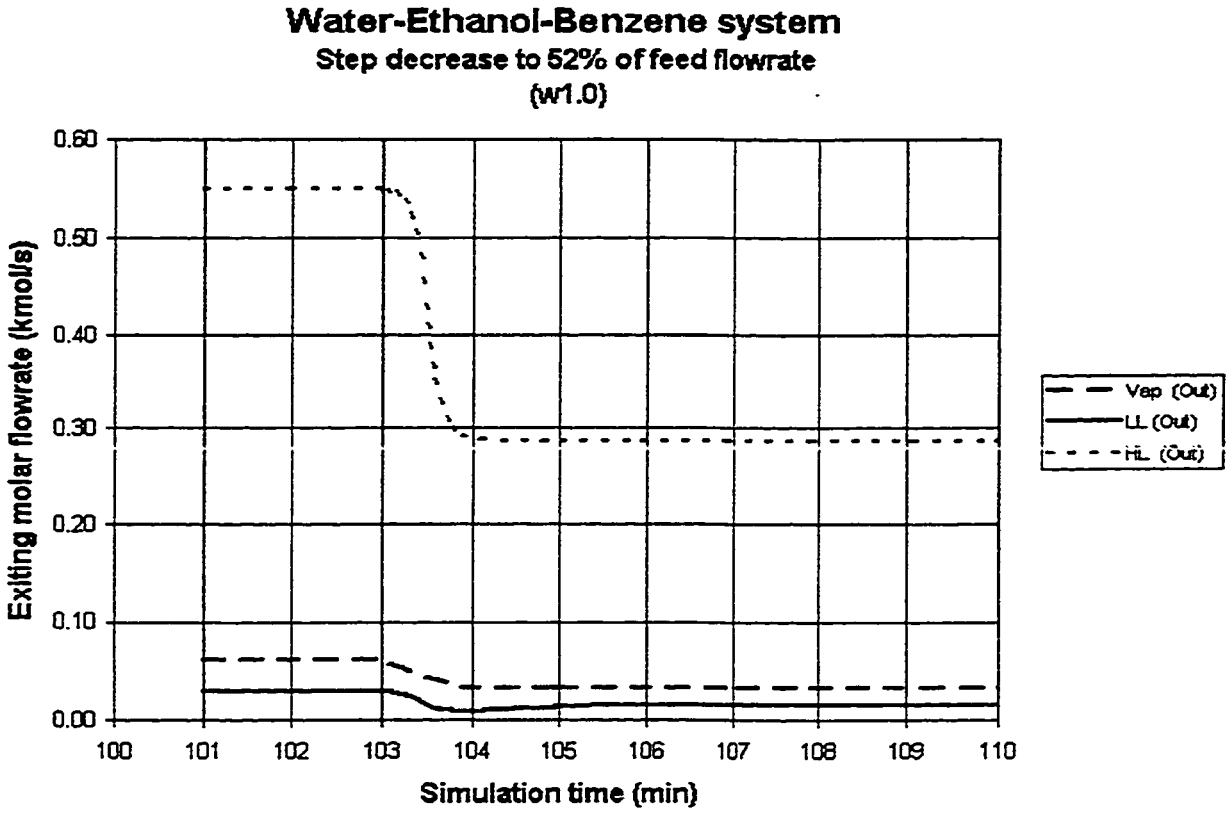

Figure 5.9 Exiting Molar Flowrate-Time profile for Run#1 Feed decrease

5.3.4 Run # 2 Dry Startup

The dry startup results are similar to the results for the mixture of water-ethanol-benzene. In Figure 5.10 the pressure peaked at 177.1 kPa from 176 kPa. The increase in pressure last longer (approximately 17 min.) than for mixture 1. For this mixture (water-

propanol-butanol), the pressure started to decrease when the light liquid level stabilized (at time = 19 minutes). The pressure further decreased to the setpoint of 176.0 kPa when the heavy liquid level reached a steady-state level (at time = 24 minutes). From t=19 min. to t=23 min., the light liquid height surpassed its steady-state level and returns to it because the heavy liquid molar holdup was still increasing, in turn increasing the light liquid level higher than the steady-state value.

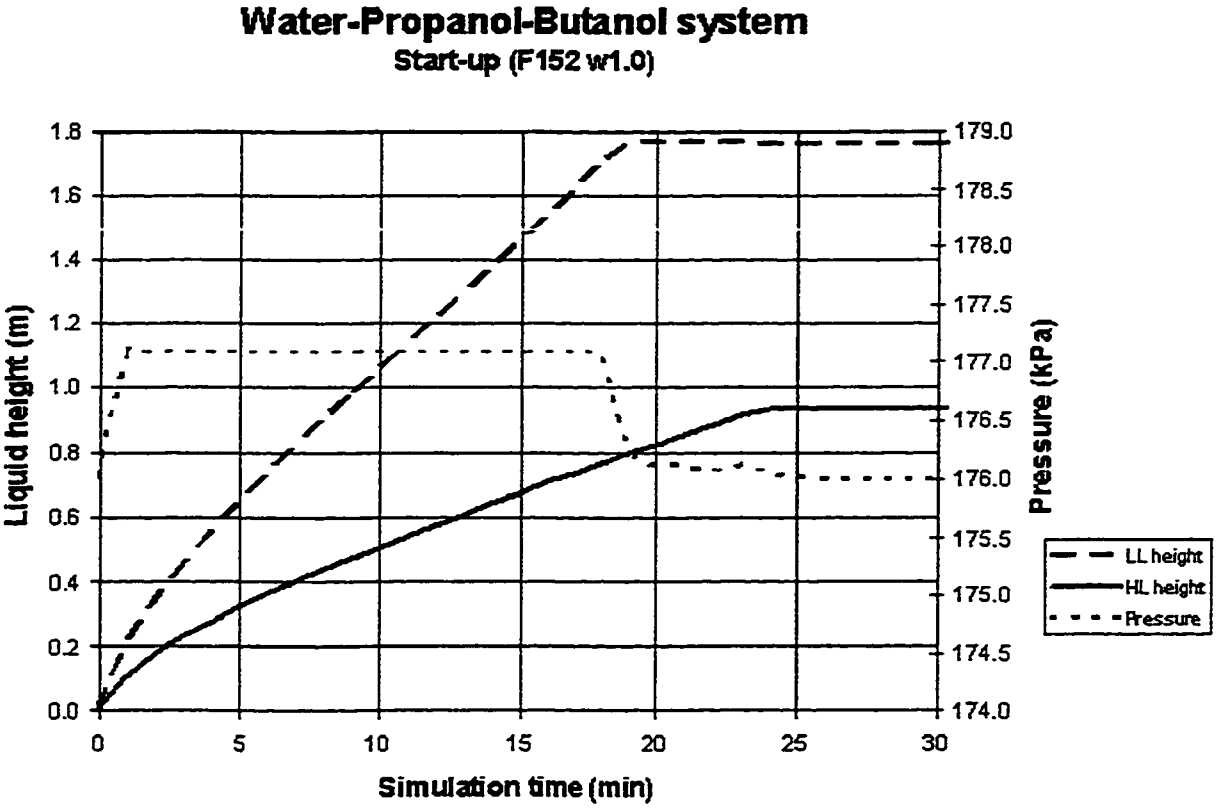

Figure 5.10 Pressure and Liquid Height-Time profile for Run#2 Dry Startup

The plot of phase temperature versus time, Figure 5.11, does indicate a stable trend. The slight increase in vapour phase temperature is a result of the thermodynamic package flash routine. This rise in temperature relates to a 0.047% relative change which can be neglected.

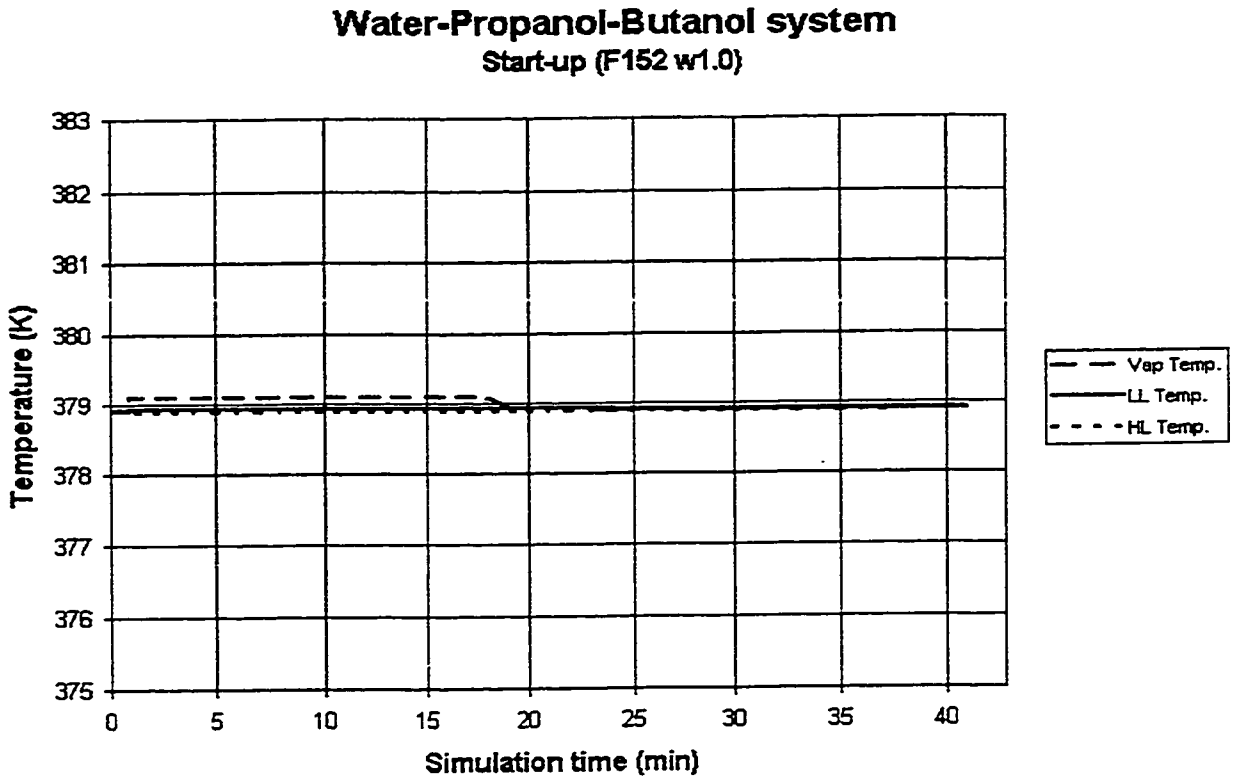

Figure 5.11 Temperature-Time profile for Run#2 Dry Startup

Figure 5.12 shows the liquid flowrates are quite dynamic and specially the light liquid. When referring to Figure 5.12 (the above exiting molar flowrates plots), it can be noted that the vapour phase flowrate, in response to the rise in pressure, jumps to 0.139

kmol/s and then at t=18 min. began to drop to 0.138 kmol/s at t=25 min. These changes are small enough to be considered negligible. The light liquid flowrate began to rise at approximately 18 minutes but exceeded the steady state flowrate value. This was due to the fact that the heavy liquid level was still increasing which forced the light liquid level to rise past its steady-state level. The heavy liquid level reached the weir height at about 24 minutes and a stable flowrate a few minutes latter.

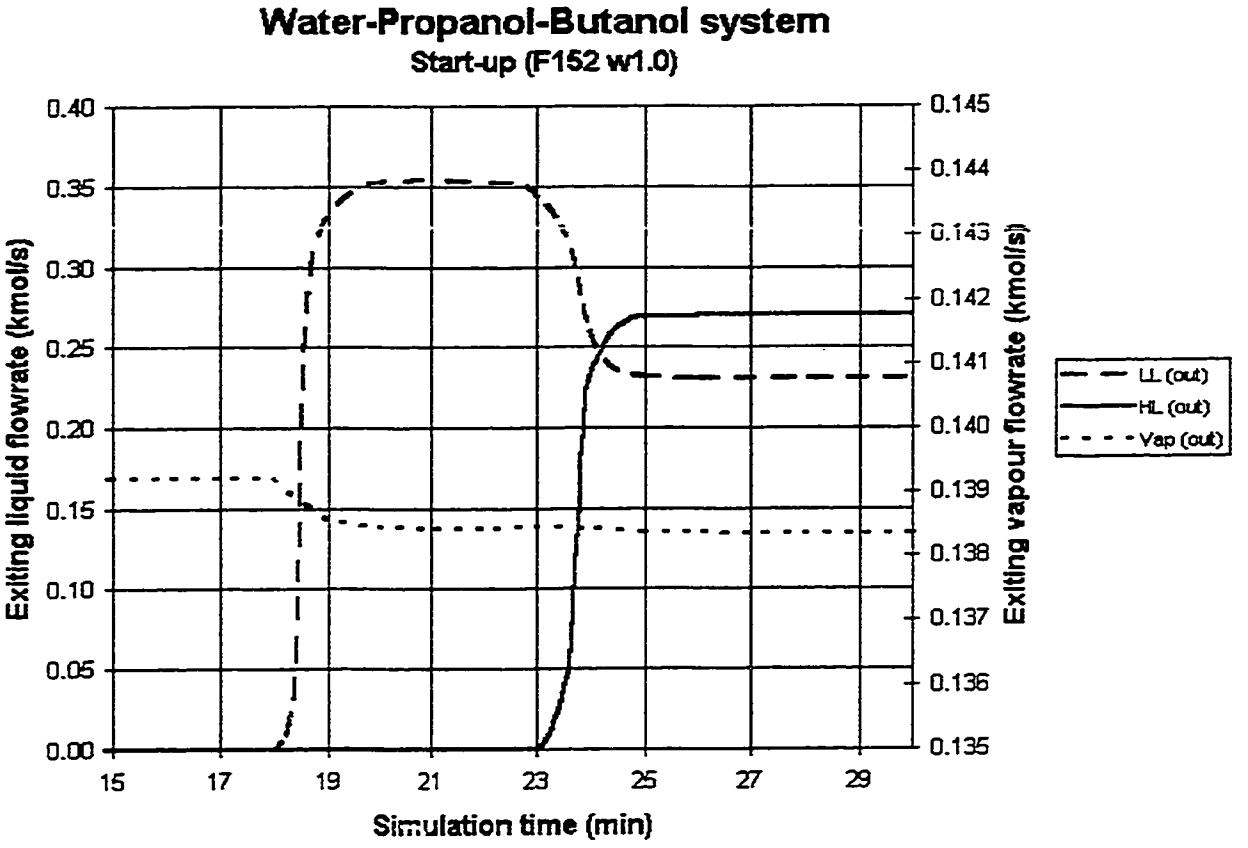

Figure 5.12 Exiting Molar Flowrate-Time profile for Run#2 Dry Startup

5.3.5 Run # 2 Feed Flowrate Increase

Figure 5.13 shows the effect of a 52% increase in feed flowrate on the pressure and liquid head responses. The pressure remained constant but the liquid levels did increase marginally. The light liquid experienced an increase in liquid height of 0.35% (liquid head change from 19.1 mm to 25.3 mm) and the heavy liquid level increased by 0.43% (liquid head change from 12.4 mm to 16.5 mm). By observing the data, the liquid head did follow a similar trend as seen in the previous run (Run#1 -Feed increase). The liquid level overshot the steady-state value then stabilized to it. Again, the phase temperatures did not fluctuate indicating thermal stability (Figure 5.14).

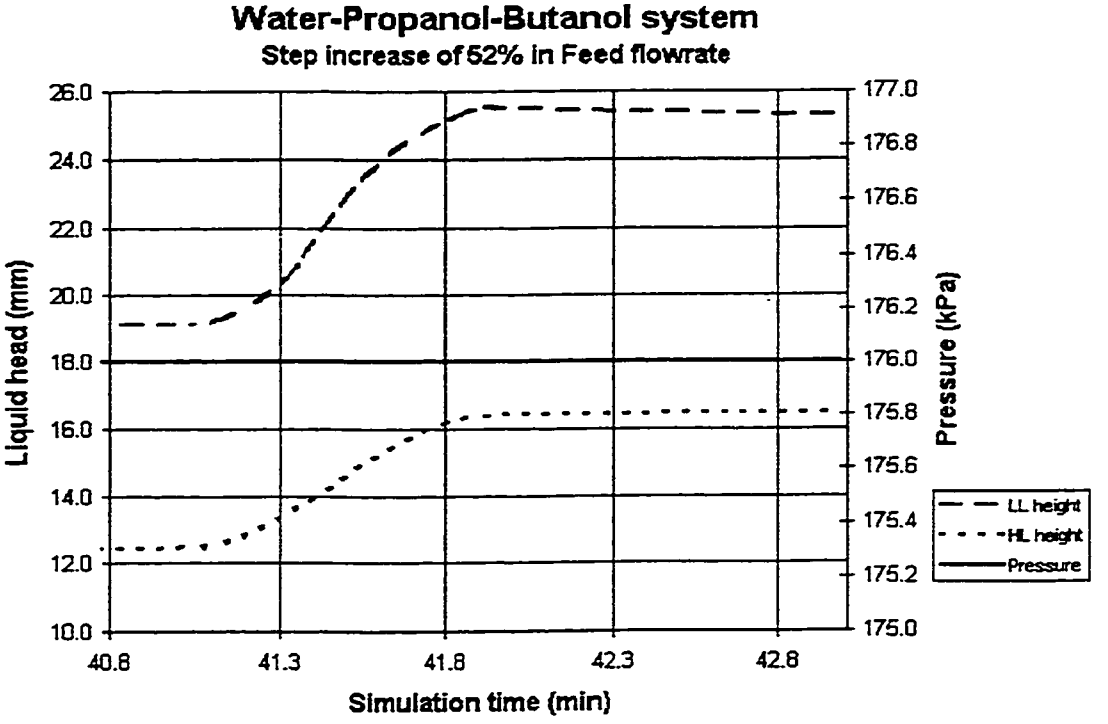

Figure 5.13 Pressure and Liquid Head-Time profile for Run#2 Feed increase

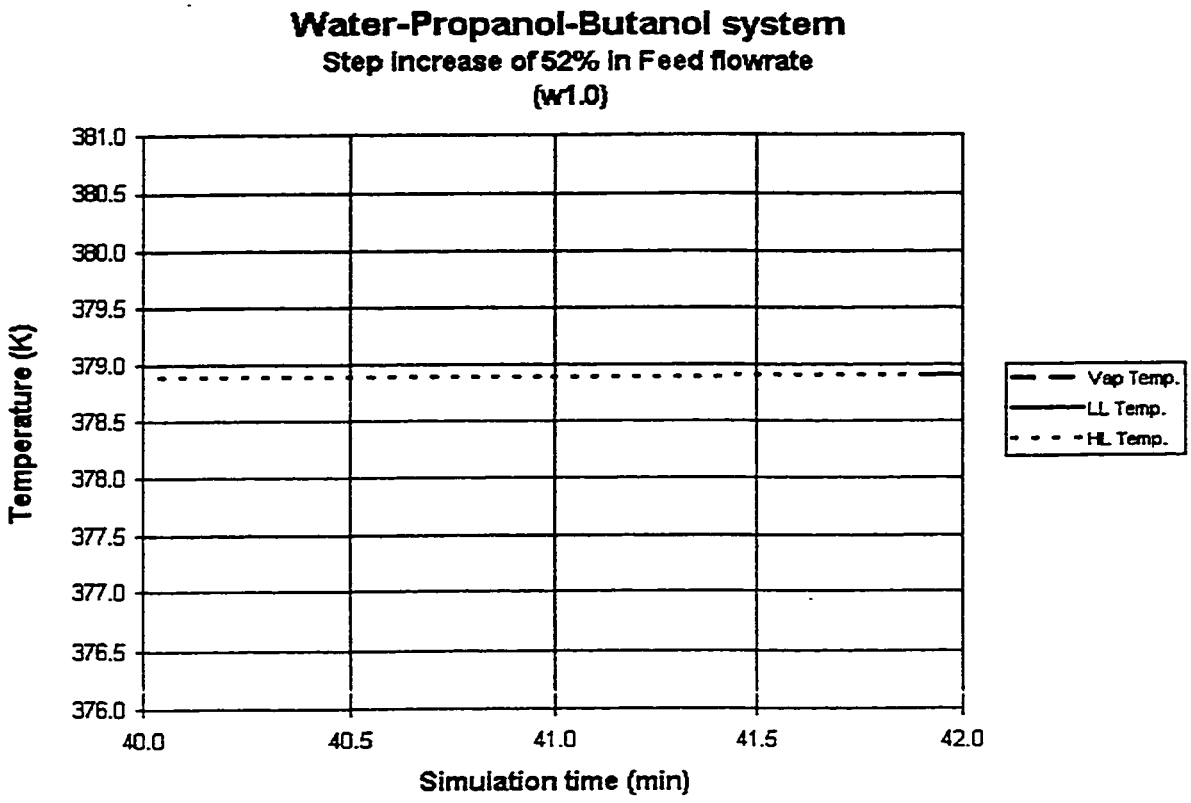

Figure 5.14 Temperature-Time profile for Run#2 Feed increase

The plots in Figure 5.15 show expected exiting flowrate responses to the feed flowrate increase. The vapour flowrate increased from 0.138 kmol/s to 0.211 kmol/s. The heavy liquid flowrate increased from 0.270 kmol/s to 0.412 kmol/s. Finally, the light liquid flowrate increased past its steady-state flowrate level and returned to its steady state value of 0.351 kmol/s.

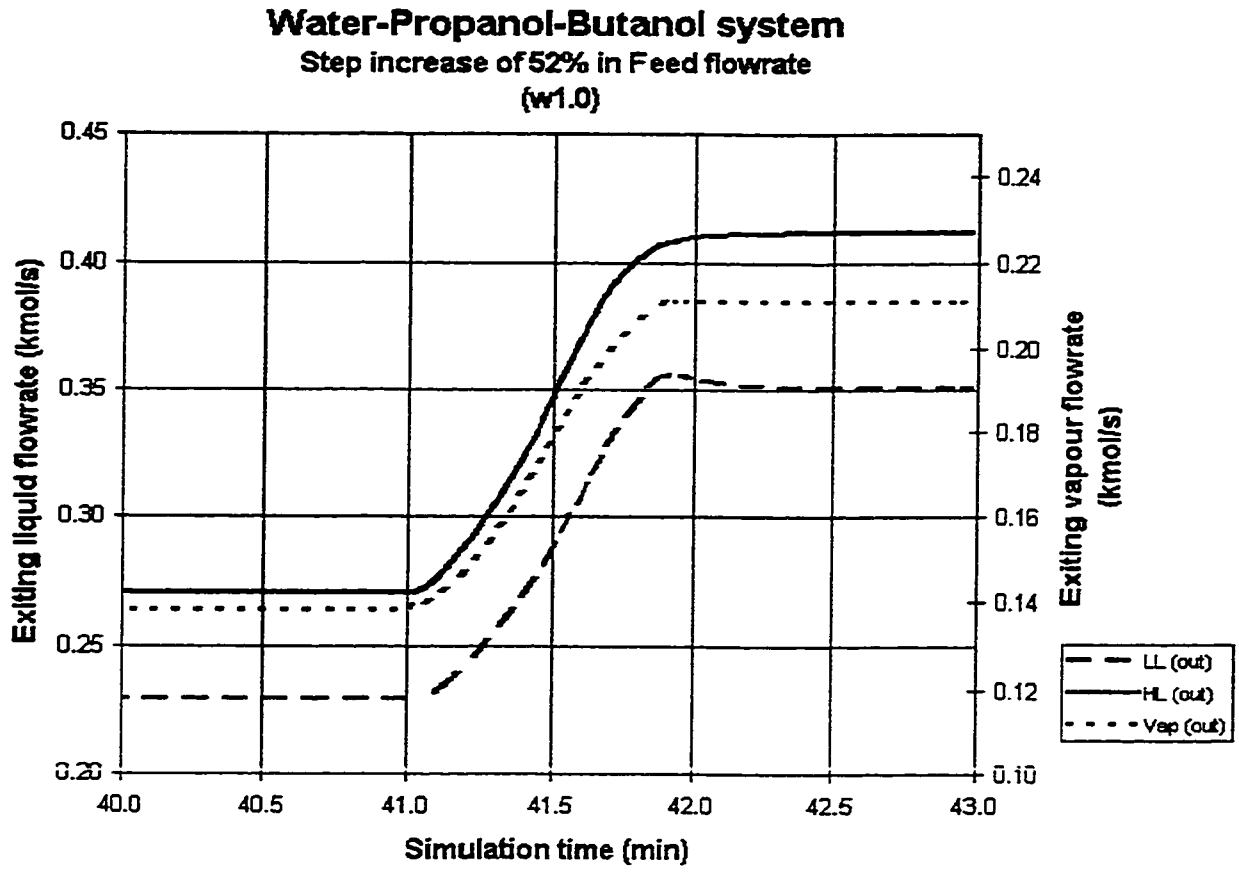

Figure 5.15 Exiting Molar Flowrate-Time profile for Run#2 Feed increase

5.3.6 Run # 2 Feed Flowrate Decrease

Figure 5.16 shows a pressure response opposite of what should be expected. The pressure increased from 176.0 kPa to 176.24 kPa (a +0.14% change) and returned to 176.0 kPa. This change in pressure is negligible as an industrial separator would not detect such minutes changes in pressure.

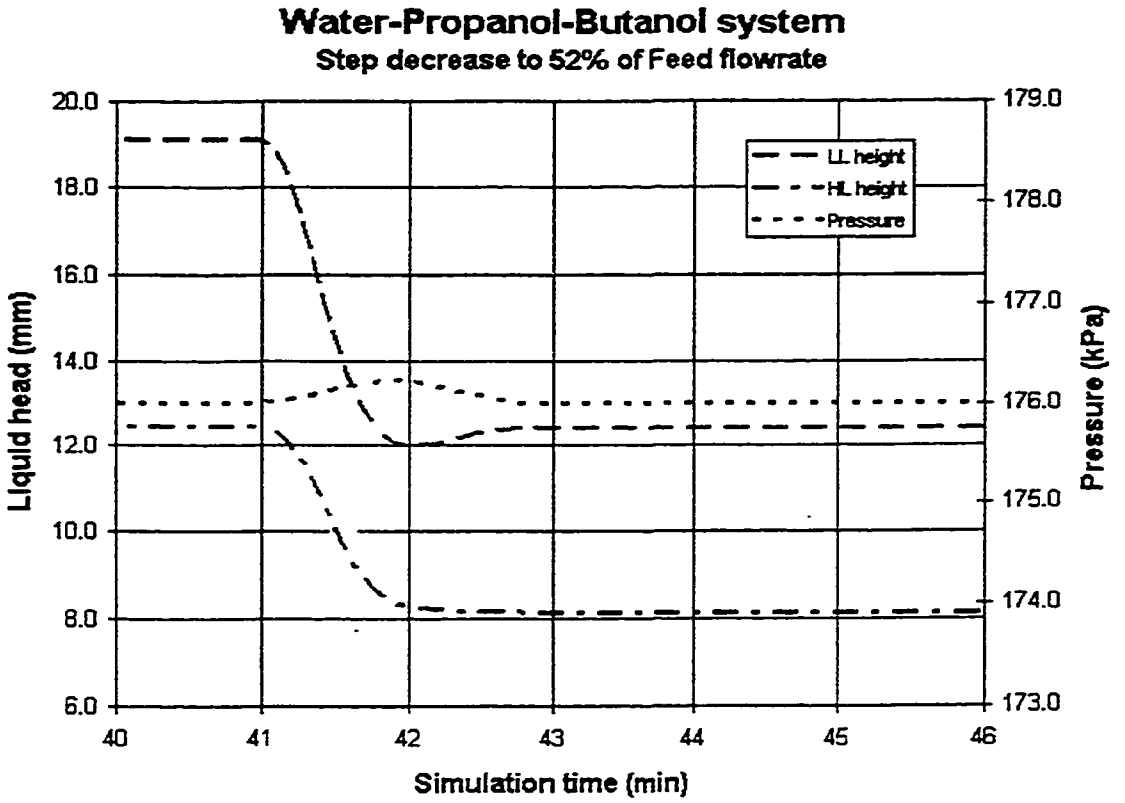

Figure 5.16 Pressure and Liquid Height-Time profile for Run#2 Feed decrease

Figure 5.17 shows stable temperature plots. Once the disturbance was applied, there was a negligible change in vapour phase temperature.

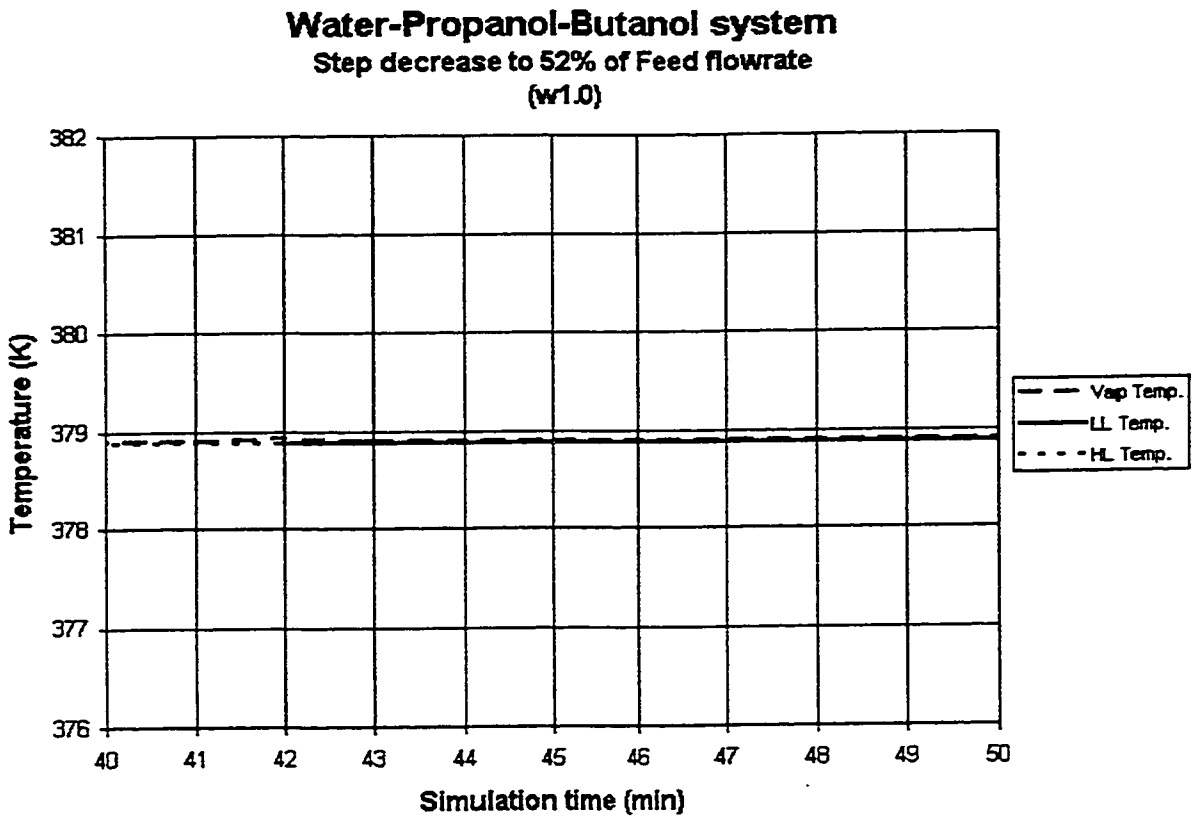

Figure 5.17 Temperature-Time profile for Run#2 Feed decrease

The corresponding exiting flowrate responses can be seen in Figure 5.18. Once the simulation time passed 41 minutes, all of the flowrates had begun to decrease. By t=44 min., all 3 flowrates had reached steady state. The steady state flowrates were precisely 52% of the original flowrates as would be expected.

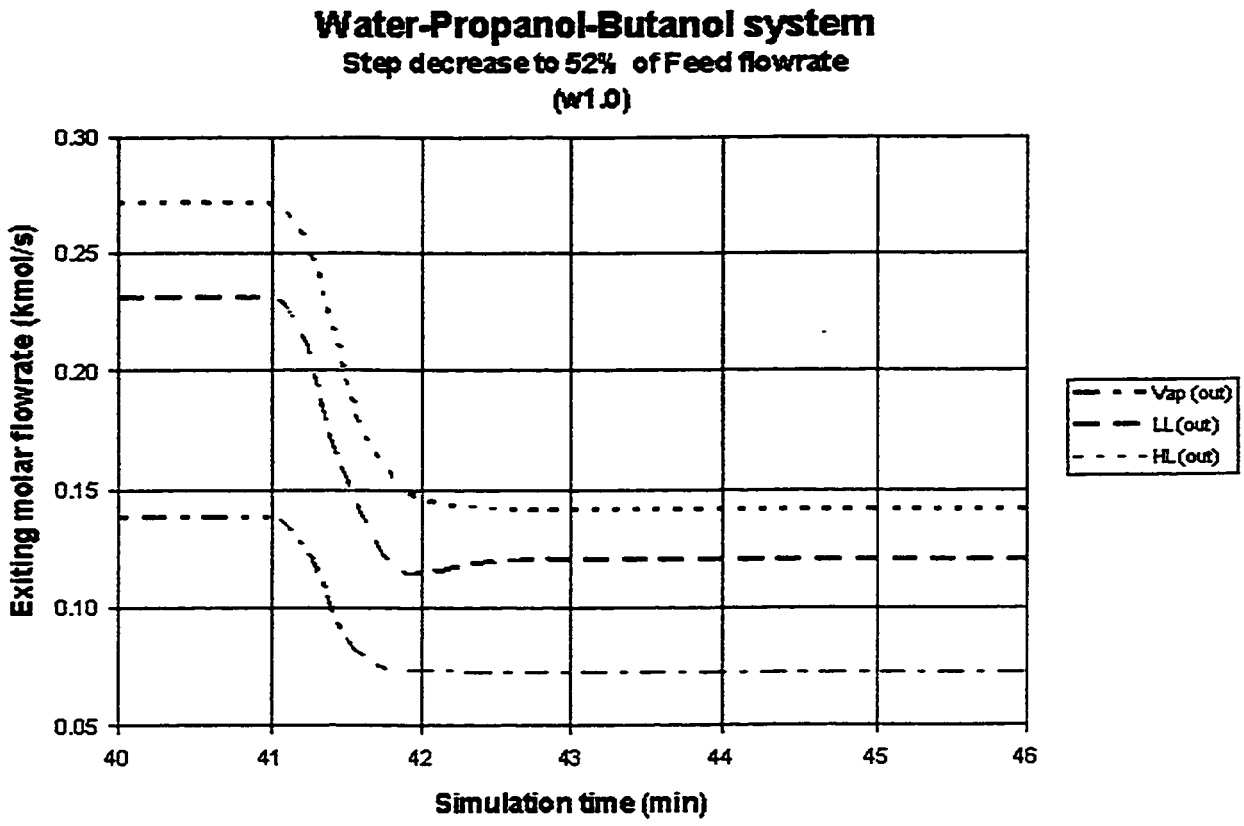

Figure 5.18 Exiting Molar flowrate-Time profile for Run#2 Feed decrease

5.3.7 Run # 2 Shutdown

The results obtained were only for the case of the step increase in feed flowrate. The data for the pressure behaviour was found to be unexpected as most of them had been. The pressure response to the feed shut off should have been a decrease in pressure rather than an increase as shown in Figure 5.19. The liquid heights behaved adequately, they decreased to exactly the weir height in order for the separator to reach steady state. If one analyzed Figure 5.20 (Temperature versus Simulation time), one could see that the vapour temperature had increased for no particular reason. This rise in temperature can

only be attributed to the results obtained from the thermodynamic package flash procedure. Certain thermodynamic properties such as the molar enthalpy, density and molar volume of the resulting phase had changed slightly. This explains the rise in pressure and vapour phase temperature.

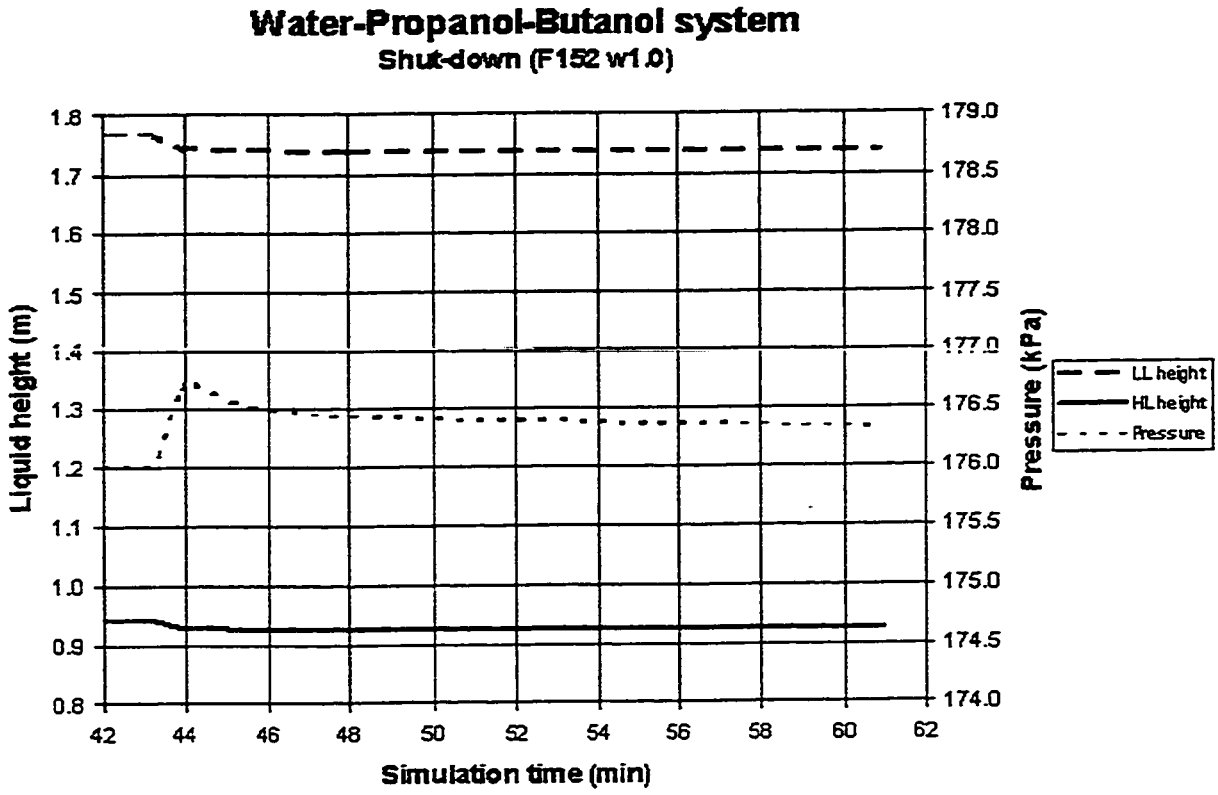

Figure 5.19 Pressure and Liquid Height-Time profile for Run#2 Shutdown

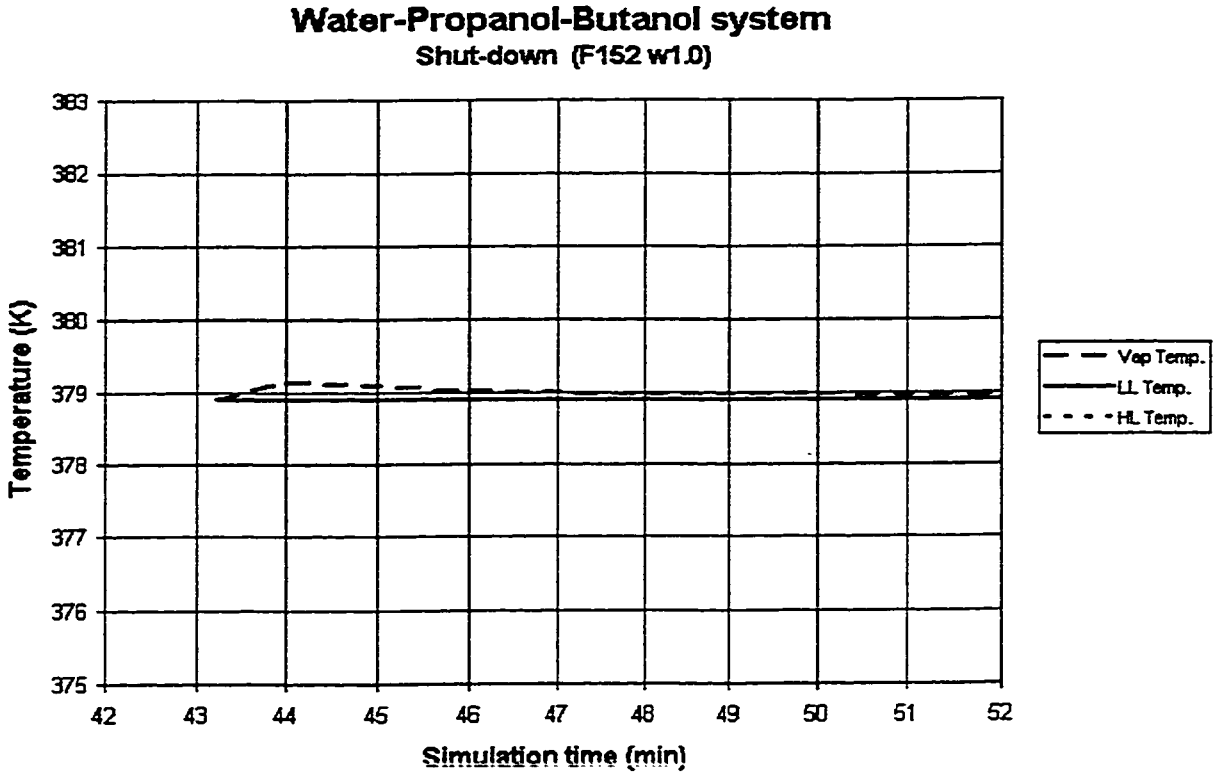

Figure 5.20 Temperature-Time profile for Run#2 Shutdown

Regardless of the unexpected change in pressure, the exiting flowrates behaved as expected, they eventually dropped to 0.0 kmol. The vapour and light liquid flowrate dropped to zero in 1 minute or less, but the heavy liquid flowrate took approximately 3 minutes to drop to essentially zero as shown in Figure 5.21.

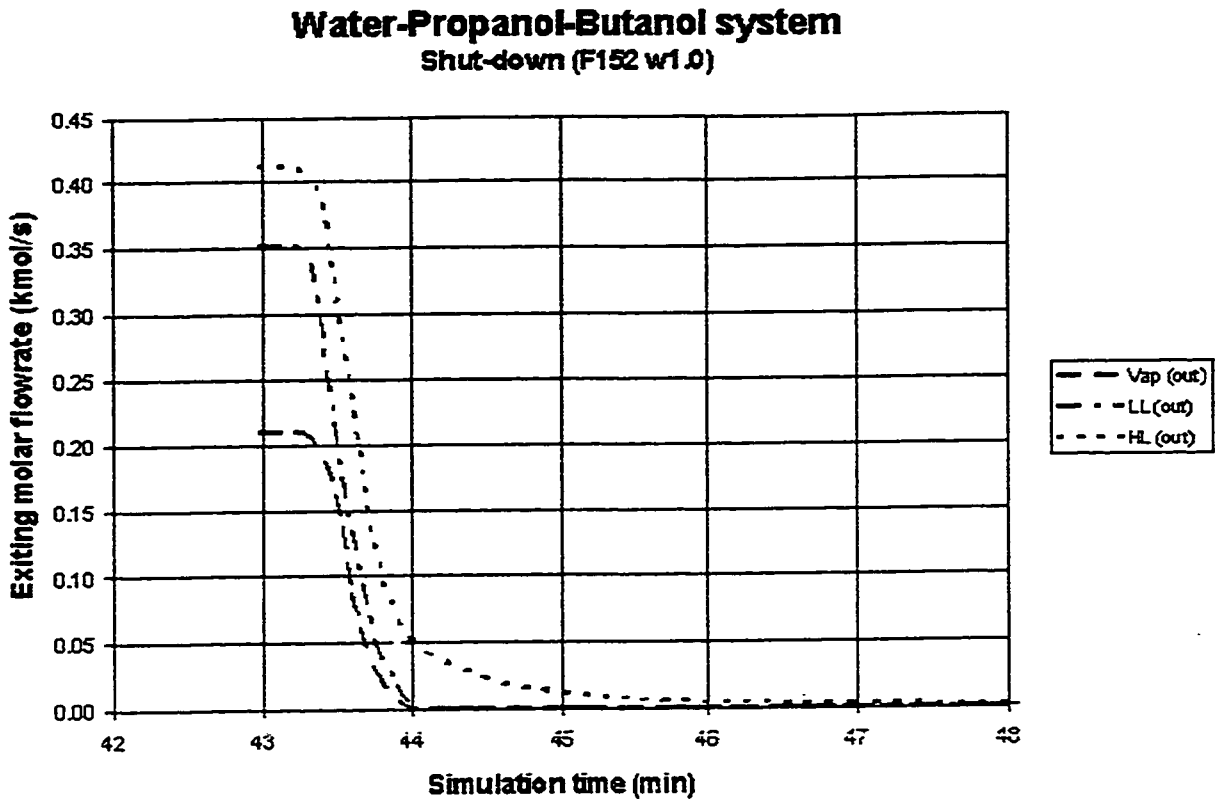

Figure 5.21 Exiting Molar Flowrate-Time profile for Run#2 Shutdown

The above discussion of the separate variable dynamic behaviour is similar for the two mixtures. The differences were mainly in the operating conditions and the separator's physical dimensions.

5.4 Effect of Weir Width

There were three tests performed to observe the effect of weir width (factor of 1.0, 0.5, 0.2) upon the separator operating behaviour. They will be designated w1.0, w0.5 and w0.2 . Both the light liquid weir and the heavy liquid weir width were decreased from run to run. All of these tests used the water-propanol-butanol mixture and the same initial operating conditions. The light liquid weir widths for the various runs were 206 cm, 103 cm, 41 cm, respectively, and the heavy liquid weir widths were 230 cm, 115 cm and 46 cm, respectively.

The original weir widths of 206 cm and 230 cm were set when the separator was designed. The widths were taken as the distance between the separator walls at the weir heights. The other widths were chosen as a fraction of the original values. The first width reduction was set at 50% of the original widths to see if the separator behaved differently. The weir widths were further reduced to 20% of the original values in order to observe any changes in separator behaviour.

5.4.1 Dry Startup

Figures 5.10, 5.22 and 5.31 show a comparison of pressure and liquid height-time profiles in the startup scenario for weir widths of w1.0, w0.5, and w0.2. Figures 5.10, 5.22 and 5.31 show that for the case of w1.0, the steady state height was 176.20 cm, while for w0.5, 177.33 cm and for w0.2 the steady state height was 179.89 cm. The rise

in liquid height was the result of narrowing the weir width to control the liquid outlet flowrate. When dealing with the weir equation, the volumetric flowrate was a function of several variables, two of which, were the width of the weir and the level of the liquid over the weir height. As the width is decreased, the level over the weir lip must increase. By cutting the weir width in half, the steady state liquid level increased by 1.13 cm. And by further reducing the weir width to 1/5th of the original value, the liquid level is increased by 2.56 cm for a total increase of 4.69 cm.

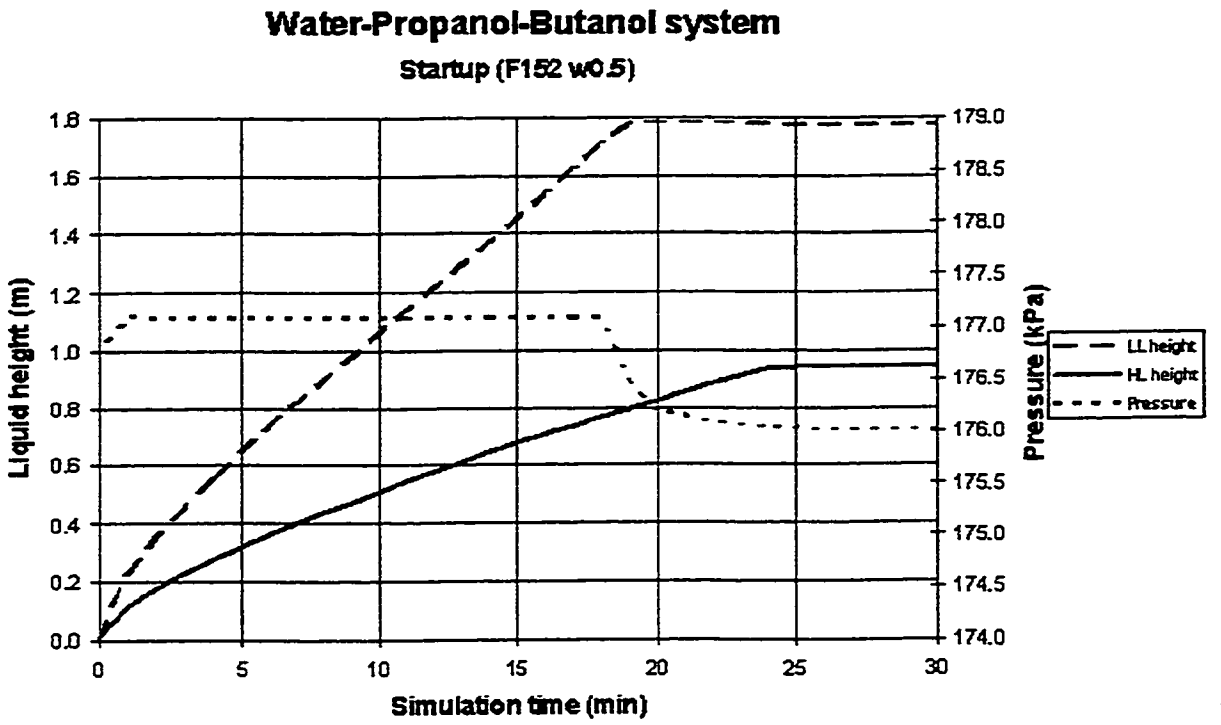

Figure 5.22 Pressure and Liquid Height-Time profile for Run#4 (w0.5) Dry Startup

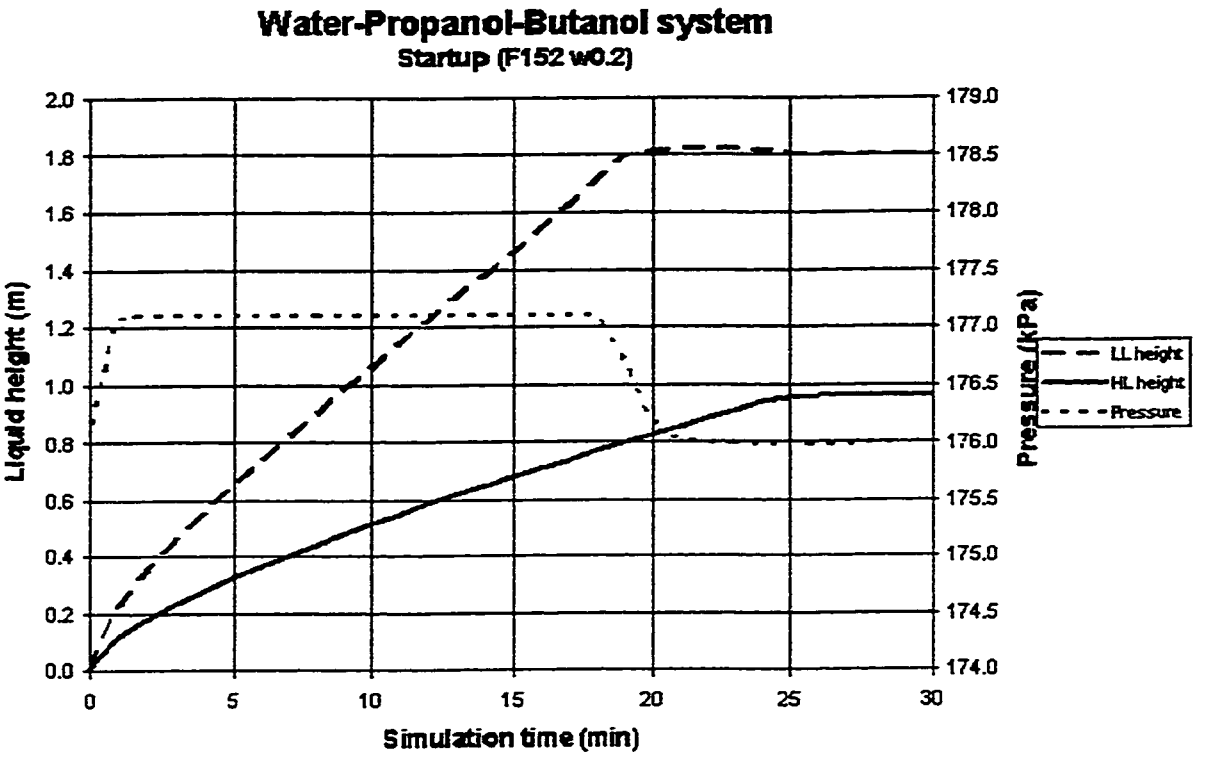

Figure 5.31 Pressure and Liquid Height-Time profile for Run#5 (w0.2) Dry Startup

An additional effect was the amount of overshoot that the light liquid level experienced. For case w1.0 the overshoot is approximately 0.65 cm. As the weir was narrowed to case w0.5 and w0.2, the overshoot increased to 1.03 cm and 1.89 cm, respectively. The reason for this increase in overshoot had to do with the rise of the heavy liquid level to its steady state value. When referring back to Figures 5.10, 5.22 and 5.31 the overshoot began shortly after the light liquid level reached the weir height and end when the heavy liquid height began to reach steady state. The rise in the heavy liquid level

forced the light liquid level to overshoot the steady state height and returned once the heavy liquid height reached its steady state.

The third effect was the response of the heavy liquid height. In the base case (w1.0), the steady state liquid level was 93.62 cm. But as the heavy liquid weir width was decreased to that of case w0.5 and w0.2, the level increased to 94.35 cm and 96.01 cm, respectively. The explanation is found in the weir equation which states that to keep a constant volumetric flowrate, the liquid height must increase if the weir width decreases, provided that the thermodynamic properties remain reasonably constant.

An additional effect was the time taken for the separator to reach steady state. For cases w1.0 and w0.5, both liquid levels stabilized in about 25 min. The vessel pressure stabilized in 26 min. For case w0.2, the liquid levels reached steady state in 27 min. and the vessel pressure around 30 min. Noting that the steady state liquid levels had increased for all the scenarios and the feed flowrate remained constant then the separator would require more time to fill up. Once the liquid levels stabilized the pressure was also able to stabilize.

Figures 5.11, 5.23, and 5.32 show the temperature response for the three cases and are virtually identical. For all practical purposes, the separator and system can be described as thermally stable.

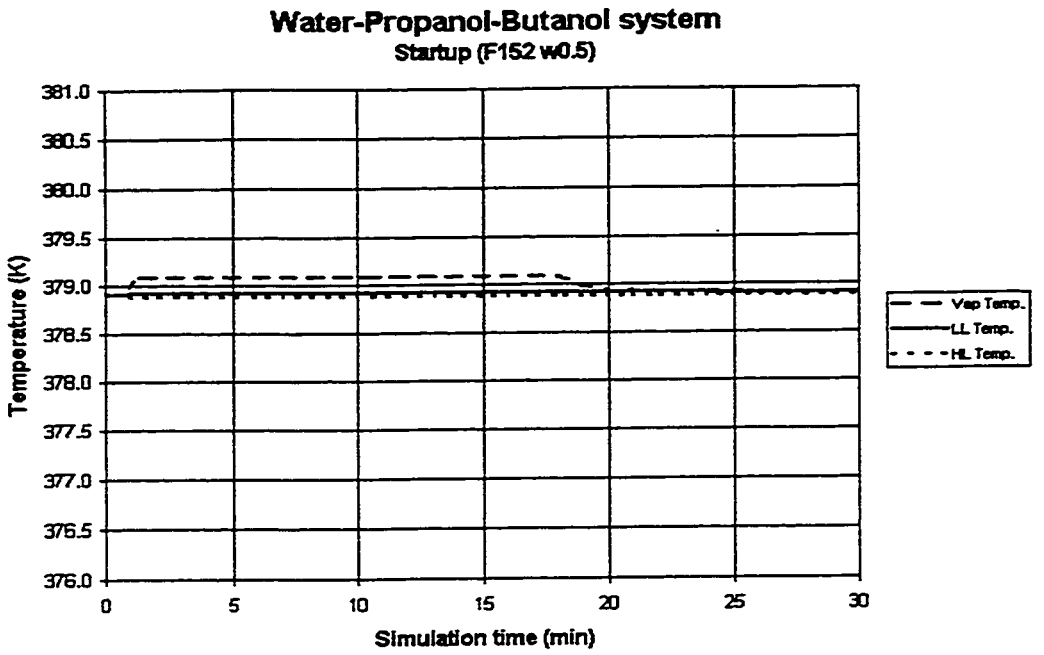

Figure 5.23 Temperature-Time profile for Run#4 (w0.5) Dry Startup

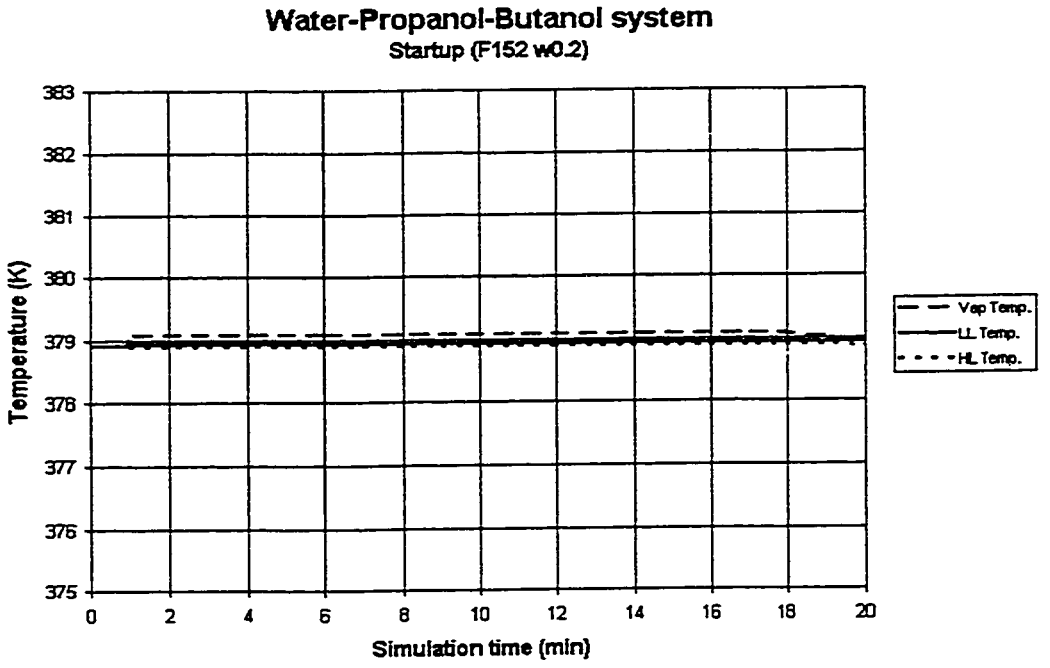

Figure 5.32 Temperature-Time profile for Run#5 (w0.2) Dry Startup

Figures 5.12, 5.24, and 5.33 show the response of the exiting flowrates. These plots were almost identical with the exception of the time required to reach steady. As the weir widths were narrowed, the time to steady state increased because the levels must rise even higher for the exiting flowrates to match the incoming flowrates. With case w1.0, the time to steady state was 26 minutes (for the liquids.. not sure of this)and approximately 25 minutes for the vapour flowrate. In case w0.5, the liquid flowrates stabilized in 27 minutes while the vapour flowrate stabilized in 26 minutes as in the previous case. For case w0.2, the vapour flowrate took the same amount of time as the 2 previous cases but the liquid flowrates reached steady state in 30 minutes. Due to the geometric configuration of the weir, the liquid levels rose higher in case w0.2 when compared to w0.5 and w1.0. There were larger volumes to fill in case w0.2, therefore the separator required the extra time to fill up and stabilize.

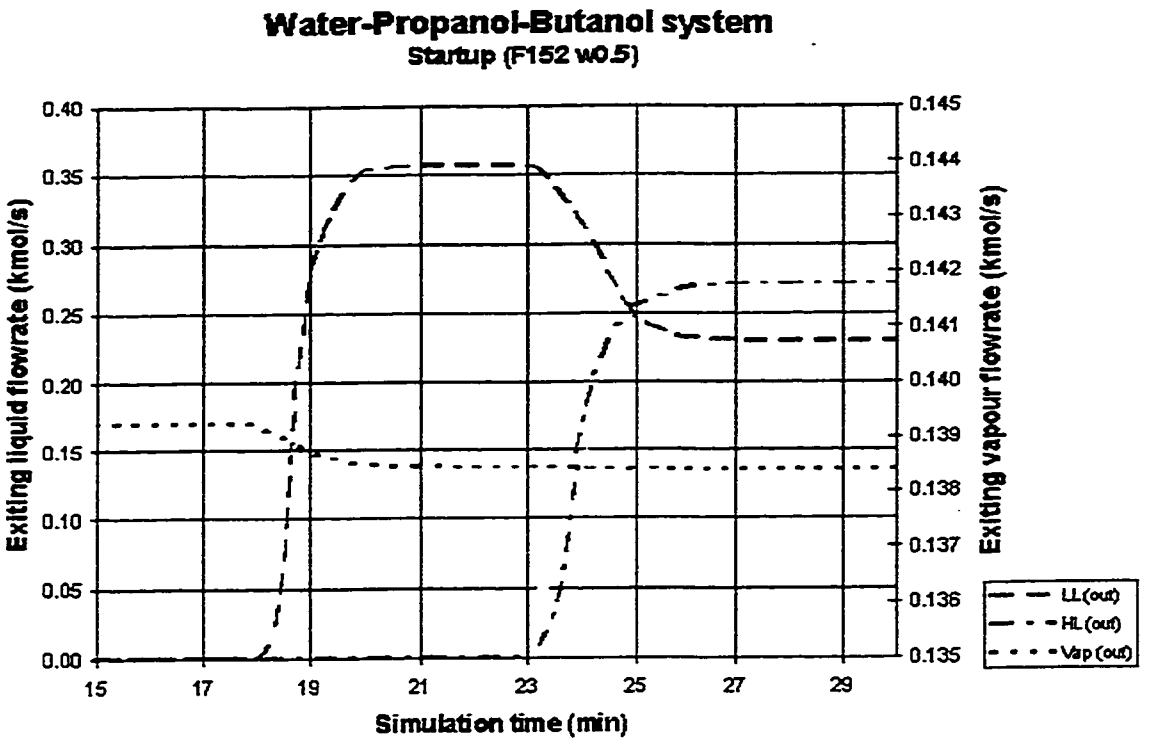

Figure 5.24 Exiting Molar Flowrate-Time profile for Run#4 (w0.5) Dry Startup

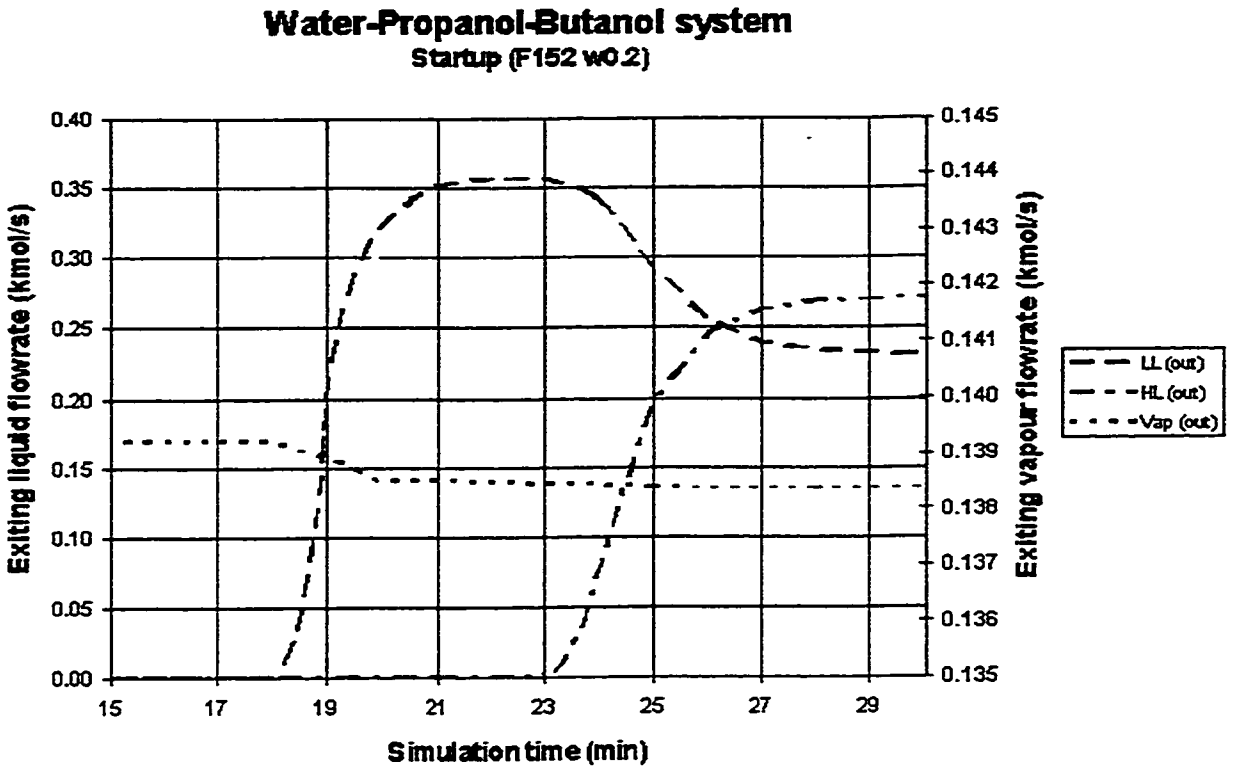

Figure 5.33 Exiting Molar Flowrate-Time profile for Run#5 (w0.2) Dry Startup

5.4.2 Feed Increase

Some of the runs showed a short post-disturbance dynamic period. For example, in case w1.0, the time required to reach steady state was only 2 minutes. In this period of time, not many data points were collected; therefore, the resulting plots are sparse.

Figures 5.13, 5.25, and 5.34 show the pressure and liquid head responses to a feed flowrate step increase of 52%. All of the responses in the three cases do show expected behaviour. The liquid heads increased and for cases w1.0 and w0.2 (Figures 5.13 and

5.34), the pressure increased then returned to the setpoint. For case w1.0, the pressure did not vary mainly because the changes in liquid heights were small enough not to affect it. The overall changes in liquid heads were 6.2 mm for the light liquid and 4.0 mm for the heavy liquid. The final levels for the light and heavy liquids were 176.82 cm and 94.02 cm respectively. For case w0.5, the overall changes in liquid heads were 9.8 mm for the light liquid and 6.5 mm for the heavy liquid. And for case w0.2, the overall changes in liquid heads were 18.2 mm for the light liquid and 11.8 mm for the heavy liquid. The liquid height response shows that the height increased beyond the steady state value and then returned to it, regardless of how small was the overshoot. The time required to reach steady state from the time of disturbance was 3 minutes.

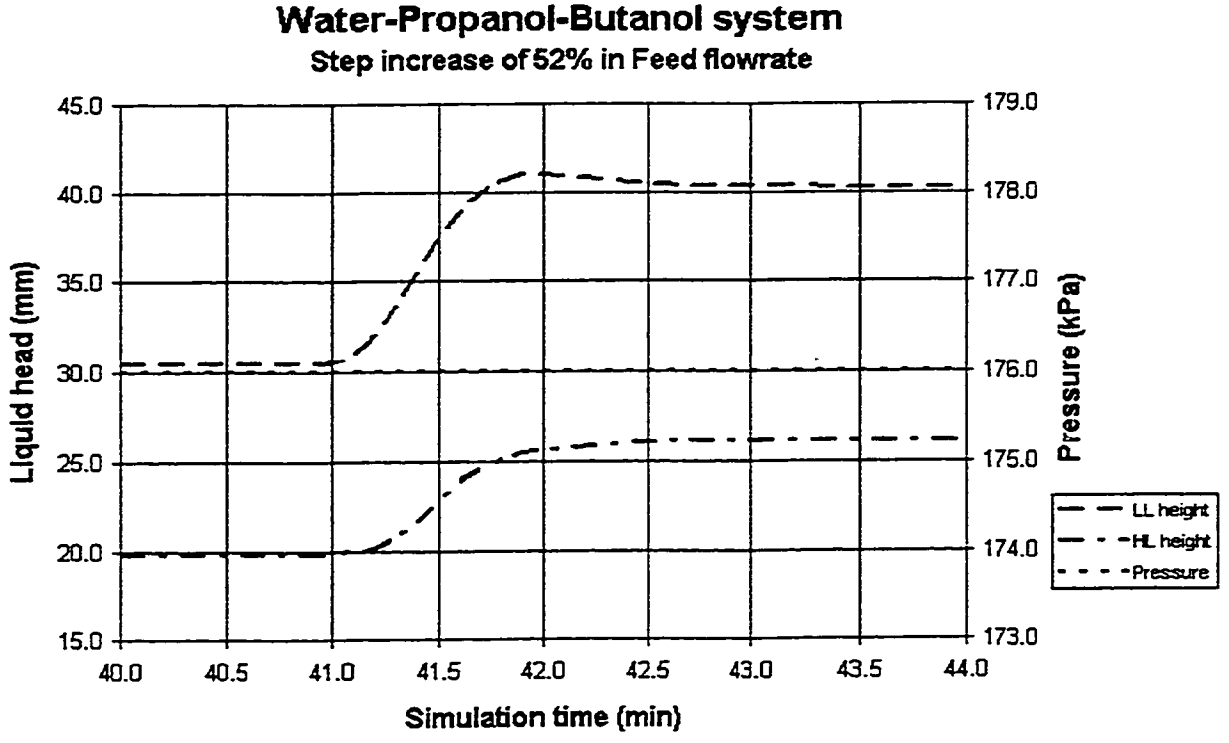

Figure 5.25 Pressure and Liquid Height-Time profile for Run#4 (w0.5) Feed increase

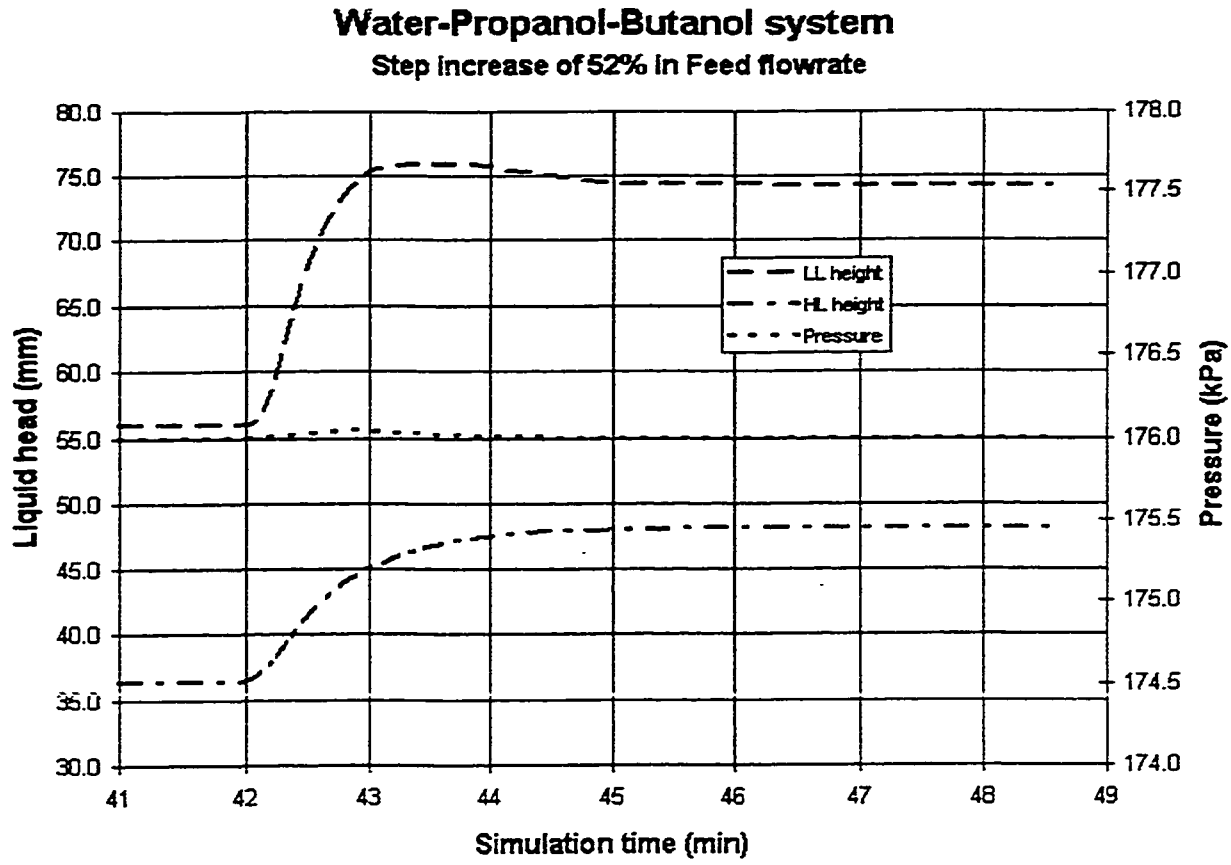

Figure 5.34 Pressure and Liquid Head-Time profile for Run#5 (w0.2) Feed increase

Basically the same observations can be made about case w0.5 (Figure 5.25). The pressure remained constant and the liquid heights increased. The final liquid heights were 178.3 cm (light liquid) and 95.0 cm (heavy liquid). Again, the steady state was reached in 3 minutes.

Case w0.2 shows a slight difference from the 2 previous cases. Just after the disturbance was applied, the pressure did rise by 0.05 kPa to 176.05 kPa and slowly

returned to its setpoint of 176.0 kPa, in about 3 minutes. The liquid levels reached their steady state values of 181.71 cm and 97.19 cm for the light and heavy liquid respectively in about 6.5 minutes.

Figures 5.14, 5.26, and 5.35 shows the temperature response to be thermally stable. The largest temperature difference experienced is that of the vapour phase by an amount of about 0.2 K. This value is small enough to be considered negligible.

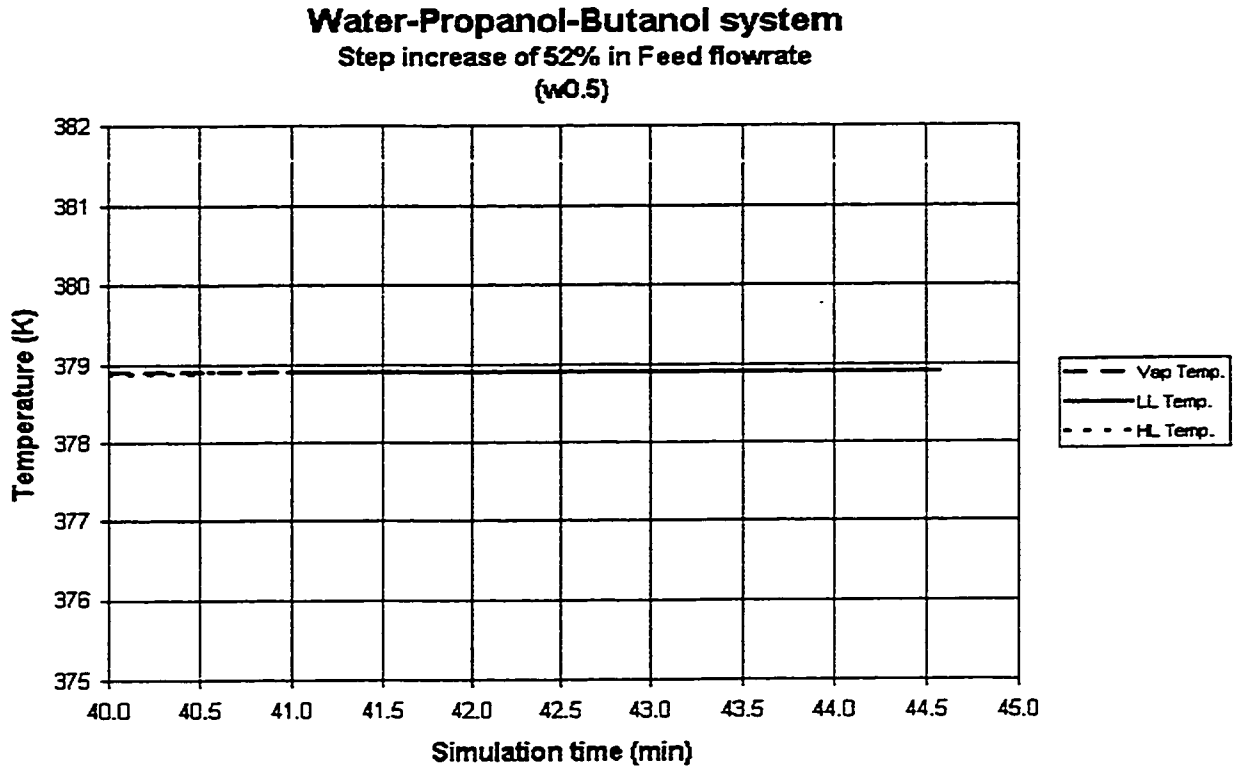

Figure 5.26 Temperature-Time profile for Run#4 (w0.5) Feed increase

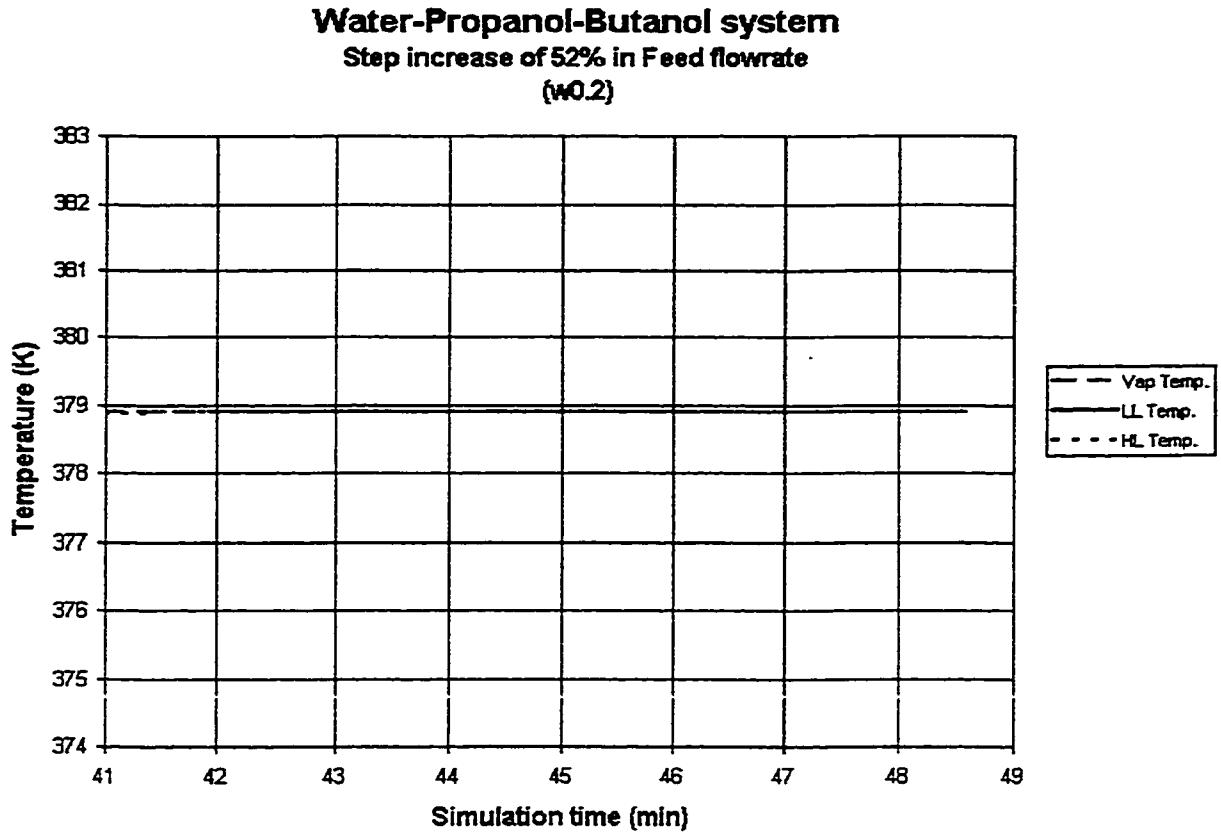

Figure 5.35 Temperature-Time profile for Run#5 (w0.2) Feed increase

Expected flowrate responses to a 52% feed flowrate increase are shown in Figures 5.15, 5.27, and 5.36. In all three cases, the vapour flowrates rapidly increased to match the vapour fraction of the feed rate. The heavy liquid rates smoothly rose to steady state flowrates, and the light liquid flowrate profiled all followed the same trend, i.e. the rates increased then overshot the steady state rates, then slowly returned. The only noticeable difference was the time required for the separator to stabilize and the amount of overshoot that the light liquid flowrate experienced. In case w1.0, the separator took 2 minutes to

stabilize while for case w0.5 and case w0.2 it took 3.6 minutes and 6.5 minutes, respectively. As for the flowrate overshoot, the values increased from 0.355 kmol/s (for case w1.0) to 0.361 kmol/s (for case w0.5) but decreased to 0.359 kmol/s (for case w0.2). This drop in overshoot shown in case w0.5 to case 0.2 is explained with equations 4.24 and 4.25 which govern the exiting flowrates of both liquid phases. The combination of both the weir width (L) and the exponent term ($h^{3/2}$) caused the flowrate value to be smaller in case w0.2 than in case w0.5 regardless of the fact that the liquid level was higher in case w0.2.

As the weir width was narrowed, the level response time lengthened and became more defined. This in turn allowed for more sampling points and the resulting plots became more realistic.

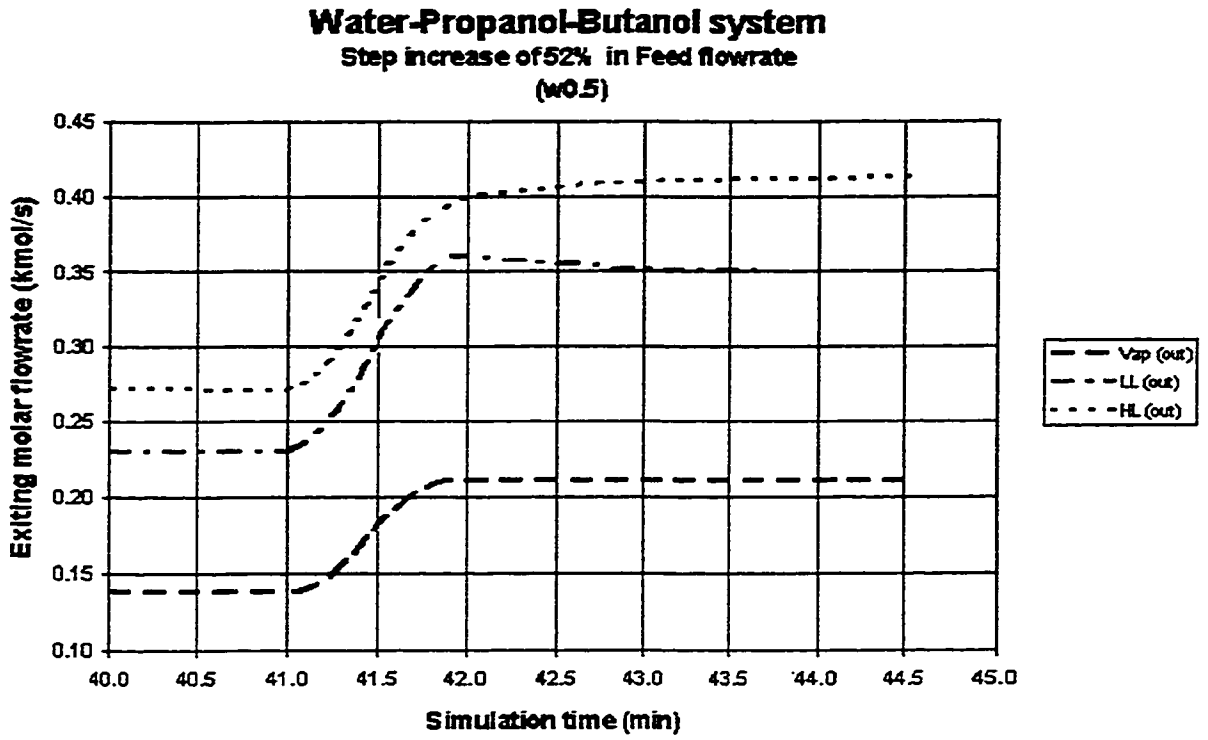

Figure 5.27 Exiting Molar Flowrate-Time profile for Run#4 (w0.5) Feed increase

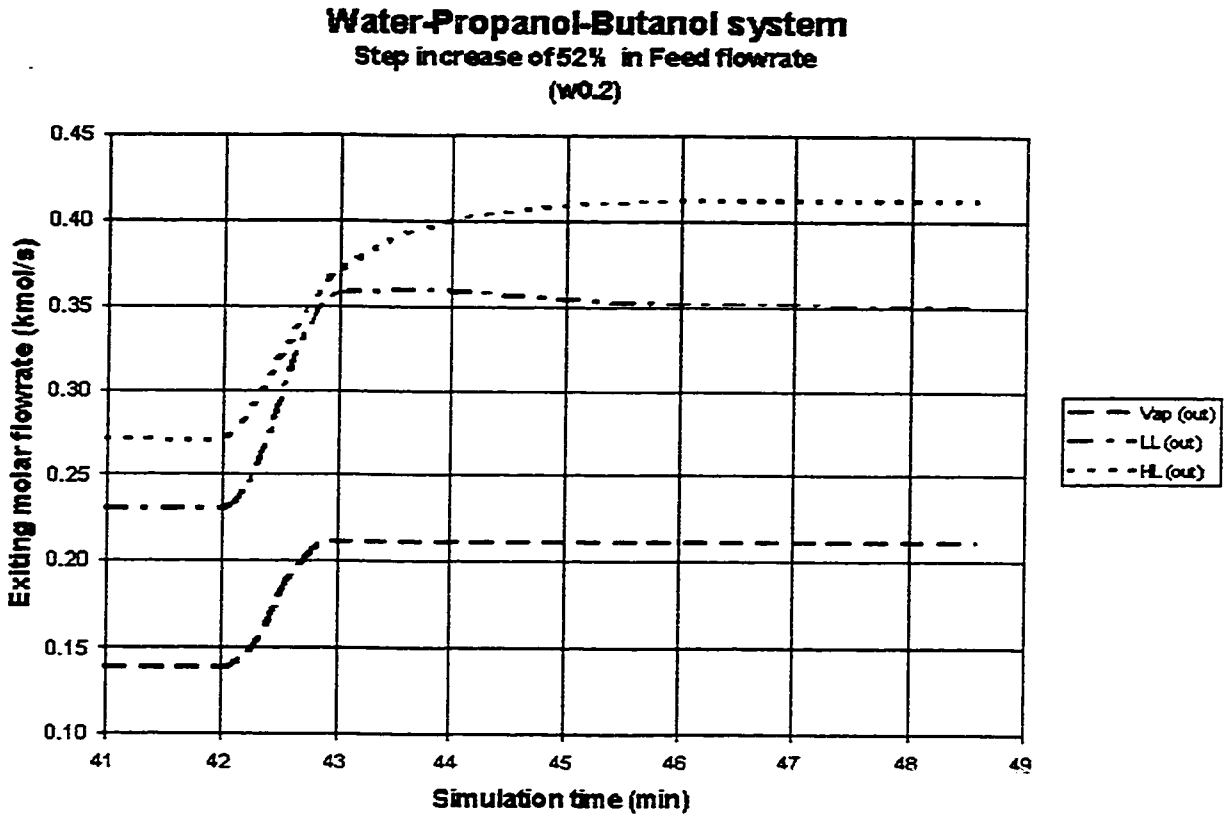

Figure 5.36 Exiting Molar Flowrate-Time profile for Run#5 (w0.2) Feed increase

5.4.3 Feed Decrease

The separator response to the decrease in feed flowrate is as expected, the opposite of that for the feed increase. The liquid levels dropped, the flowrates decreased, and the light liquid level and flowrate undershot the steady state values and returned to them. Again, the interaction of the light liquid and the heavy liquid response played an important role in the lighter liquid response. The pressure rose then returned to the setpoint, with the exception of case w0.2. It would appear that a slight change in

thermodynamic properties is responsible for the reversed pressure response to the step decrease in feed flowrate. The phase temperatures remained constant.

Figures 5.16, 5.28, and 5.37 show the liquid level and pressure responses for cases w1.0, w0.5 and w0.2. The pressure increased to 176.24 and 176.17 kPa, then dropped to the setpoint of 176.0 kPa. The pressure in case w0.2 initially decreased to 175.97 kPa and then overshot to a value of 176.1 kPa and finally stabilized to 176.0 kPa. This quasi-sinusoidal behaviour could have been produced by the combination of both the increase in the light liquid height and the pressure controller response. For cases w1.0, w0.5 and w0.2, the time needed for the levels and pressure to reach steady state are 5 minutes, 5 minutes and 7 minutes, respectively.

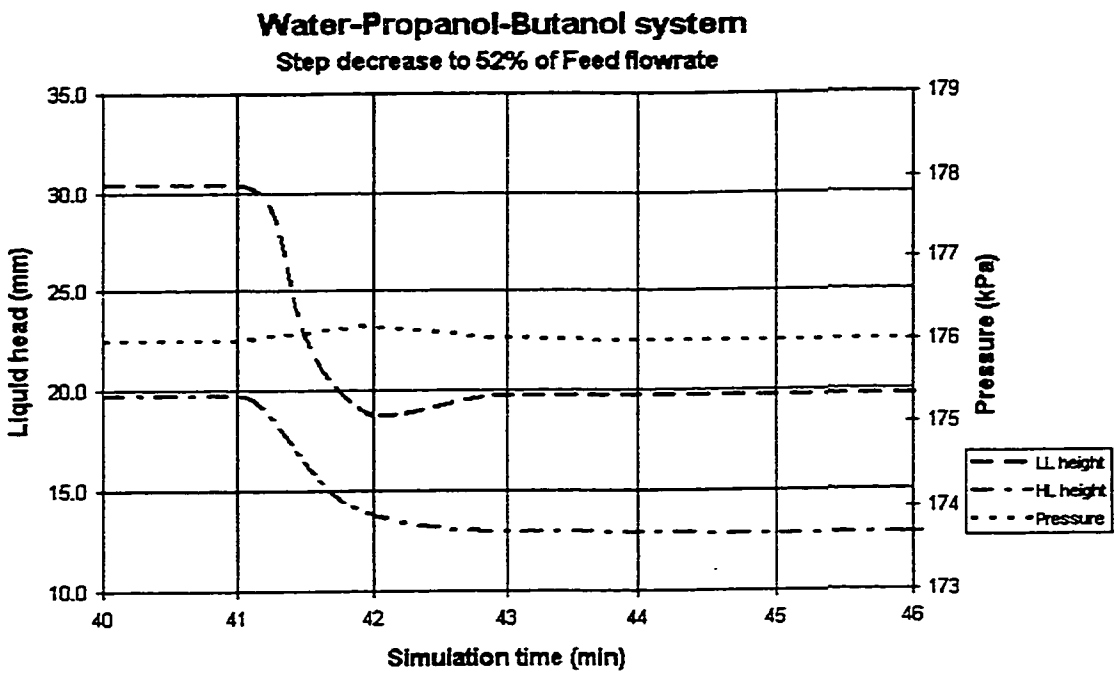

Figure 5.28 Pressure and Liquid Head-Time profile for Run#4 (w0.5) Feed decrease

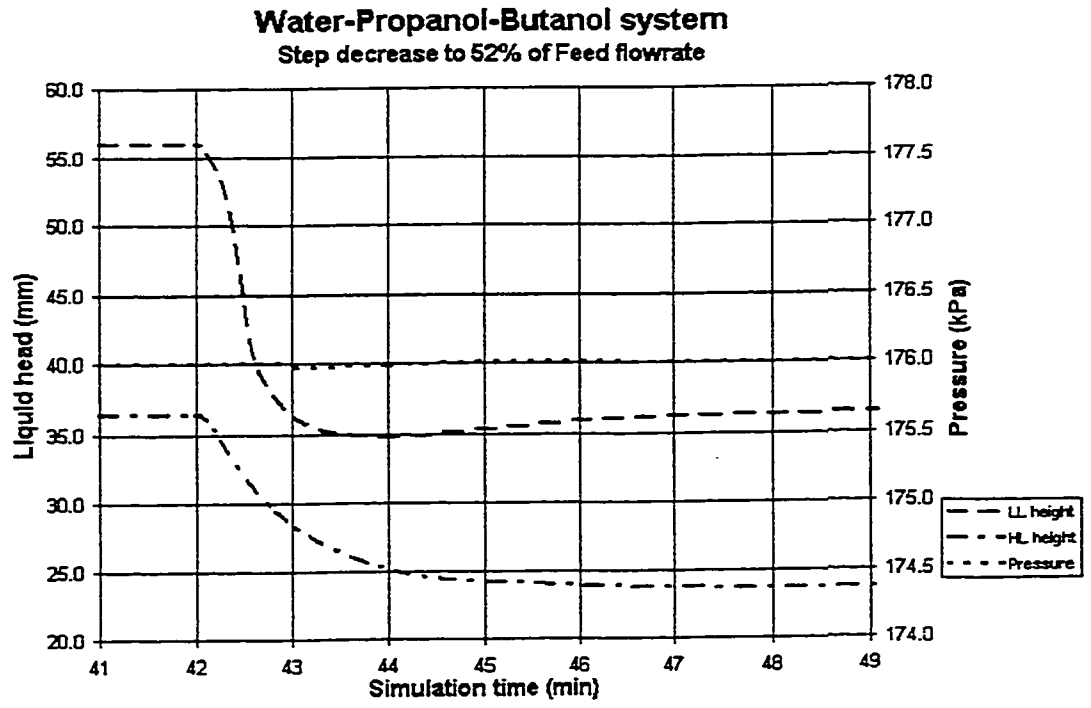

Figure 5.37 Pressure and Liquid Head-Time profile for Run#5 (w0.2) Feed decrease

Figures 5.17, 5.29, and 5.38 shows the temperature responses. Again, the system is thermodynamically stable.

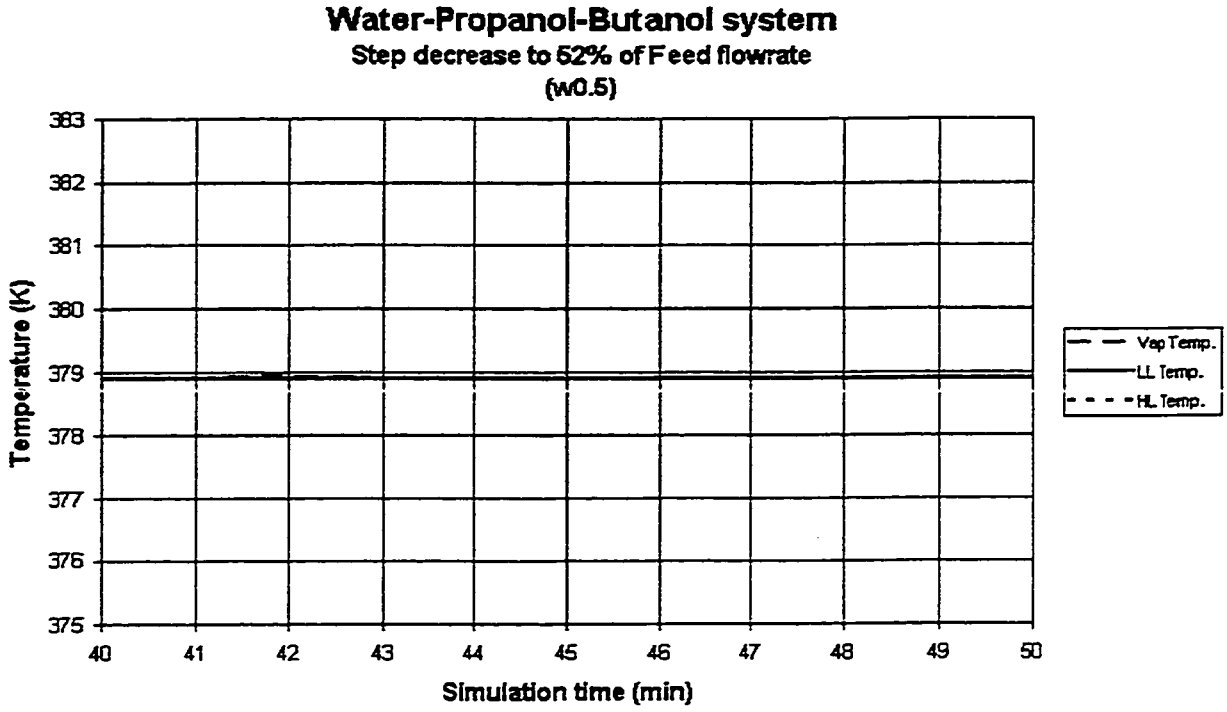

Figure 5.29 Temperature-Time profile for Run#4 (w0.5) Feed decrease

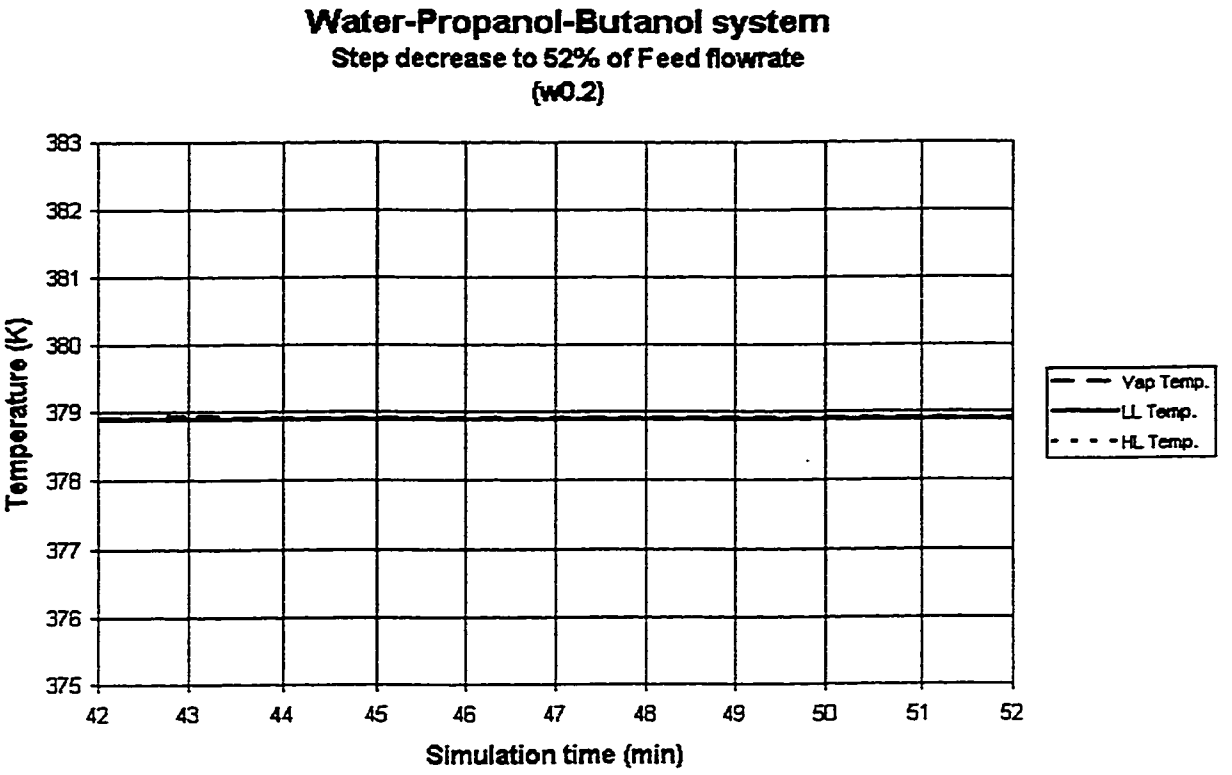

Figure 5.38 Temperature-Time profile for Run#5 (w0.2) Feed decrease

The flowrate responses are shown in Figures 5.18, 5.30, and 5.39. As mentioned, when the weir width was reduced, the time to steady state increased and more data points were collected, hence the smoother, more realistic plots. At steady state, the final flowrates equaled the feed flowrates.

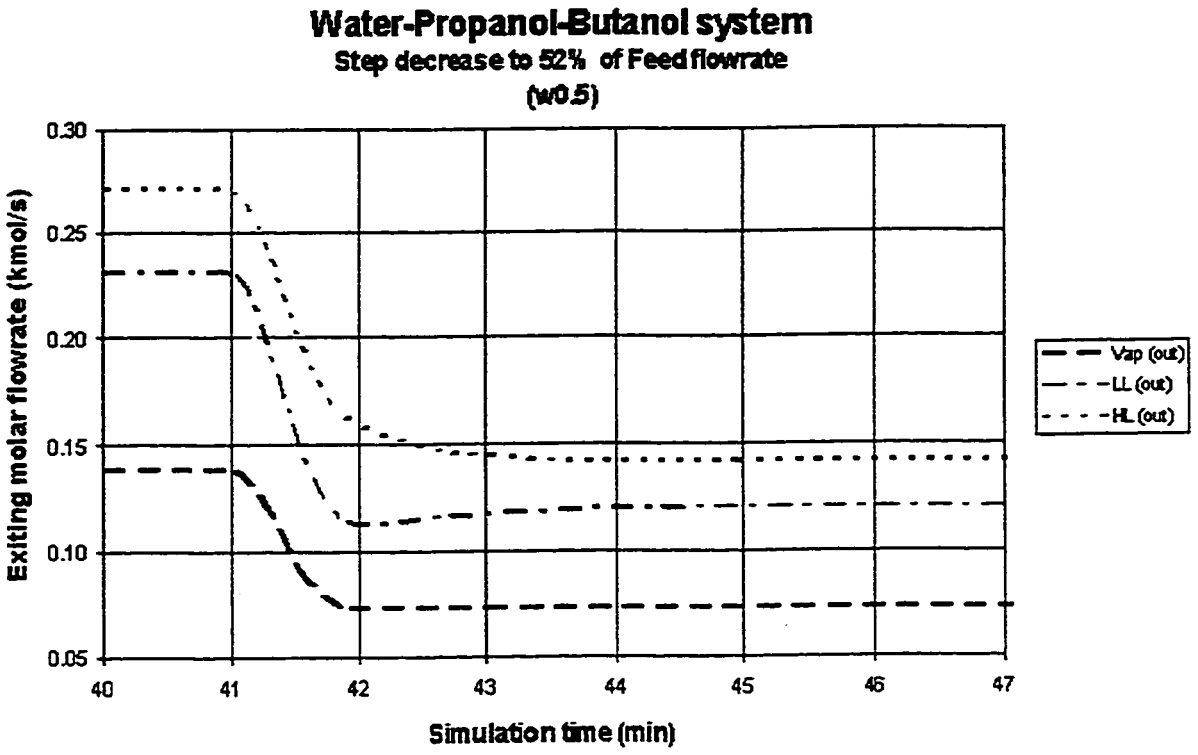

Figure 5.30 Exiting Molar Flowrate-Time profile for Run#4 (w0.5) Feed decrease

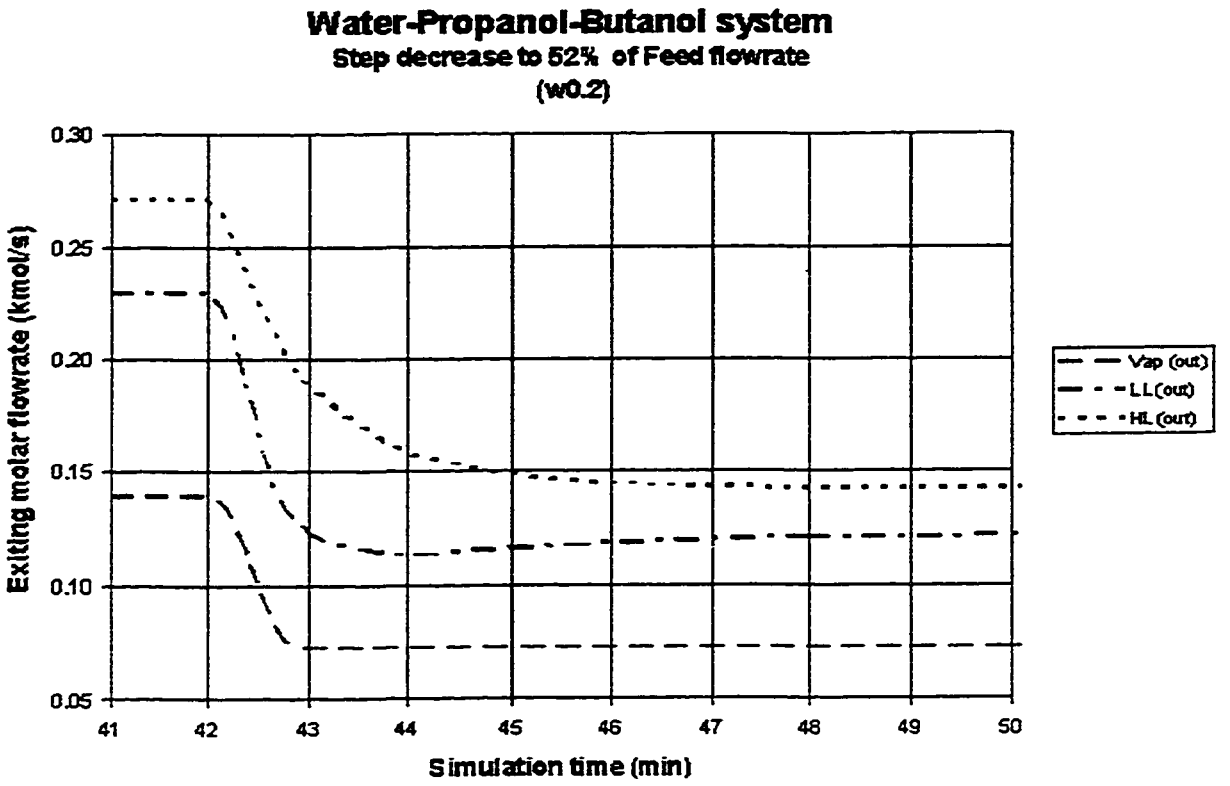

Figure 5.39 Exiting Molar Flowrate-Time profile for Run#5 (w0.2) Feed decrease

Summary

Various tests were performed in order to adequately simulate the most important operating scenarios of the three phase separator. The dry startup, the feed step changes and the shutdown are the main scenarios of separator operation that were simulated. The tests were performed to observe the following: any effects of various chemical systems on the separator design, the effects of feed flowrate change and weir width upon the vessel pressure, temperature, liquid heights and exiting molar flowrate.

The varying thermodynamic properties of the different chemical mixtures (water-ethanol-benzene and water-propanol-butanol) produced negligible changes in the designed separator's physical dimensions.

The comparison of Runs #1 and #2 revealed similar trends in separator behaviour during the dry startup, feed step changes and the shutdown. The similarities were noticed in the responses of the liquid levels, temperature, exiting flowrates, and pressure.

During the dry startup, the pressures increased then returned to the setpoint. The liquid levels increased. The phase temperatures remained constant. The exiting molar flowrates increased to the values equal to the feed flowrates.

During the feed step increase, tendencies were similar to those observed during the dry startup. The liquid levels and exiting molar flowrates increased. The temperatures basically remained constant. The pressure responded differently. In one case, it decreased then returned to the setpoint and in the other case it remained constant.

The feed step decrease caused the separator to respond in the reverse manner as found during the feed step increase. The liquid levels and exiting molar flowrates decreased. The pressure increased then stabilized to the setpoint.

Only run #2 possessed an adequate shutdown simulation. The separator responses were similar to those experienced during the feed step decrease. The pressure increased and slowly returned to the setpoint. The exiting molar flowrate reduced to zero. The liquid levels decreased to exactly the weir heights. The temperatures did not fluctuate.

The reversed variations in pressure is caused by slight changes in thermodynamic properties which resulted from the numerical calculations of the borrowed property package.

The various chemical mixtures also affected the time required to reach steady state. The two mixtures have three phase regions that are very different. The corresponding phase fractions and compositions were different as well. The variation in phase fractions caused differences in the feed flowrates. The feed flowrates filled the individual phase holdups at different rates, thus, the time required to reach steady state were not the same.

The effect of weir width on certain separator properties were investigated in runs #3, #4 and #5. As the weir width is decreased, the liquid levels increased as explained by the weir equation that governs the exiting molar flowrate. The equation states that as the width is decreased, the liquid level above the weir height must increase in order to keep the flowrate the same.

The increase in steady state liquid levels signified an increase in phase volume or holdup. This also signified that the time required to reach steady state increases as the weir width decreases. The longer the simulation time span, the more data points are collected. This in turn allows smoother more realistic plots to be graphed.

For runs #3, #4 and #5 similar trends in the liquid levels, exiting molar flowrates and pressure behaviour were observed during the main separator operating scenarios. During the operating scenarios, certain responses experienced an overshoot and undershoot. This was observed in the liquid level and exiting liquid flowrates responses. In the dry startup and feed step increase, there was overshoot in the liquid levels and exiting flowrates. During the feed step decrease, the responses displayed an undershoot. All the responses that overshot or undershot the stable values did return to them. As the weir width was decreased, the magnitude of the overshoot and undershoot increased.

Chapter 6 -Conclusions and Recommendations

6.1 Conclusions

A dynamic rate based mathematical model was developed for a three phase bucket and weir separator. The detailed mathematical model consisted of the enthalpy and mole balance equations, composition change equations and the mass transfer equations. The component mixtures used in the simulation were the water-ethanol-benzene and water-propanol-butanol ternaries at low pressure.

In particular, the rate based mathematical model developed by Lao and Taylor can be used to simulate separation unit operations, in this case a three phase separator with suitable modifications to the model.

The mass transfer correlation (Xu and Shen, 1992) was adapted to model the mass transfer fluxes in the separator. The necessary modifications included using multicomponent diffusivity coefficients to determine the multicomponent binary mass transfer coefficient. Then converting the binary mass transfer coefficients in the overall mass transfer coefficients. The assumptions made to adapt the correlation to the separator model were the following: the mass transfer occurs in equimolar counter diffusion, the separator would behave as a single stage of a distillation tower and the phase with the largest resistance would be the mass transfer rate determining phase.

The model appeared to be adequately developed to describe a three phase separator. The stratified liquid flow model (Lao and Taylor, 1994) applied in this work was the most adequate model of the ones described by Lao and Taylor (Lao and Taylor, 1994). It was found that the developed model worked well in steady state and dynamic periods. Under dynamic conditions, the model demonstrated that it was capable of handling disturbances applied to the three phase separator during most operating scenarios. The results showed that the separator behaved appropriately during the dry

startup and the feed disturbance. Most of the separator operating variables (liquid levels, exiting molar flowrates) demonstrated proper dynamic responses.

One of the first steps in the execution of the simulator was to design a separator according to the chosen feed. The feed flowrate and the densities of the various phases were some of the variables that affected the design of the separator. As a result of this and the similarities in the chemical ternary mixtures, the designed separators were virtually identical. The differences in the separator dimensions ranged from 2% to 7% relative difference.

The other effect of using different ternary mixtures was the effect of phase fraction upon the separator behaviour. The major difference was caused by the location of the feed mixture within its' three phase region. For example, the ternary mixture of water-ethanol-benzene (at the separator operating conditions of 346.5 K and 140 kPa) was in a three phase region where the heavy liquid fraction was more than 80%. This meant that more than 80% of the feed flowrate would be the flowrate of the heavy liquid phase. The heavy liquid phase responses would dominate the separator response behaviour of the entire separator. The heavy liquid level would stabilize first and the heavy liquid exiting flowrate would be the first to stabilize during all operation scenarios. The ternary mixture of water-propanol-butanol (at the separator operating conditions of 378.9 K and 176 kPa) was located in a three phase region where the vapour phase and the two liquid phase fractions varied from 28% to 36%. As a result, the feed flowrate was split in similar fractions between the three phases. The time required for each of the associated phase responses to stabilize were similar.

These trends and behaviours were observed in the vessel pressure, liquid levels, exiting molar flowrates and the phase temperatures during all operation scenarios. During all dry startup scenarios the liquid levels increased and the exiting molar flowrates increased once the levels reached the weir height. As well, the pressure increased until the

liquid levels stabilized, then returned to the pressure setpoint. The phase temperatures fluctuated minimally at the beginning of the dry startup, then stabilized.

Similar trends were observed when the feed flowrate was increased and decreased. When the feed was increased, the liquid levels and exiting molar flowrates increased and stabilized to a new steady state. The opposite occurred when the feed flowrate was decreased. The only variable that did not change in a similar trend was the pressure.

The results of the tests performed to observe the effect of weir width produced similar trends as those found in the previous tests. During all the operation scenarios the liquid levels, pressure, exiting molar flowrate and the phase temperatures behaved as those found in the previous tests. However, an additional trend was observed in these tests. As the weir width was decreased the liquid volumes and levels increased along with the time required for the separator to reach steady state. The weir equation governed this change in levels. To compensate for the decrease in weir width, the level of liquid over the weir lip had to increase in order for the exiting molar flowrate to match the incoming feed. This increase in liquid levels signified increases in the liquid volumes. As the feed flowrate was keep constant during the dry startup for all the tests, then the time required for the separator to reach steady state was also increased. During these longer transient periods more data was collected which in turn produced more realistic plots. The changes in weir width also demonstrated that the geometry of the separator played an important role in the separator behaviour during the dry startup and the feed disturbances. For example, a vertical separator would respond differently to a perturbation than would the horizontal separator.

Another response to the feed disturbance was the minor changes in the phase thermodynamic properties. These changes can be attributed to the pressure enthalpy (PH) flash response to the applied perturbation. These small changes in the intensive properties were responsible for the unexpected pressure responses to the disturbances.

When the weir widths were narrowed (using water-propanol-butanol), the similar trends and behaviours were observed. By reducing the weir width, the liquid levels increased. These increased liquid levels translated into increases in phase volumes thus requiring longer transient times to reach steady state.

The NRTL model appeared to have well represented the aqueous mixtures. When using the NRTL for the residual curve map utility, the HYCON software produced three phase regions that were easier to find than with other thermodynamic models. This enabled the author to run the separator simulator at the specific temperature and pressure of the desired three phase region. The choice in thermodynamic models would affect the simulation results. Using various thermodynamic models would affect almost all of the separator operating variables, thus, could result in very different simulation outputs.

6.2 Recommendations

The following is a list of items that should be addressed for future work.

1) When developing a complex rate based model of this type, it would be advantageous if the thermodynamic package was written specifically for the model.

2) Most of the runs performed as part of the thesis had to be performed in three separate stages; the dry startup, the feed disturbances and the shutdown. All three stages could not be performed in one run. Further work could be focused on the dry startup and shutdown in an effort to develop efficient and smooth scenarios, possibly for operator training.

3) As this study of the dynamic simulation of a 3 phase separator was theoretical, experimental results could be obtained from a small scale separator in order to compare and validate the theoretical results.

4) Add detail to the model by including heat loss to the environment and heat transfer coefficient for the separator outer walls.

5) Re-run the tests using various other thermodynamic models in order to observe differences in the separator behaviour during the operating scenarios.

REFERENCES

Baden, Niels and Michael L. Michelsen, "Computer Methods for Steady-State Simulation of Distillation Columns", Institute of Chemical Engineers Symposium Series, No. 104, 1987, pp. A425-A435.

Bakr, Abu, S.H. Salem, Magdi Fekri, "Rigorous Computation of Binary Distillation Systems", 1994.

Benallon, A., D.E. Seborg, D.A. Mellichamp, "Dynamic compartemental models for separation processes", AIChE Journal, July 1986, Vol.32, No7, pp. 1067-1078.

Block, Ulrich, Bernd Hegner, "Development and Application of a Simulation Model for Three- Phase Distillation", AIChE Journal, May 1976, Vol.22, No.3, pp. 582-589.

Cairns, Brett P., Ian A. Furzer, "Multicomponent Three-Phase Azeotropic Distillation 1) Extensive Experimental Data and Simulation Results", Industrial Engineering and Chemical Research, 1990, Vol. 29, pp. 1349-1363.

Carta, R., G. Tola, A. Servida, M. Morbidelli, "Performance of collocation models for simulation transient multistage separation units", Computers and Chemical Engineering, Vol. 19, No.11, 1995, pp. 1141-1151.

Eckert, E., M. Kubícek, "Dynamic simulation of a distillation column with multiple liquid phases", Computers and Chemical Engineering, Vol.19, Suppl., 1995, pp. S393-S398.

Eckert, E., M. Kubícek, "Modelling of Dynamics for Multiple Liquid-Vapour Equilibrium Stage", Computers and Chemical Engineering, Vol. 49, No.11, 1994, pp. 1783-1788.

Ferraris, G. B., Morbidelli, M., "Distillation Models for 2 Partially Immiscible Liquids", AIChE Journal, Vol. 27, No. 6, Nov. 1981, pp. 881-888.

Floudas, C.A., "Separation Synthesis of Multicomponent Feed Streams into Multicomponent Product Streams", AIChE Journal, April 1987, Vol.33, No.4, pp.540-550.

Franks, G. E., "Modeling and Simulation in Chemical Engineering", Wiley-Interscience, 1972, 411 p.

Grottoli, M.G., G. Biardi, L. Pellegrini, "A new simulation model for a real tray absorption column", Computers and Chemical Engineering, Vol.15, No.3, 1991, pp.171-179.

Heh, Jiing-Shiuan, Ming-Yaw Lay and Shan-Hill Wong, "Simulation of Single and Multi-Stage Operation with Vapor-Liquid-Liquid Equilibrium", Journal of the Chinese Institute of Chemical Engineers, Vol.18, No. 5, 1987, pp.329-337.

Hyprotech Ltd., "HYSYS-Conceptual Design Application reference manual".

Iribarren, Oscar A., Omar J. Chiotti, "Simplified Analytical Prediction of distillation column startup time @ total reflux", The Canadian Journal of Chemical Engineering, Vol. 69, Feb. 91, pp. 377-382.

Kienle, A., E.D. Gilles, W. Marquardt, "Computing Multiple Steady States in Homogeneous Azeotropic Distillation Processes", Computers and Chemical Engineering, Vol.18, Suppl., 1994, pp. S37-S41.

Kingsley, Jeffrey P., Angelo Lucia, "Simulation and Optimization of Three Phase Distillation Processes", Industrial Engineering and Chemical Research, 1988, Vol. 27, pp.1900-1910.

Kinoshita, Masahiro, "Simple model for dynamic simulation of stage separation processes with very volatile components", AIChE Journal , May 1986, Vol. 32, No 5, pp. 872-874.

Kooijman, Hendrik A. and Ross Taylor, "A Nonequilibrium Model for Dynamic Simulation of Tray Distillation Columns", AIChE Journal, August 1995, Vol.41, No.8, pp.1852-1863.

Kooijman, Hendrik A., Ross Taylor, "Dynamic Simulation of Distillation Columns using a Nonequilibrium Model", AIChE 1993 Annual Meeting, UNPUBLISHED.

Krishnamurthy, R., R. Taylor, "A Nonequilibrium Stage Model of Multicomponent Separation Processes", AIChE Journal, Vol. 31, No. 3, March 1985, pp. 449-465.

Kruse, Ch., G. Fieg, G. Wozny, L. Jeromin, W. Johannisbauer, "Experimental verification of equilibrium stage model for the dynamics of multicomponent distillation considering the effects of energy loss", Industrial Engineering Chemistry and Research, Vol. 34, 1995, pp. 1810-1822.

Lacey, J.W., Svrcek, W.Y., "Computers and Chemical Engineers.", Presented at 40th Canadian Chemical Engineering Conference, Halifax, NS, Canada, 1990.

Landwehr, B., G. Wozny, H. Hartmann, "Simulation of coupled columns with 3 phase", European Symposium on Computer Aided Process Engineering, 1992, Suppl., pp. S395-S402.

Landwehr, B., G. Wozny, and H. Hartmann, "Steady state and dynamic simulation of three phase distillation for industrial application", ICHEME Symposium Series, No.128, 1992, pp. B11-26.

Luyben, W.L., "Process Modeling, Simulation, and Control for Chemical Engineers.", McGraw-Hill, New York, 1973.

Lao, Miaozhen, Ross Taylor, "Modelling mass transfer in three phase distillation", Industrial Engineering and Chemical Research, 1994, Vol. 33, pp. 2637-2650.

Liu, Fang-Zhi, Hideki MORI, Setsuro HIROAKA, Ikuho YAMADA, "Phase Equilibrium and simulation for heterogeneous azeotropic distillation", Journal of Chemical Engineering of Japan, Vol.26, No.1, 1993, pp.41-47.

Marquardt, W., "Dynamic Process Simulation-Recent Progress and Future Challenges.", Proceedings of CPIV (Ed: Arkun, Y., Ray, W.H., AIChE) New York, 1991, p. 131-180.

Monnery, Wayne D., William Y. Svrcek, "Successfully Specify Three-Phase Separators", Chemical Engineering Progress, September 1994, pp. 29-40.

Morris, Craig G., "Dynamic Simulation of Multicomponent distillation", Thesis, University of Calgary, 1980.

Overjero, Gabriel, Rafael van Grieken, Lourdes Rodriguez, Jose Luis Valverde, "Simulation of multicomponent Distillation using a non-equilibrium stage model", Separation Science and Technology, Vol. 29, No.14, 1994, pp. 1805-1821.

Pucci, A., P. Mikitenko, L. Asselineau, "Three-Phase Distillation. Simulation and Application to the Separation of Fermentation Products", Chemical Engineering Science, Vol.41, No.3, 1986, pp. 485-494.

Ross, Bradley A., Warren D. Seider, "Simulation of 3 phase distillation towers", Computers and Chemical Engineering, Vol.5, 1980, pp. 7-20.

Rovaglio, Maurizio , Michael F. Doherty, "Dynamics of Heterogeneous Azeotropic Distillation Columns", AIChE Journal, January 1990, Vol.36, No.1, pp. 39-52.

Ruiz, C.A., I.T. Cameron, R. Gani, "A generalized dynamic model for distillation columns.-III study of startup operations", Computers and chemical engineering, Vol.12, No.1, 1988, pp. 1-14.

Salazar-Sotelo, Daniel, "3Phase Distillation Simulation", Thesis, Instituto Mexicano Del Petroleo, 1992.

Sayama, Hayatoshi, Kengo Shimizu, Yoshimara Kameyama, Kazuhiko Suzuki, "Modeling and stage to stage computation of multicomponent distillation processes as a multistage optimization problem", Journal of Chemical Engineering of Japan, vol23, No4, August 1990.

Smith, J. M., H. C. Van Ness, "Introduction to Chemical Engineering Thermodynamics", McGraw-Hill, 1987, 698 p.

Stewart, Warren E., Keith L. Levien, Manfred Morari, "Simulation of fractionation by orthogonal collocation", Chemical Engineering Science, Vol.40, No.3, 1985, pp. 409-421.

Taylor, Ross, Hendrik A. Kooijman, "Dynamic simulation of distillation columns using a non-equilibrium model", 1993

Taylor, R. and Angelo Lucia, "Modelling and Analysis of Multicomponent Separation Processes", Separation System Synthesis and Design, 1995, pp.19-28.

Vickery, D.J., Ross Taylor, "Path following approaches to the solution of multicomponent, multistage separation process problems", AIChE Journal , Apr. 1986, Vol. 32, No 4., pp. 547-554.

Walas, Stanley M., "Phase Equilibria in Chemical Engineering", Butterworth-Heinemann, 1985, 671 p.

Wasylkiewicz, S., "Simulation of 3phase distillation", ICHEME Symposium Series No.128, 1992, pp.B205-B212.

Wong, C. F., W. Hayduk, "Correlations for Prediction of Molecular Diffusivities in Liquids at Infinite Dilution", The Canadian Journal of Chemical Engineering, Vol. 68, October 1990, pp. 849-859.

Wong, D.S.H., S.S. Jang, C.F. Chang, "Simulation of dynamics and pattern changes for an azeotropic distillation column", Computers and Chemical Engineering, Vol.15, No.5, 1991, pp. 325-335.

Xu, Xiao-Ming, Fu Shen, "Use of Estimated Transfer Rate to Calculate Binary Mass Transfer Coefficients and Model Multicomponent Fractionation", Teoreticheskie Osnovy Khimicheskoi Tekhnologii, Vol. 26, No. 4, July-August 1992, pp. 486-493.

Appendix A

All of the data obtained during the five various simulation runs were tabulated prior to generating the different plots and graphs. The table, as shown below, is an example of the generated data obtained during Run #2 or #3. The pressure displayed is in kiloPascal (kPa), the temperatures are in degrees Kelvin (K), and all exiting molar flowrates (vapour, light liquid and heavy liquid) are in kmol/s. The liquid heights are in centimeters (cm).

Startup									
Time	Pressure	Vap Temp.	Vap (out)	LL Temp.	LL height	LL (out)	HL Temp.	HL height	HL (out)
0.00	176.00	378.90	0.000	378.90	0.00	0.000	378.90	0.00	0.000
0.00	176.11	378.90	0.138	378.90	2.33	0.000	378.90	1.17	0.000
0.92	177.08	378.90	0.139	378.90	21.23	0.000	378.90	10.68	0.000
0.95	177.12	379.08	0.139	378.92	21.71	0.000	378.88	10.92	0.000
0.98	177.12	379.08	0.139	378.92	22.18	0.000	378.88	11.15	0.000
1.98	177.09	379.08	0.139	378.92	34.94	0.000	378.88	17.52	0.000
2.99	177.09	379.08	0.139	378.92	45.89	0.000	378.88	22.93	0.000
3.97	177.09	379.08	0.139	378.92	55.60	0.000	378.88	27.67	0.000
5.00	177.09	379.08	0.139	378.92	65.03	0.000	378.88	32.21	0.000
5.98	177.09	379.08	0.139	378.92	73.54	0.000	378.88	36.26	0.000
6.99	177.09	379.08	0.139	378.92	82.06	0.000	378.88	40.25	0.000
7.98	177.09	379.08	0.139	378.92	90.15	0.000	378.88	43.99	0.000
8.97	177.09	379.08	0.139	378.92	98.14	0.000	378.88	47.61	0.000
10.00	177.09	379.08	0.139	378.92	106.25	0.000	378.88	51.23	0.000
11.00	177.09	379.08	0.139	378.92	114.11	0.000	378.88	54.66	0.000
11.98	177.09	379.08	0.139	378.92	121.76	0.000	378.88	57.92	0.000
12.98	177.09	379.08	0.139	378.92	129.64	0.000	378.88	61.20	0.000
13.98	177.09	379.08	0.139	378.92	137.57	0.000	378.88	64.41	0.000

14.98	177.09	379.08	0.139	378.92	145.60	0.000	378.88	67.55	0.000
16.00	177.09	379.08	0.139	378.92	153.94	0.000	378.88	70.71	0.000
16.99	177.09	379.08	0.139	378.92	162.30	0.000	378.88	73.73	0.000
17.99	177.09	379.08	0.139	378.92	171.11	0.000	378.88	76.76	0.000
18.99	176.24	378.94	0.139	378.92	176.76	0.336	378.88	79.73	0.000
19.98	176.11	378.92	0.138	378.92	176.85	0.356	378.87	82.66	0.000
21.00	176.12	378.91	0.138	378.91	176.85	0.356	378.87	85.61	0.000
21.99	176.07	378.91	0.138	378.91	176.85	0.356	378.87	88.48	0.000
23.00	176.11	378.92	0.138	378.91	176.85	0.356	378.87	91.38	0.000
23.99	176.06	378.91	0.138	378.90	176.47	0.282	378.87	93.44	0.212
24.98	176.01	378.90	0.138	378.90	176.22	0.233	378.87	93.61	0.269
25.99	176.00	378.90	0.138	378.90	176.20	0.230	378.88	93.62	0.270
26.98	176.00	378.90	0.138	378.90	176.20	0.230	378.88	93.62	0.270
28.00	176.00	378.90	0.138	378.90	176.20	0.230	378.88	93.62	0.270
28.99	176.00	378.90	0.138	378.90	176.20	0.230	378.88	93.62	0.270
29.98	176.00	378.90	0.138	378.90	176.20	0.230	378.88	93.62	0.270
30.99	176.00	378.90	0.138	378.90	176.20	0.230	378.88	93.62	0.270
31.98	176.00	378.90	0.138	378.90	176.20	0.230	378.88	93.62	0.270
33.00	176.00	378.90	0.138	378.90	176.20	0.230	378.88	93.62	0.270
33.99	176.00	378.90	0.138	378.90	176.20	0.230	378.88	93.62	0.270
35.00	176.00	378.90	0.138	378.90	176.20	0.230	378.88	93.62	0.270
35.99	176.00	378.90	0.138	378.90	176.20	0.230	378.88	93.62	0.270
36.98	176.00	378.90	0.138	378.90	176.20	0.230	378.88	93.62	0.270
38.00	176.00	378.90	0.138	378.90	176.20	0.230	378.89	93.62	0.270
38.99	176.00	378.90	0.138	378.90	176.20	0.230	378.89	93.62	0.270
40.00	176.00	378.90	0.138	378.90	176.20	0.230	378.89	93.62	0.270
40.99	176.00	378.90	0.138	378.90	176.20	0.230	378.89	93.62	0.270

Feed increase									
Time	Pressure	Vap Temp.	Vap (out)	LL Temp.	LL height	LL (out)	HL Temp.	HL height	HL (out)
41.90	176.00	378.90	0.211	378.90	176.84	0.355	378.90	94.01	0.408
41.92	176.00	378.90	0.211	378.90	176.84	0.355	378.90	94.01	0.408
41.93	176.00	378.90	0.211	378.90	176.84	0.355	378.90	94.01	0.409
41.94	176.00	378.90	0.211	378.90	176.84	0.355	378.90	94.01	0.409
41.96	176.00	378.90	0.211	378.90	176.84	0.355	378.90	94.01	0.409
41.97	176.00	378.90	0.211	378.90	176.84	0.354	378.90	94.01	0.409
41.99	176.00	378.90	0.211	378.90	176.84	0.354	378.90	94.01	0.409
42.90	176.00	378.90	0.211	378.90	176.82	0.351	378.90	94.02	0.412
42.91	176.00	378.90	0.211	378.90	176.82	0.351	378.90	94.02	0.412
42.92	176.00	378.90	0.211	378.90	176.82	0.351	378.90	94.02	0.412
42.94	176.00	378.90	0.211	378.90	176.82	0.351	378.90	94.02	0.412
42.95	176.00	378.90	0.211	378.90	176.82	0.351	378.90	94.02	0.412
42.97	176.00	378.90	0.211	378.90	176.82	0.351	378.90	94.02	0.412
42.98	176.00	378.90	0.211	378.90	176.82	0.351	378.90	94.02	0.412

Shutdown									
Time	Pressure	Vap Temp.	Vap (out)	LL Temp.	LL height	LL (out)	HL Temp.	HL height	HL (out)
43.24	176.00	378.90	0.211	378.90	176.82	0.351	378.90	94.02	0.412
43.99	176.78	379.16	0.000	378.89	174.24	0.000	378.89	92.78	0.053
44.98	176.57	379.08	0.000	378.89	173.94	0.000	378.89	92.52	0.011
45.99	176.49	379.03	0.000	378.89	173.85	0.000	378.89	92.45	0.004
46.98	176.45	378.99	0.000	378.89	173.82	0.000	378.89	92.42	0.002
47.98	176.43	378.97	0.000	378.89	173.80	0.000	378.89	92.40	0.001
48.99	176.41	378.97	0.000	378.89	173.79	0.000	378.89	92.39	0.001
49.98	176.40	378.97	0.000	378.89	173.79	0.000	378.89	92.39	0.000
50.99	176.39	378.96	0.000	378.89	173.78	0.000	378.89	92.38	0.000
51.98	176.38	378.96	0.000	378.89	173.78	0.000	378.89	92.38	0.000
52.99	176.38	378.96	0.000	378.89	173.78	0.000	378.89	92.38	0.000
53.98	176.37	378.96	0.000	378.89	173.78	0.000	378.89	92.38	0.000
54.98	176.36	378.96	0.000	378.89	173.78	0.000	378.89	92.38	0.000
55.99	176.35	378.96	0.000	378.89	173.77	0.000	378.89	92.38	0.000
56.98	176.35	378.96	0.000	378.89	173.77	0.000	378.89	92.38	0.000
57.99	176.34	378.95	0.000	378.89	173.77	0.000	378.89	92.38	0.000
58.98	176.33	378.95	0.000	378.89	173.77	0.000	378.89	92.38	0.000
59.99	176.33	378.95	0.000	378.89	173.77	0.000	378.89	92.37	0.000
60.96	176.32	378.95	0.000	378.89	173.77	0.000	378.89	92.37	0.000

Table A.1 Run 2 : Water-Propanol-Butanol system with a 52% increase in Feed flowrate

Appendix B

This appendix contains the residue curve maps that were employed for the purpose of this work. The graphs were used to initially determine the three phase regions in which the feed and separator mixtures operated. These curve maps were generated by the thermodynamic software HYCON developed at Hyprotech Ltd.

The first step in locating the three phase region was to set the pressure in which the vessel and the feed operated. Then the composition of the feed mixture was chosen so that the mixture fell within the two liquid phase region which can be seen on both generated graphs (Figures B.1 and B.2). Then once the composition was determined, HYCON's Stream Manager was used to find the three phase region by varying the temperature of the mixture.

Figures B.1 and B.2 show the residue curve maps for the two chemical mixtures used in this work. The first mixture (water-ethanol-benzene) existed as a three phase mixture at the conditions of 140 kPa, 346.5 K and mole fractions of 0.8, 0.1, and 0.1 respectively. The second mixture (water-propanol-butanol) existed as a three phase mixture at the conditions of 176 kPa, 378.9 K and the same mole fractions of 0.8, 0.1 and 0.1 respectively.

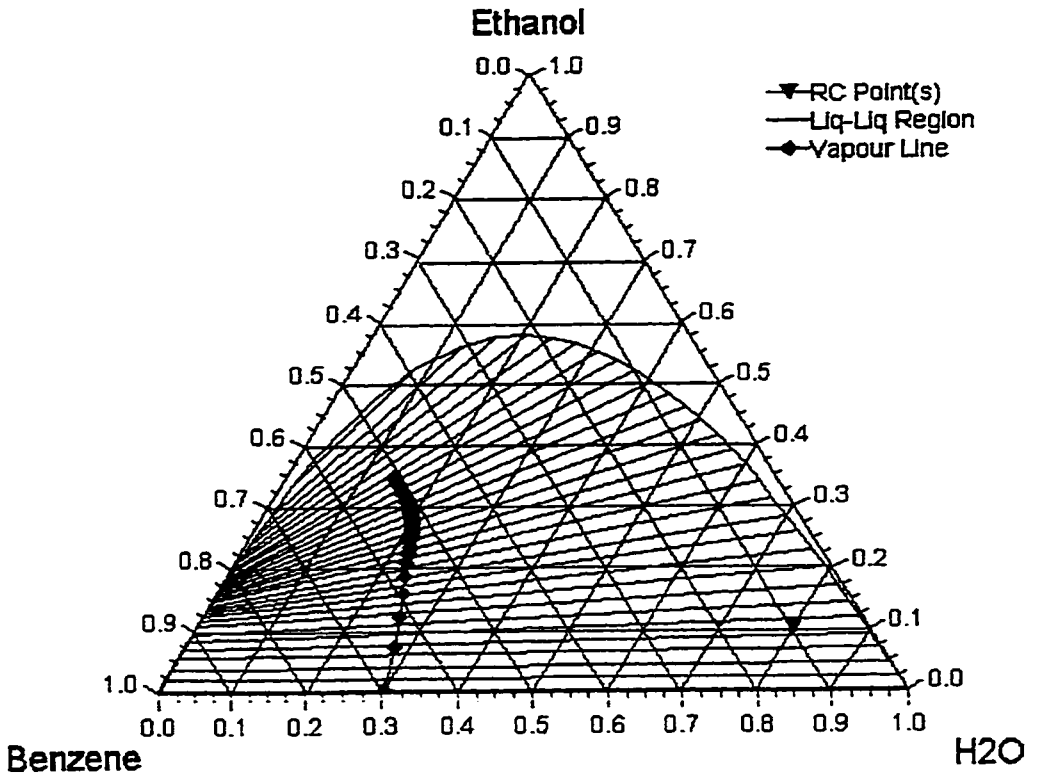

Figure B.1: Residue curve map for the water-ethanol-benzene mixture at 140 kPa

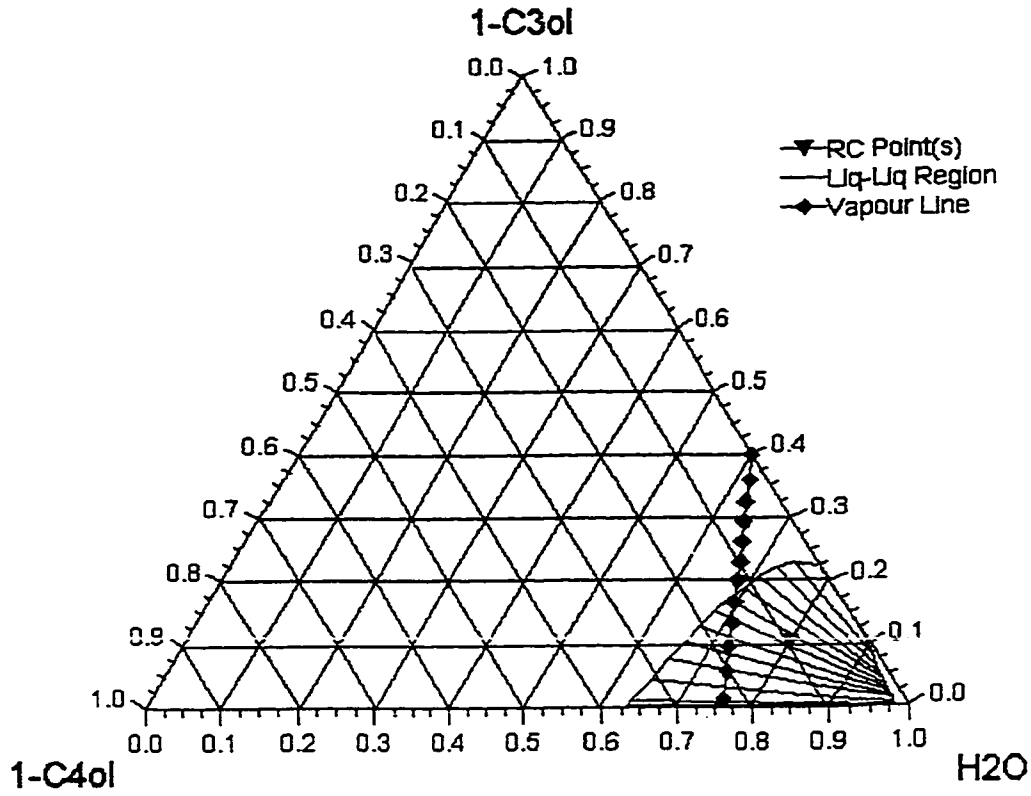

Figure B.2: Residue curve map for the water-propanol-butanol mixture at 176 kPa